Volume 46 | Number 8 | 21 April 2017 | Pages 2031–2366

Chem Soc Rev

Chemical Society Reviews

rsc.li/chem-soc-rev

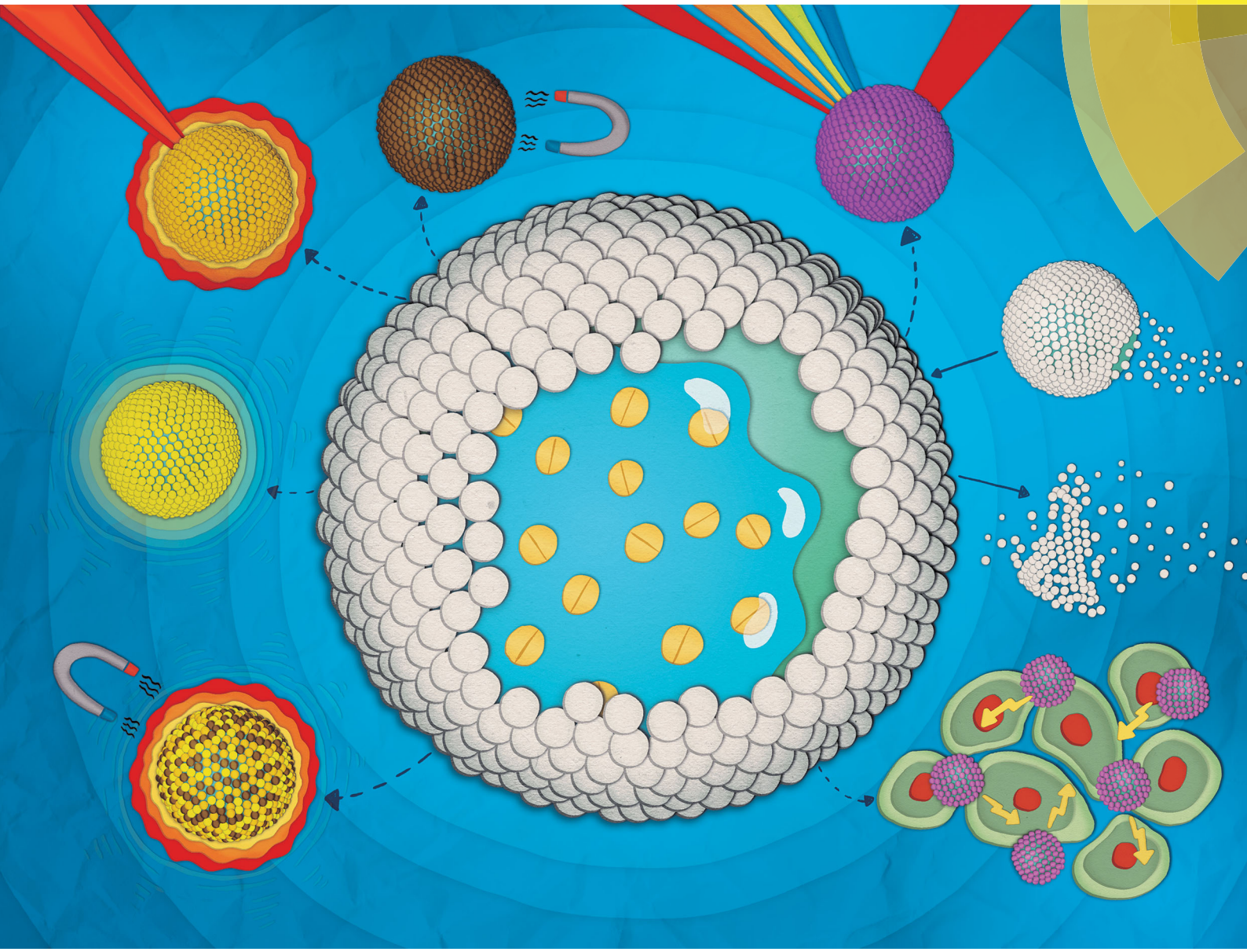

ISSN 0306-0012

ROYAL SOCIETY OF CHEMISTRY

REVIEW ARTICLE

Tobias Bollhorst *et al.*

Colloidal capsules: nano- and microcapsules with colloidal particle shells

Chem Soc Rev

REVIEW ARTICLE

View Article Online
View Journal | View Issue

Cite this: *Chem. Soc. Rev.*, 2017, **46**, 2091

Colloidal capsules: nano- and microcapsules with colloidal particle shells

Tobias Bollhorst,* Kurosch Rezwan and Michael Maas

Utilizing colloidal particles for the assembly of the shell of nano- and microcapsules holds great promise for the tailor-made design of new functional materials. Increasing research efforts are devoted to the synthesis of such colloidal capsules, by which the integration of modular building blocks with distinct physical, chemical, or morphological characteristics in a capsule's shell can result in novel properties, not present in previous encapsulation structures. This review will provide a comprehensive overview of the synthesis strategies and the progress made so far of bringing nano- and microcapsules with shells of densely packed colloidal particles closer to application in fields such as chemical engineering, materials science, or pharmaceutical and life science. The synthesis routes are categorized into the four major themes for colloidal capsule formation, *i.e.* the Pickering-emulsion based formation of colloidal capsules, the colloidal particle deposition on (sacrificial) templates, the amphiphilicity driven self-assembly of nanoparticle vesicles from polymer-grafted colloids, and the closely related field of nanoparticle membrane-loading of liposomes and polymersomes. The varying fields of colloidal capsule research are then further categorized and discussed for micro- and nano-scaled structures. Finally, a special section is dedicated to colloidal capsules for biological applications, as a diverse range of reports from this field aim at pharmaceutical agent encapsulation, targeted drug-delivery, and theranostics.

Received 23rd August 2016

DOI: 10.1039/c6cs00632a

rsc.li/chem-soc-rev

1. Introduction

Various methods for the synthesis of nano- and microcapsules with densely packed colloidal particle shells have been introduced and greatly advanced over the course of the last two decades. These mainly include self-assembly routes based on Pickering-emulsification, templating of (sacrificial) particles, or the amphiphilicity-driven capsule formation from polymer-grafted colloids. And even though these diverse synthesis techniques rely on different assembly principles, the resulting structures feature one concurrent characteristic: a shell formed from one or more closely packed layers of colloidal particles.

Advanced Ceramics, Department of Production Engineering & MAPEX Center for Materials and Processes, University of Bremen, 28359 Bremen, Germany. E-mail: bollhorst@uni-bremen.de

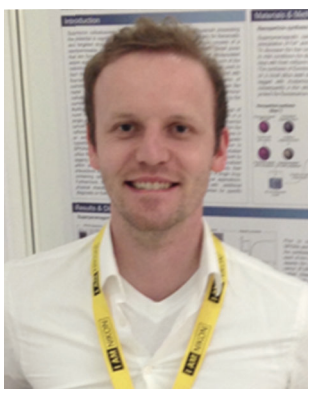

Tobias Bollhorst

Tobias Bollhorst is currently a PhD student at the Department of Production Engineering at the University of Bremen. He received his MSc from the University of Bremen in 2012 and his BSc in Materials Science from the Technical University of Berlin in 2010. His research is focused on the synthesis and surface functionalization of inorganic and polymeric nanoparticles, nanoparticle self-assembly, and colloidal particles for drug delivery.

Kurosch Rezwan

Kurosch Rezwan is a professor of Advanced Ceramics at the University of Bremen. He earned his Materials Science and Engineering Diploma (2001) and PhD degree (2015) from the ETH Zurich in Switzerland. Subsequently, he was a postdoctoral fellow at the Imperial College of Science and Engineering in London, before he joined the Faculty of Production Engineering Department at the University of Bremen in 2006. His research focuses on the interaction of advanced ceramics at the biointerface for biomedical and biotechnological applications.

Generally, micro- and nanoscaled capsules, which have been of intense research interest for many decades, comprise an organic, metallic, or inorganic shell to separate themselves from the surrounding environment and to protect a solid, liquid- or gas-filled interior. Such structures may be used for the encapsulation of a wide variety of compounds, including; pharmaceuticals,[1] nutrients,[2] catalysts,[3,4] or fragrances.[5] Until recently, the outer layer of nano- and microcapsules has mainly been utilized for the controlled interaction with its environment and for the protection and release of encapsulated cargo. Here, the outer layer functions either as a non-, partially, or highly permeable membrane. However, lately this paradigm is shifting and the shell itself is subjected to significant engineering efforts, with the goal to add distinct morphological, chemical, or physical properties; increasingly often by taking advantage of specific interactions of colloidal particles in the shell of a nano- or microcapsule. Utilizing modular colloidal building blocks to form one or more densely packed layers of a capsule's shell can lead to unprecedented material properties and may be advantageous in comparison to conventional encapsulation structures.

For instance, liposomes[6–8] and polymersomes,[9–11] artificial vesicles formed from natural and synthetic amphiphiles (phospholipids or block-copolymers), have been successfully developed for the entrapment and transport of active ingredients and play a critical role *e.g.* in the biomedical field for targeted pharmaceutical delivery. To further improve and to meet the growing demand for new multifunctional vesicular structures, a dense loading of the membrane of liposomes or polymersomes with nanoparticles or the self-assembly of capsules with a densely packed shell of colloidal particles can lead to advanced material properties. By carefully selecting the types of the shell-forming colloidal particles tailor-made exploitable characteristics can be achieved within such vesicle-like capsules.

In analogy to liposomes and polymersomes, these structures are often described as colloidosomes,[12] after this term was coined for a distinct type of capsule with a shell of densely packed colloidal particles. However, it has come to our attention that the term 'colloidosome' may not be the most ideal match for the description of spherical structures with colloidal particle shells. The term was initially introduced to solely describe Pickering emulsion-based capsules, but was recently also used for capsules based on other assembly routes, *e.g.* template-based structures.[13,14] In contrast, other terms were introduced by different authors who may have felt that their structures did not satisfy the original colloidosome definition, *e.g.* 'nanoparticle vesicles',[15] 'nanoparticle-stabilized nanocapsules',[16] or 'raspberry-like nanocapsules'.[17] This, and a clear evidence of a lack of cross-citation of the herein reviewed fragmented research fields, calls for a more general term that unifies the herein reviewed capsules. This would also greatly simplify the review of the literature from this field in the future. We think that the previously introduced term 'colloidal capsule'[18] fulfills the description of all types of capsules with a closely packed shell of colloidal particles more clearly. Hence, we advise the future use of this term to unify this research field.

Since the pioneering works by Caruso and Möhwald *et al.*,[19] Dinsmore and Weitz *et al.*,[12] and Nie and Kumacheva *et al.*,[20] research on colloidal capsules has gained substantial momentum and shows great promise for their application in a wide range of fields, such as drug delivery,[21] catalysis,[22] energy storage,[23] or photonics.[24,25] The successful implementation of these colloidal capsules will strongly depend on the possibility to precisely control structural characteristics, such as size, morphology, and surface chemistry of the capsule itself as well as the shell-forming building blocks, and will further depend on the mechanical stability, shell permeability, monodispersity, and biocompatibility of the resulting colloidal capsule.

Recently, an increasing research interest has been dedicated to the novel physical features that may be derived from forming a closely packed spherical shell from modular colloidal building blocks. Here, plasmonic near-field coupling promoted by the accumulation of gold nanoparticles,[26,27] the enhancement of various bioimaging techniques by *e.g.* utilizing the distinct superparamagnetic properties of iron oxide nanoparticles,[28] the decreased fluorescence intensity proximity quenching of fluorophore-doped core–shell silica particles,[29] or the integration of different nanoparticles with distinct functionalities in a single capsule[30,31] underscore just a few functionalities of such novel nano- and microcapsules. Beyond the utilization of these aforementioned modular building blocks with specific physical properties, building blocks with unique morphological and biological characteristics from the materials and life sciences fields have also been employed to form densely packed shells of colloidal particles. These include *e.g.* cubical metal organic frameworks,[32] mesoporous silica particles,[33] janus particles,[34] nanodiamonds,[35] carbon nanotubes,[36] nano-/microrods,[37,38] as well as polymersomes,[39,40] enzyme-loaded liposomes,[41] or viruses (bionanoparticles).[42] Furthermore, proteins are also being intensively explored as shell-forming biological building blocks, bringing about the nascent field of proteinosomes.[43] These protein capsules, representing a special class of so called protocells,[44–47] may be

Michael Maas

Michael Maas is a senior scientist at the Advanced Ceramics group at the University of Bremen. He received his diploma in chemistry in 2005 and completed his PhD in Physical Chemistry in 2008 at TU Dortmund. He then spent two years as a postdoc at Stanford University. His research focuses on the colloidal assembly of nanostructured materials from nano-sized building blocks, (bio)-molecules and minerals. His work includes fundamental research on thin films for the formation of multifunctional colloidal capsules, utilizing biomineralization strategies for designing biodegradable nanocarriers, and exploring assembly and functionalization techniques for the preparation of anisotropic and patchy nanoparticles.

utilized as a tool for the investigation of the early origin of primitive cell-like structures.[48] Hence, the inclusion of functional building blocks, particularly through specific nanoparticles, is inherent to this colloidal capsule platform and one of the main features of these structures. Furthermore, a strong focus in colloidal capsule research lies in pushing the structures ever closer towards biomedical applications, specifically for parenteral drug delivery, bioimaging and hyperthermia treatment. Here, the main challenges were found in miniaturization[16,49,50] of the structures to nano-scaled sizes with tailor-made pharmaceutical agent release[51] and controlled capsule disassembly, combined with particle clearance from the body *in vivo*.[52]

In the following sections we will review and discuss recent advances of the varying synthesis strategies of forming colloidal capsules, the exploitation of various building blocks with different chemical, physical, and morphological properties, capsule miniaturization, and their potential utilization for bionanotechnology applications. It should be noted that the structures described here are clearly to be distinguished from colloidal/nanoparticle clusters[53,54] which represent another class of supraparticles. The goal of this review is to give a comprehensive overview on the recent progress in the field of nano- and microcapsules with colloidal particle shells and closely related structures. Although the majority of the herein discussed papers have been published in the last 10 years, we will also discuss seminal papers that defined a subfield of colloidal capsule research and preceded the bulk of the publications from the last years. We will start the discussion by introducing the different methods for the creation of colloidal capsules and nanoparticle membrane-loaded vesicles. Thereafter, we categorize the capsules based on their size and the building block materials. The review will then close with an overview of recent colloidal capsules for biological applications, including a critical discussion on whether such structures should be considered for in-human use.

2. Strategies for the synthesis of colloidal capsules

Various approaches for the synthesis of spherical structures with densely packed colloidal particle shells have been investigated in the past two decades. We categorize these into their four major themes, *i.e.* their Pickering emulsion-based synthesis (Section 2.1),

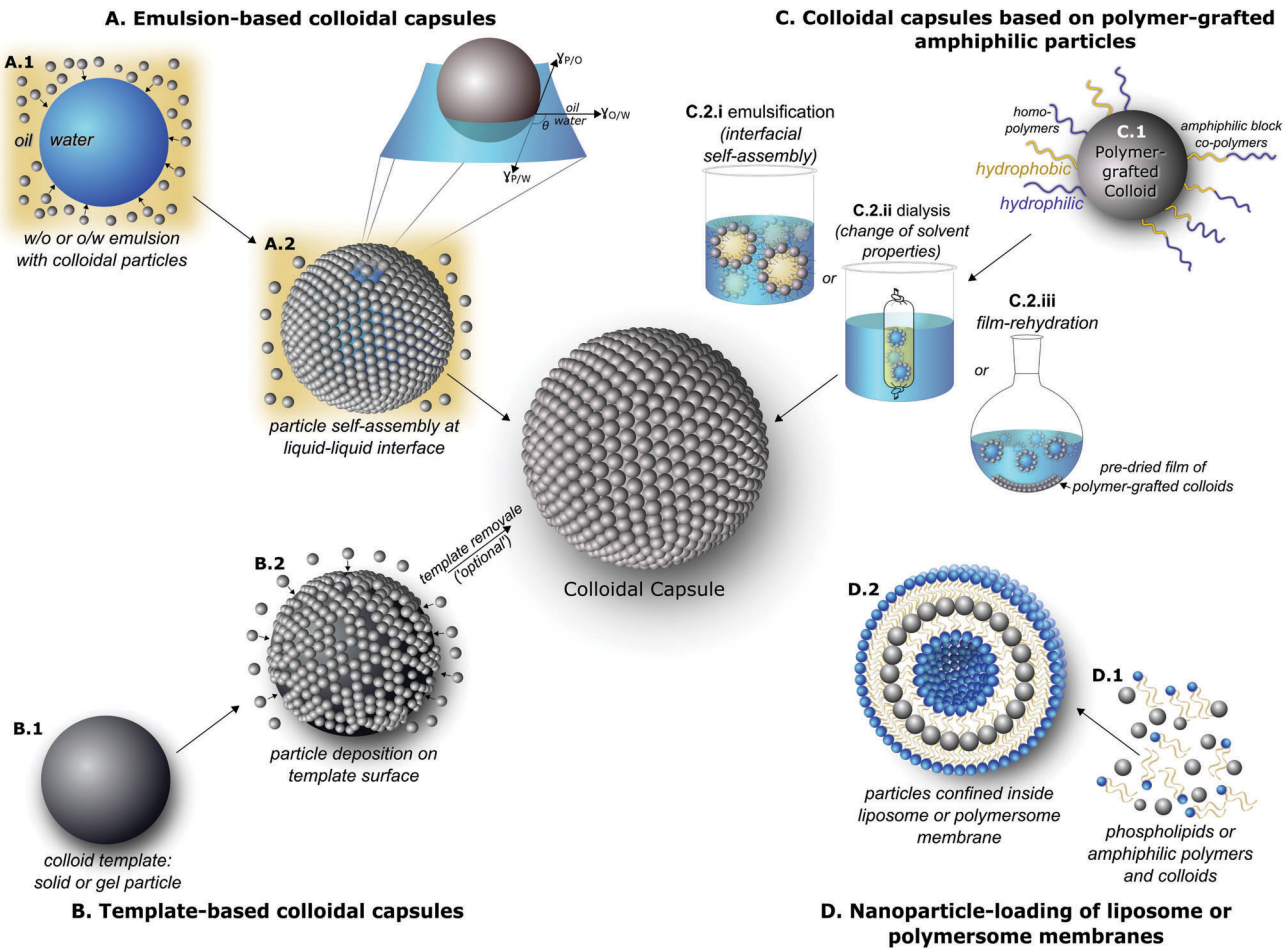

Fig. 1 Overview of utilized routes for the formation of colloidal capsules: (A) emulsion-based colloidal capsules *via* interfacial assembly of particles at the oil–water interface of droplets; (B) colloidal capsules formation *via* templating against (sacrificial) particles; (C) colloidal capsule synthesis *via* amphiphilicity-driven self-assembly of polymer-grafted nanoparticles; (D) dense nanoparticle loading of the membrane of liposomes/polymersomes.

the deposition and formation of densely packed colloids on template particles (Section 2.2), the amphiphilicity-driven self-assembly of polymer-brush functionalized colloids to 'nanoparticle vesicles' (Section 2.3), and the closely related field of liposomes and polymersomes with nanoparticle-loaded membranes (Section 2.4). The formation of these structures is based on bottom-up self-assembly processes of systems usually forced into a non-equilibrium state which are directed towards a thermodynamic minimum-energy state. The synthesis routes will be introduced and discussed in sequence of their historical appearance in the literature.

2.1 Emulsion-based synthesis routes for colloidal capsule assembly

Beginning in 1996, Velev *et al.*[55–57] published pioneering works on the formation of supraparticles from oil–water emulsions, utilizing latex particles for the formation process. The latexes were sulfated or amidined to induce negative or positive surface charges to perform an interaction-tailored colloidal assembly in the particle/droplet system. This was followed by Dinsmore's 2002 paper who accomplished a further stabilization of these Pickering[58]–Ramsden[59]-emulsion-capsules which enabled their transfer to a fresh water phase resulting in water dispersed capsules with an aqueous core.[12]

In general, the original synthesis route for the formation of colloidal capsules *via* Pickering-emulsions, involves three major steps, which are depicted in Fig. 1A(A.1) the emulsification of a water-in-oil phase, with colloidal particles either dispersed in the oil or water phase, Fig. 1B(B.1) the confinement of the colloidal particles at the emulsion droplet oil–water interface, and finally a transfer of the stabilized emulsion-based capsule to a fresh continuous phase, usually water. Fig. 2 shows an example of one of the first dried 'colloidosomes', which was assembled from 0.9 μm sized polystyrene (PS) particles, whilst the PS particles were slightly sintered to form a stable shell.[12]

A great number of research papers and several reviews[18,60,61] have since been published on emulsion based colloidal capsules, including a recent review by Thompson *et al.*[62] which we like to point out for secondary citations. This review particularly summarizes the key routes for the stabilization of the shell of the particle-stabilized emulsion droplet, *i.e.*, thermal annealing (shell sintering),[12,63,64] gel trapping,[65–67] covalent cross-linking,[68–70] and the polymerization of either the inside or the surface of the emulsion droplet.[71–74]

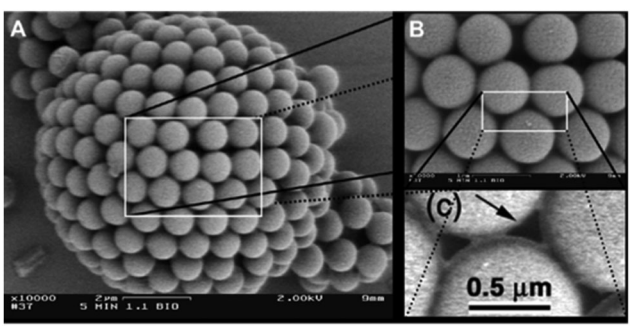

Fig. 2 Initial 'colloidosome', formed from polystyrene particles (From ref. 12. Reprinted with permission from AAAS (2002).).

2.1.1 Particle confinement at the liquid–liquid interface.

To successfully synthesize colloidal capsules *via* Pickering emulsification, a confinement of colloidal particles at the liquid–liquid interface of the emulsion droplet is a major prerequisite. The self-assembly of colloidal (nano-)particles at liquid–liquid interfaces is driven by the reduction in Helmholtz free energy, where the fluid–fluid surface area is replaced with particle–fluid surface area.[12] Additionally, the tendency for colloidal particles to adsorb and stay at the interface depends on various factors, including the particles surface chemistry, which influences the particles wettability by the oil and water phase, and the particles radius (r). Fig. 1B.1 (zoom-in) schematically depicts a particle confined at the emulsion-droplet interface, including the contact angle (θ) of the particle with the interface, which depends on the surface free energies (interfacial tensions ($\gamma_{i/j}$)) at the particle–water (P/W), particle–oil (P/O) and oil–water interface (O/W).[75] The energy change (ΔE) for one particle confined at the interface, reducing the total free energy, was initially introduced by Pieranski[76] and has been greatly used by other authors for the description of particle behaviour at liquid–liquid interfaces since then:[75,77,78]

$$\Delta E = -\frac{\pi r^2}{\gamma_{O/W}}\left[\gamma_{O/W} - \left(\gamma_{P/W} - \gamma_{P/O}\right)\right]^2$$

Hence, with decreasing particle sizes, ΔE is decreased as well and approaches similar values as k_BT (k_B: Boltzmann constant) making the colloidal particles more susceptible to momentum transfer from solvent molecules. Consequently, for very small particles ($d \ll 50$ nm) and depending on particle wettability by either phase, this can result in diminished confinement at and possible detachment of particles from the liquid–liquid interface due to thermal fluctuations.[78] This makes the emulsion-based synthesis of miniaturized colloidal capsules with small particles more complex.

Significant research interest is dedicated to the study and advancement of the adsorption and desorption of colloidal particles at fluid interfaces. However, the elucidation of the full details of this field would go well beyond the scope of this review, as why we would like to redirect the interested reader to the books by Binks[75] and Ngai *et al.*[79] (which both include detailed mathematical descriptions) and recent research studies,[80–91] novel measurement techniques,[92–95] and recent reviews[96–105] for further information.

2.1.2 Microfluidic-based colloidal capsule synthesis.

The formation of colloidal capsules *via* classical emulsification approaches tends to lead to a fairly broad size range of the capsule diameters in a single sample. To decrease the rather high polydispersity observed in emulsion-based capsules, various groups investigated the utilization of microfluidics to further control the synthesis of these structures. For instance, Subramaniam *et al.* utilized a three-channel hydrodynamic focusing device to assemble 4 μm polystyrene colloids to a "jammed shell".[106] Similarly, Utada and Weitz *et al.* used microcapillaries to control the formation of double emulsions,[107] which were later used for capsule synthesis. Within the double-emulsion synthesis route, hydrophobic particles

are usually dispersed in the organic phase of a water-in-oil-in-water double-emulsion, and the evaporation of the organic solvent then leads to the final colloidal capsule formation.[108] This method has since been extended by Weitz and co-workers to form nonspherical colloidal capsules,[109] to incorporate a Pluronic polymer core for thermally switched release,[110] for the generation of stimuli-responsive capsules formed from poly(*N*-isopropylacrylamide) particles,[111] and by Sanders and Studart *et al.* by utilizing nanoparticles with magnetic, photocatalytic, and potentially biocompatible functionalities in the shell.[112] Additionally, Park and Kumacheva *et al.* synthesized closely related structures, by assembling poly(styrene-*co*-acrylic acid) particles on CO_2 bubbles.[113] In a follow-up report the process was further tailored by using a temperature-dependent dissolution of CO_2.[114] Nie and Kumacheva *et al.* also investigated an ''inside-out'' approach by emulsifying a dispersion in a particle-free continuous phase.[115] Besides this, Abell *et al.* used polymer–gold nanoparticles to also synthesize micrometer-sized colloidal capsules.[116] Albeit, two challenges within this synthesis route remain, the first being a controlled miniaturization of the final structures, which has been approached by Nie *et al.* with block-copolymer (BCP)-tethered colloids,[117,118] and secondly an increase of the overall yield and throughput of this method.

2.2 Templated synthesis of colloidal capsules

In 1998 Caruso laid ground for the field of the templated formation of colloidal capsules by first reporting the sequential adsorption of SiO_2 nanoparticles and oppositely charged polyelectrolytes on polystyrene (PS) template particles[119] *via* electrostatic interactions. Shortly afterwards, this process was advanced by etching the PS particles and creating hollow capsules[19] (Fig. 3). This layer-by-layer (LbL) templating approach allows for a precise control of the thickness of the shell by depositing a defined number of layers on the template, which at the same time also determines the capsule's size and morphology. Various template structures have been investigated, including inorganic and hard or soft polymeric colloids. Since the introduction of this technique, numerous excellent reviews on layer-by-layer templating routes have been published, including articles by Caruso *et al.*[120,121] and a review by X. Lou *et al.*,[122] which we would like to point out for secondary citations. Also discussing various types of capsules and other superstructures with non-colloidal particle shells. For means of a simpler overview, we divided this section into hard (Section 2.2.1) and soft (Section 2.2.2) template-based structures.

2.2.1 Hard templates. The initial synthesis route utilizing hard colloids as templates is illustrated in Fig. 3 and consists of polymers (polyelectrolytes) (1) and nanoparticles (2) which are sequentially assembling on the template particle *via* electrostatic interactions. This may be followed by either a solvent-induced dissolution of the template core or by calcination, which, besides the dissolution of the template particle, usually also removes the polyelectrolyte layers, only leaving behind the self-assembled nanoparticle shell. In 2000, Caruso published a concept paper further elucidating this process.[123] Recently, Caruso *et al.* utilized polyphenol-conjugated colloidal building blocks, which, among the formation of other colloidal superstructures,

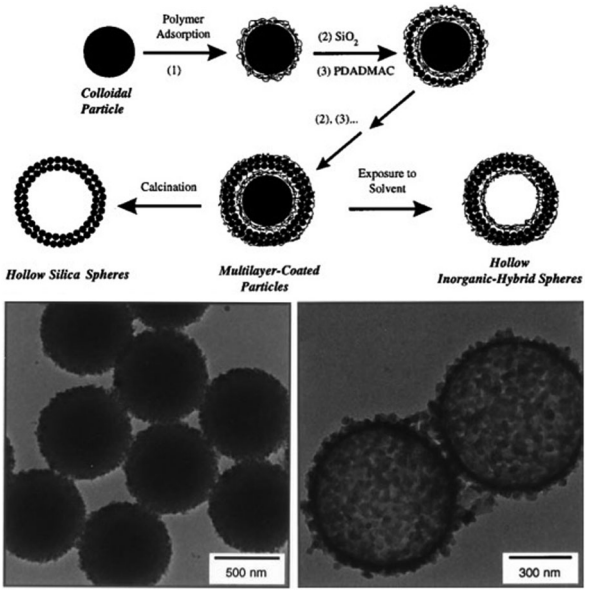

Fig. 3 (top) Template based synthesis route; (bottom) colloid templated structures before (left) and after (right) core etching. (From ref. 19. Reprinted with permission from AAAS (1998).)

could be assembled on spherical PS templates for colloidal capsule formation. After the assembly process, the shell-forming building blocks were linked and stabilized *via* metal–phenol complexation utilizing different metal ions.[124] Another templating route also without using polyelectrolytes, solely based on the deposition of PS nanoparticles onto silica microspheres, was introduced by Fleming and co-workers. Here, the PS particles are sintered prior to the etching of the silica template, leading to a fused surface.[125] In addition to the direct use of nanoparticles for the assembly on a colloidal template, ionic precursor solutions have been investigated as well, to initiate nucleation and growth of nanoparticles on the template. For instance, Kim *et al.*[126] coated thiolated silica particles with a palladium precursor and induced a formation of approx. 10 nm-sized Pd nanoparticles, and subsequently etched the core with hydrofluoric acid (HF) to retrieve hollow capsules.

Besides the use of solid colloidal particles for the formation of the capsule's shell, proteins have also been employed as building blocks. Merz and Caruso *et al.* have prepared nano- and microcapsules with a protein building block shell from human serum albumin (HSA) on nonporous silica templates,[127] doxorubicin-conjugated capsules using various different types of proteins,[128] and nano-scaled HSA based capsules with MRI and gene-silencing functionalities by using a mesoporous silica template for encapsulation prior to the templating step.[129]

2.2.2 Soft (gel) templates. Along with hard particle templates, ''soft'' gel-like particles have also been studied significantly for the formation of a closely packed layer of colloidal particles on their surface. In many works, a full coverage of the soft/gel-like templates is achieved by shrinking the bulk template after covering its surface with a certain amount of particles. In 2007, Kim and Weitz *et al.* used temperature sensitive microgel templates with sizes ranging from 50–60 μm which were based on poly(*N*-isopropylacrylamide) (PNIPAm). The PNIPAm particles were

first sparely covered with smaller polystyrene particles and then jammed by shrinking the PNIPAm template to achieve a closely packed particle coverage on the surface.[13] A very similar strategy was shortly later applied by Karg *et al.* for smaller poly-(NIPAM-*co*-allylacetic acid) nanogel templates featuring final sizes of approx. 320 nm. The nanogels were templated with gold-nanorods to investigate their shifted resonance peak, induced by the near-field plasmonic coupling of the Au rods.[37] Gawlitza and Karg *et al.* later on also used spherical gold nanoparticles for a more sparse decoration of PNIPAm microgels.[130] Additionally, PNIPAm was also used as a template material by Du *et al.* who added a pre-silanized aqueous TEOS solution (silica sol) to form a closed shell of silica particles on PNIPAm aggregates.[131] In contrast to these previous reports utilizing PNIPAm, we recently investigated chitosan nanoparticles as substrates for the adsorption of 5 nm and 15 nm fluorescent SiO_2 particles with the intention to increase the biocompatibility of the template material.[132] Another approach was reported by Destribats *et al.* who adsorbed CTAB-coated silica particles on molten wax droplets, which were in turn able to release the wax upon heating to approx. 44 °C.[133] The release of various agents from microgel templates enclosed with colloids was shortly afterwards examined systematically by Rosenberg and Dan and co-workers.[134–136] Recently, Huang *et al.* reported a novel approach by templating vesicles formed from poly(3-ethyl-3-oxetanemethanol)-PEO block-*co*-polymers by *in situ* formation of gold, silver, or platinum nanoparticles on the vesicle surface,[137] which is however different from the works described in the next section of colloidal capsules formed from polymer-grafted particles.

2.3 Amphiphilicity-driven colloidal capsule self-assembly from polymer brush grafted nanoparticles

Two decades ago, Eisenberg *et al.* pioneered the self-assembly of amphiphilic block copolymers into various morphologies, including spherical vesicular structures.[9,138,139] Shortly after, the term polymersome was coined by Disher *et al.*[10] to describe polymer vesicles, in analogy to liposomes. Diblock or triblock copolymers are now ubiquitous and widely used for the synthesis of polymersomes, by making use of the hydrophobic effect[140] which induces a water-mediated association of the hydrophobic polymer units, while the hydrophilic units protrude towards aqueous media.[141] Numerous reviews have since been published on polymersomes.[11,142,143]

Recently, the principle of amphiphilicity-driven self-assembly has been transferred to colloidal particles for the formation of capsules with colloidal particle shells. Among this, three routes have mainly been used to control the self-assembly of amphiphilic polymer-grafted particles to vesicle-like capsules, including emulsification by preparing oil-in-water emulsions and subsequently evaporating the organic solvent (Fig. 1C.2.i),[52] dialysis from a selective solvent against water with the intention to slowly change the solvent composition (Fig. 1C.2.ii),[144] or by drying a thin-film of the particles on the wall of a vial and then rehydrating the film (Fig. 1C.2.iii).[145] Due to various similarities to molecular amphiphile based vesicles – liposomes and polymersome – these structures are often termed 'nanoparticle vesicles'.[15] However, their overall structural build-up and inherent properties are correspondent to colloidal capsules.

Following a first report on the assembly of polymer-conjugated nanoparticles to spherical aggregates,[146] in 2006 Zubarev *et al.*[147] and in 2007 Nie *et al.*[20] published the first works on the three dimensional self-assembly of polymer-brush functionalized colloids to hollow tubular and spherical structures. Zubarev *et al.* grafted a V-shaped PS_{40}–PEO_{50} amphiphile to the surface of 2 nm gold or silver particles and then induced the self-assembly by first slowly adding a certain amount of water to a dispersion of the particles in organic media (*i.e.* DMF or THF) and secondly dialyzed this mixture against water to remove the remaining organic media. Depending on the NP concentration and organic solvent either worm-like or vesicular assemblies were reported by the authors. Similarly, 'Pom-pom'-like gold nanorods (Fig. 4 – left), coated with CTAB and conjugated on each end with hydrophobic polystyrene brushes reported by Nie *et al.*, showed, in analogy to ABA block-copolymers, a self-assembly to structures with varying geometries, including vesicle-like capsules (Fig. 4 – right), which depended on the solvent composition. Grubbs mainly attributed this solvent-tuned self-assembly process of the amphiphilic-like colloids to a non-thermodynamically stable 'trapping' of the structures based on a solidification of the polymer domains in 'kinetically stable amorphous phases'.[148]

Since these two pioneering reports, an especially strong focus has laid on polymer-brush functionalization of gold nanoparticles with their subsequent self-assembly to nanoparticle vesicles. Due to the distinct association of the hydrophobic units with each other, most of these vesicle-like structures feature a closed hydrophobic polymer membrane layer on their surface, allowing for an efficient encapsulation of a wide variety of active agents. The main focus in this field has since been on forming vesicles from nanoparticles with either diblock, mixed, or Janus[149] polymer brush architectures. Nie *et al.* as well as Song *et al.* have published a series of papers, including various recent reviews by each,[26,27,150,151] bringing significant progress to this field, with a strong focus on utilizing these vesicles for biomedical applications. Nie and co-workers concentrated on grafting gold

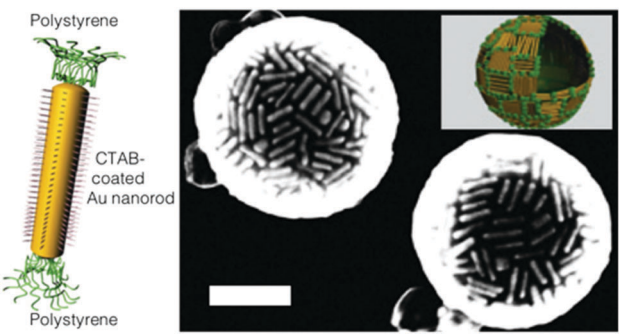

Fig. 4 (left) Illustration of a hydrophilic CTAB-mediated gold nanorod with hydrophobic polystyrene brushes at its ends; utilized for nanoparticle vesicle formation, represented in the SEM micrograph (right). The inset in the SEM micrograph schematically showcases the arrangement of the Au nanorods in the capsule shell (Reprinted with permission from Macmillan Publishers Ltd: [Nature Materials] ref. 20, copyright (2007).).

nanoparticles with block-copolymers, whilst Song and co-workers laid their focus on grafting gold nanoparticles with a mixed homopolymer architecture (see Fig. 1C.1).

Song *et al.* used combinations of PEG with either PMMA/PMMAVP,[49,152] PNBA,[153] PLA,[154] or PLGA[52,155] for vesicle formation, conjugating the particles either *via* a two step grafting-"To" and subsequent grafting-"From" approach, or by concurrently bonding pre-synthesized hydrophilic and hydrophobic homopolymers onto the nanoparticles *via* grafting-"To". Song *et al.* also recently published a comprehensive summary of the various protocols for the synthesis and characterization of the previously reported polymer-grafted gold particles and self-assembled capsules.[156]

Following their work on the self-organization behaviour of PS-grafted 'Pom-Pom'-like gold nanorods,[20,157,158] Nie *et al.* mainly focused on conjugating gold colloids with block copolymers. When utilizing PEO_x-*b*-PS_y BCPs, the tendency of the polymer-grafted colloids to form vesicles was observed to depend on a combination of the size of the colloidal particles and the length of the hydrophilic and the hydrophobic polymer units.[15] Submicron-sized vesicles were assembled from nanoparticles with a flower-like[145] or spherical[144,159] morphology and larger, micron-sized vesicles,[160] were formed from gold-nanrods. The capsules could be synthesized using varying assembly methods and PEO-*b*-PS BCPs of different lengths, and allow for a near-infrared light triggered release of encapsulated cargo due to a red shift of the plasmon resonance bands. In addition to this light-triggered disaggregation, light (ultra violet) has also been used to assemble vesicles from various thiol-capped inorganic nanoparticles by oxidation of mercapto containing ligands which supposedly induces a rearrangement of the ligands.[161] By further controlling the grafting density of the BCPs on gold nanoparticles, vesicles with string-like assemblies could be formed.[162,163] In another report, the hydrophobic PS block was substituted for a biodegradable poly(ε-caprolactone) block for increased biocompatibility.[50]

In addition to Song's and Nie's works, Förster *et al.* described the spontaneous self-assembly of hydrophobic CdSe/CdS particles, also featuring a hydrophilic PEO chain, into various structures, including large vesicles. They compared the self-assembly behaviour of the particles to that of surfactants and lipids.[164] Moffitt *et al.* coated CdS NPs with a PS-*b*-PAA-*b*-PMMA triblock copolymer and were also able to form vesicle-like assemblies.[165] Hu *et al.* synthesized polymer-grafted nanoparticles with a Janus-like brush architecture, by binding the central block of an amphiphilic triblock copolymer (PEO-*b*-P(LAMP-*co*-GMA)-*b*-PS) to 2.0–3.8 nm sized gold nanoparticles. The particles assembled to various structures, including vesicles that are believed to form a polymersome-like double-layer of particles.[149] Overall, the here described colloidal capsules feature some physico-chemical similarities to the structures reviewed in the following section. However, in the next section the colloidal building blocks are not functionalized with polymer brushes to mimic the behavior of amphiphilic molecules, but instead conjugated with hydrophobic ligands to enable their dense confinement in a vesicle's membrane formed from free lipids or block copolymers.

2.4 Liposomes and polymersomes with nanoparticle-loaded membranes

With the first works on liposomes dating back to the 1960s by Bangham *et al.*,[166–168] liposomes are now omnipresent and have found their way into numerous consumer applications and represent a crucial instrument in the pharmaceutical field.[169] A large amount of research was and still is devoted to the functionalization of liposomes. We are aware of a myriad of excellent studies in the field of liposomes/polymersomes in general and vesicle–nanoparticle hybrids specifically, for instance previously reviewed by Al-Jamal *et al.*[170] as well as Amstad and co-workers.[171] However, we will here exclusively concentrate on amphiphile-assembled vesicles which resemble a colloidal capsule by featuring a closely packed spherical layer of nanoparticles inside the membrane of liposomes or polymersomes, as depicted in Fig. 1D.2.

2.4.1 Liposomes with nanoparticle-loaded bilayers. In 2003 Cha *et al.* demonstrated the incorporation of quantum dots in the shell of poly-L-lysine vesicles.[172] Following this and other pioneering works of sparely loaded particles in a vesicle membrane,[173–185] in 2010 Rasch *et al.* were the first to assemble closely packed nanoparticles inside the lipid bilayer of liposomes from phosphatidylcholine and thoroughly characterized them *via* cryo-TEM (Fig. 5).[186] Here, dodecanethiol-coated gold nanoparticles were used for the membrane loading, where the core was merely 2 nm in diameter. The small particle size was reportedly chosen to inhibit lipid adsorption around the nanoparticle and to reduce disrupting effects to the bilayer, which might be induced if larger nanoparticles are intended to be loaded into the membrane. The dodecanethiol-coated NP were loaded inside the membrane of the vesicles using a synthesis route based on a combination of film-rehydration and mini-extrusion, leading to vesicle sizes as low as 50 nm. Interestingly, only vesicles with either no particles or a closely packed monolayer of particles were formed. In a follow-up report, Rasch *et al.* further examined parameters that lead to vesicle disruption.[187]

The particle size in relation to the membrane thickness, which is usually in the range of 5 nm, plays a pivotal role regarding the particle confinement inside the bilayer of liposomes. Ultrasmall particles with diameters below 2 nm form densely packed layers, particles with diameters between 2 and 6.5 nm tend to disrupt the bilayer and may create small cavities in their close periphery or bridge adjacent liposomes, whilst particles above 6.5 nm tend to adsorb the lipids, which inhibits vesicle formation and leads to micellization.[188] For a thorough discussion on the interaction of nanoparticles with liposome and polymersome membranes we recommend the review by Schulz and co-workers.[189]

Besides embedding Au NP in the lipid bilayer of liposomes, a strong focus in this field also lays on the incorporation of ultra small iron oxide nanoparticles (USPIONs) inside the bilayer, which accordingly fall into the field of magnetoliposomes.[190] Amstad *et al.* incorporated palmityl-nitroDOPA stabilized <5.5 nm iron oxide NPs in the membrane of liposomes from 2-dis-tearoyl-*sn*-*glycero*-3-phosphocholine (DSPC).[191] Using an alternating magnetic field to heat the embedded iron oxide NP, the authors were able

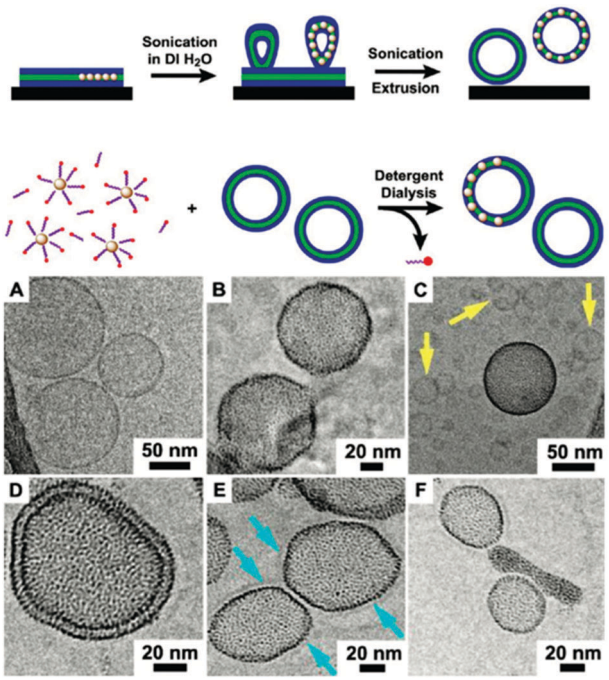

Fig. 5 (top) Illustration of the initially reported synthesis routes for densely nanoparticle-loaded liposome membranes; (top) either *via* the rehydration of lipid Au NP thin film followed by extrusion through a 50 nm-sized filter, or (bottom) by dialyzing pre-formed and unloaded liposomes in combination Au NP and detergents. (bottom) Cryo-TEM micrographs of (A) unloaded vesicles and (B–F) Au NP-loaded liposomes with the particles embedded in the phospholipid bilayer (Adapted with permission from ref. 186. Copyright (2010) American Chemical Society.).

to change the permeability of the membrane, allowing for a controlled release of an encapsulated fluorescent dye from the liposomes. A similar process was later examined by Qiu and co-workers.[192,193] Furthermore, Katagiri *et al.* also used Fe_3O_4 NP in the lipid bilayer to synthesize magnetoresponsive liposomes which were additionally conjugated with thermosensitive polymers.[194]

2.4.2 Polymersomes with nanoparticle-loaded membranes. Analogous to liposomes, polymersomes also possess particle incorporation capacities within their membrane and are gaining significant momentum as multivalent nanocontainers. For instance, Wei *et al.* synthesized HOOC–PEG–PLA BCP based polymersomes, which were first loaded with a dense spherical layer of 6 nm-sized hydrophobic Fe_3O_4 particles, and subsequently conjugated with an antibody using EDC-NHS cross-linking chemistry.[195] The polymersomes were then used as novel immunosensors. Similarly, Sanson and Lecommandoux *et al.* incorporated <8 nm γ-Fe_2O_3 NP in the membrane of poly(trimethylene carbonate)-*b*-poly(L-glutamic acid) (PTMC-*b*-PGA) based polymersomes using a nanoprecipitation approach.[196] In a follow-up report, Oliveira and Lecommandoux *et al.* used these PTMC-*b*-PGA vesicles as stimuli-responsive magneto-polymersomes for the local induction of a hyperthermia effect in tissue in close proximity to the polymersome membrane.[197] Furthermore, various reports in this magneto-polymersome field were made by Park *et al.*, who achieved a control of the architectural build-up of magneto-polymersomes and nanoparticle–micelle hybrids (magneto-micelles). The structures were formed using poly(acrylic acid) and PS BCPs and the resulting morphology could be controlled by varying the relative volume ratio of the hydrophilic and the hydrophobic blocks.[198] Recently, Park *et al.* also accomplished a precise tailoring of the size of magneto-polymersomes and thoroughly characterized the morphological properties of the structures. The authors were able to control the size of the polymersomes via the incorporation of iron oxide particles with different sizes.[199] Additionally, Park *et al.* were able to create multicompartment polymersomes by utilizing 11-mercapto-1-undecanol-capped gold nanoparticles for the membrane loaded polymersome synthesis.[200] Interestingly, it was also recently reported that the combination of PEG–PS BCP-tethered colloids and a second free amphiphile PS–PEO BCP led to the concurrent assembly of further Janus-like polymersome–nanoparticle hybrid structures, including (hemi-) spherical janus, disc-like janus, and patchy vesicle morphologies (Fig. 22).[201] In follow-up report, Nie *et al.* further advanced these janus vesicles by incorporating hydrophobic Fe_3O_4 NP along with Au NP grafted with PS-*b*-PEO inside the membrane of vesicles formed from free PS-*b*-PAA BCPs.[202]

3. Micron-sized colloidal capsules

Micron-sized colloidal capsules have been covered extensively in the scientific literature in the past decades and are usually more simple to synthesize and to characterize than their smaller submicron-sized siblings. Due to their larger size, there will most likely not be much reasoning to implement them in advanced applications. However, they are indispensable tools for the investigation of colloidal self-assembly phenomena at the micron-scale, allowing for a simple *in situ* visualization.

Most of the above described routes have been utilized to generate >1 μm colloidal capsules. However, there is clearly a great majority of structures created *via* the emulsion route in comparison to the other techniques. Since emulsion-based colloidal capsules are either themselves Pickering emulsions or a derivative of them, there are a myriad of structures formed and described in the literature based on this route. Hence, it would go well beyond the scope of this review to describe every structure ever generated and described in the available literature which is based on the Pickering-emulsion route. Besides recent reviews on Pickering-emulsions[61,203] and the recently published book by Bon and Ngai,[79] we like to again point out the review by Thompson *et al.*[204] and another review by Patra *et al.*,[18] which summarized a majority of structurally stabilized colloidal capsules from Pickering emulsions and we will refrain from describing the therein reviewed works in detail. Therefore, in the following section of micron-sized colloidal capsules, we will mainly focus our descriptions on recently reported structures with unique morphological and physical properties, formed from any of the above described synthesis routes.

3.1 Building blocks and colloidal capsules with distinct morphological characteristics

In the past few years a broad range of colloidal capsules with unique morphological characteristics have been reported

in the literature. Capsules were *e.g.* formed from cubical metal organic frameworks (MOFs) based on a solvothermal synthesis route (Fig. 6). Here, Pang and co-workers heated a precursor solution to 120 °C that eventually formed Fe-soc-MOF particles which then spontaneously self-assembled on emulsion droplets.[32] Further colloidal capsules also formed from MOFs and eventually termed by the authors as ''MOFsomes'' were prepared by incorporating spherical MOF particles into the surface of hollow polystyrene capsules.[205] Utilizing a one-pot synthesis route, Xu *et al.* formed homogeneous and 'particle-doped' (Fig. 7) colloidal capsules by assembling the shell-forming building blocks at a water–gas bubble interface. A precursor solution either containing a certain amount of phenol monomer, or a combination of the phenol monomer with $AgNO_3$ or $HAuCl_4$ led to the formation of a phenol formaldehyde resin (PFR) shell, giving rise to homogeneous Ag@PFR or Au@PFR colloidal capsules. When the authors added some pre-synthesized Ag@PFR particles to the initial reaction system they observed the formation of novel ''doped Ag@PFR-PFR colloidosomes''.[206] Further structures formed from a set of differently sized particles of silica or polystyrene microspheres and silica or titania nanoparticles were described by Cho and co-workers. By combining two particle types of different length scales, bimodal colloidal clusters were reported by the authors. Removale of larger PS particles *via* calcination at 500 °C then led to hollow colloidal structures (Fig. 8).[207] For more colloidal capsules with a patchy surface structure we recommend the recent review by Rozynek and Jozefczak.[208]

Besides these MOF-based and bimodal structures, a variety of capsules with oblong building blocks have been reported. Noble and co-workers first reported the use of microrods for the stabilization of a Pickering-like emulsion and subsequent capsule formation. They adsorbed SU-8 polymeric microrods at the interface of an aqueous agarose microgel which was intermediately washed with an ethanol–water solution and finally dispersed in pure water. To further retain the microrods in the shell, the authors stabilized the shell by using small amounts of glutaraldehyde to cross-link the shell-forming rods.[38] Similarly, Datskos *et al.* also used a Pickering-emulsion approach to form colloidal shells from silica microrods.[209] Vanadium pentoxide (V_2O_5) nanorods were formed by Cao *et al.* from a vanadium(III) acetylacetonate precursor.[23] Using a process based on the Kirkendall[210] effect Liu and Zeng formed ''Dandelion'' structures with a shell of ZnO nanrods.[211] Furthermore, the authors also investigated Dandelion-like hollow capsules with a shell of CuO nanoribbons[212] and smaller unidirectionally attached ZnO nanorods.[213] Hollow capsules with a shell of multi-walled carbon nanotubes (MWNT), termed as ''carbon nanotubosomes'', were synthesized by Paunov an co-workers. In their first work, the authors explored an emulsion-based approach[214] and in a second report templated aminated MWNTs against sulfated PS particles which were later dissolved in toluene.[36] In both approaches the MWNT shell was cross-linked with glutaraldehyde.

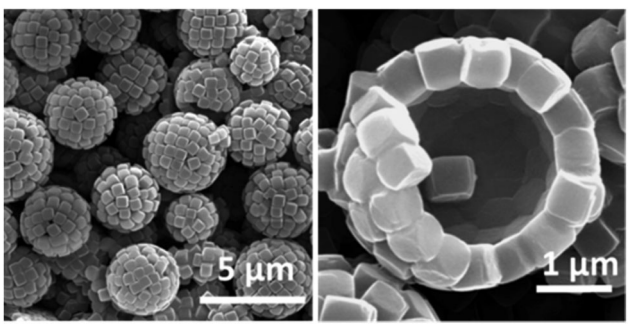

Fig. 6 SEM images of colloidal capsules prepared from metal organic framework building blocks (Reprinted (adapted) with permission from ref. 32. Copyright (2013) American Chemical Society.).

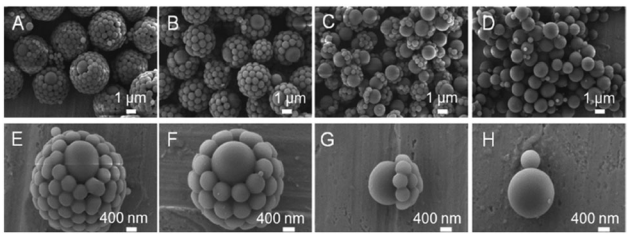

Fig. 7 SEM images of ''doped Ag@PFR-PFR colloidosomes (Reprinted with permission from ref. 206. Copyright (2013) American Chemical Society.).

Plate-like building blocks have also been utilized for the stabilization of Pickering-emulsions[215] and utilized in other approaches. For instance, Wang *et al.* formed $Ni(OH)_2$-based nanoflakelets on styrene-acrylic acid copolymer particles and retrieved hollow structures after dissolving the cores in toluene.[216] Subramaniam *et al.* synthesized semi-permeable capsules from natural clay montmorillonite building blocks by assembling the clay from water on gas bubbles.[217] Sander and Studart used double-emulsions prepared *via* microfluidics to assemble monodisperse capsules from 8–10 μm sized montmorillonite clay particles. In addition to these oblong- and plate-like shaped building blocks further particles with unique morphological properties for the formation of the capsule's shell include cross-linked polymersomes,[39] mesoporous silica particles,[33] or Janus particles.[34,218–221] A distinct kind of the latter anisotropic colloid type with a 'snowman-like' shape and hydrophobic and hydrophilic moieties, was recently explored by Evers *et al.* for colloidal capsule formation. Based on 'colloidal bond hybridization', defined by the authors as a redistribution of flexible surface groups of mutually attractive and deformable anisotropic particles, in analogy to bond hybridization, 3.7 ± 0.8 μm sized capsules were prepared.[222]

3.2 Distinct physical properties of building blocks and resulting colloidal capsules

Colloidal particles with distinct physical properties such as iron oxide nanoparticles with superparamagnetic properties and noble metal colloids with near-field plasmonic coupling characteristics have been significantly investigated to create tailor-made functionalities in micron-sized colloidal capsules. Taking advantage of adjacent particles in the shell of colloidal capsules is a unique characteristic of these structures and has allowed

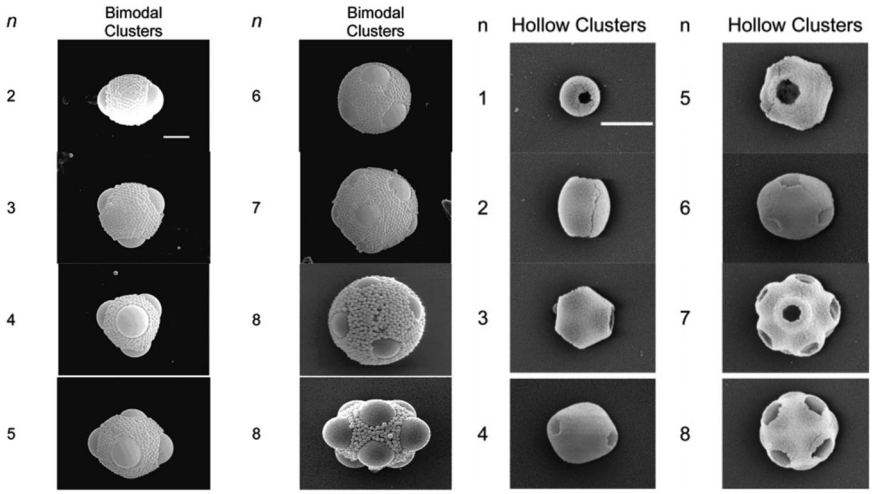

Fig. 8 Left: SEM micrographs of structures formed from two sets of silica particles (scale bar: 2 μm). Right: Structures formed from larger PS and silica NP after removal of PS particles *via* calcination. (Adapted with permission from ref. 207. Copyright (2005) American Chemical Society.)

the development of distinct material properties in colloidal capsules.

3.2.1 Colloidal capsules with magnetic nanoparticles. Duan *et al.* formed micron-sized colloidal capsules from hydrophobic iron oxide nanoparticles with different sizes (4.0, 5.0, and 8.0 nm). The authors dispersed 2-bromo-2-methylpropionic acid capped particles in toluene and then assembled the particles on emulsion droplets from pure water or from a heated aqueous agarose solution. Decreasing the temperature, and by that gelling the agarose core, led to a structural stabilization of the capsules. The resulting colloidal capsules could easily be washed by magnetic separation.[67] Based on a Cu(I)-catalyzed Huisgen click reaction, Rotello *et al.* cross-linked iron oxide nanoparticles at oil–water interfaces. Here, 11 nm-sized oleic acid-capped particles were functionalized prior to their assembly *via* a ligand-exchange reaction with alkyne and azide groups and led to capsules with diameters of 49 ± 15 μm.[223] In addition to iron oxide nanoparticles, Rotello and co-workers also used magnetic FePt particles for the creation of colloidal capsules. The FePt particles featured sizes of 7 ± 1 nm which were capped with terpyridine thiol groups and dispersed in toluene. Upon emulsification with an aqueous Fe(II) tetrafluoroborate hexahydrate solution, the particles assembled and formed a stable interconnected membrane at the droplet interface.[69] Sander *et al.* successfully increased the monodispersity of magnetic capsules *via* a microfluidic w/o/w double-emulsion approach. Here, the capsules were assembled from a combination of Al_2O_3 and Fe_3O_4 particles which were dispersed in an organic toluene phase with the surfactant sorbitan trioleate. The authors were able to track the movement of the capsule with a microscope, where a magnetic field rearranged the particles within the shell leading to Janus-like capsules.[112] Zhang and co-workers assembled magnetic colloidal shells from rod-like Fe_3O_4–SiO_2 Janus nanoparticles. Stemming from the superparamagnetic properties of the rod-like janus particles, the capsules could be aligned under a magnetic field (Fig. 9).[218] Furthermore, colloidal capsules formed *via* an emulsion-based synthesis were also created

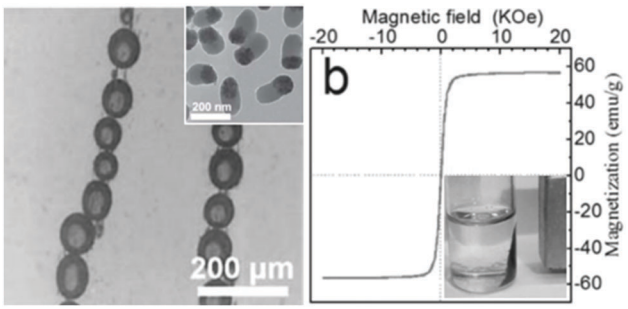

Fig. 9 (left) Emulsion-based capsules aligned under a magnetic field; inset: shell-forming rod-like SiO_2–Fe_3O_4 Janus particles; (right) Superparamagnetic properties of rod-like particles and magnetic response of capsules to an external magnetic field (From ref. 218. Reproduced with permission from The Royal Society of Chemistry.)

from PS-coated FeO_x particles by Kaiser *et al.* were investigated to serve as a controlled release system.[224] Akartuna *et al.* used Fe_3O_4 – among other particles – for the stabilization of oil-in-water colloidal capsules which were *in situ* hydrophobized with water-soluble surfactants.[225] Liu *et al.* reported drug-containing colloidal capsules with a gelled agarose core and a Fe_2O_3 shell.[226]

3.2.2 Colloidal capsules with noble metal particles or quantum dots. As briefly mentioned above, quantum dots and noble metal particles have been explored as well for the creation of micron-sized colloidal shells. In specific, noble metal particles may induce plasmonic near field coupling of particles in close proximity to each other. Here, new optical properties may be created due to the coupling of surface plasmons, which is indicated by shifts of the coupled plasmon modes towards longer wavelengths.[227] We will start the discussion of this section with quantum dots.

In one of the first reports, in 2003, Lin *et al.* pioneered the crosslinking of colloidal shells from vinylbenzene-capped CdSe nanoparticles. The cross-linking was performed at a toluene emulsion droplet interface within an aqueous solution of 2,2′-azobis(2-(2-imidazolin-2-yl)propane) dihydrochloride at 60 °C

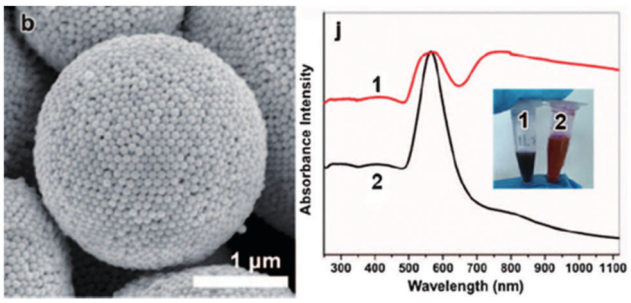

Fig. 10 (left) "Black Gold" colloidal capsule, (right) displaying plasmonic coupling (curve 1) in comparison to freely dispersed gold particles (curve 2). (Reproduced with permission ref. 235. Copyright 2015, Wiley-VCH Verlag GmbH & Co. KGaA.)

for 6 h.[228] Skaff *et al.* later advanced this approach with cyclic olefins-capped CdSe/ZnS nanoparticles and interfacial cross-linking *via* so called ring-opening metathesis polymerization (ROMP).[229] Rotello and co-workers investigated another approach of ligand-capped colloidal shells. The authors pre-synthesized hydrophilic and hydrophobic gold nanoparticles, by respectively capping a first type of colloid with beta-cyclodextrin and a second type with adamantane. Interaction of the two moieties at a droplet interface led to stable colloidal capsules. However, in contrast to cross-linked shells, the particle interaction could be mitigated by adding an amphiphilic molecule that led to partial coalescence and eventually capsule growth.[230] Beyond this, Rotello *et al.* also used enzymes (*Candida rugosa* lipase), similar to their work on nanoscaled colloidal capsules discussed below, to stabilize micron-sized oil-in-water gold particle shells.[231] Using MF particles as templates, Caruso *et al.* prepared near-infrared (NIR) responsive polyelectrolyte–gold nanoparticle capsules. The resulting capsules could be ruptured by pulsing them with laser light allowing a controlled release of encapsulated cargo.[232,233] Also utilizing gold nanoparticles, Glogowski *et al.* assembled PEGylated 2 nm gold colloids at the interface of an oil-in-water emulsion. The colloidal shells were assembled on large 60–200 μm droplets and could be downsized by extrusion through polycarbonate membranes with defined pore sizes to diameters below 10 μm.[234] Gold nanorods tethered with PEO_{45}-*b*-PS_{211} were assembled to giant vesicles with diameters of up to 2 μm *via* a microfluidic-based continuous self-assembly.[160] In contrast, Liu *et al.* used larger gold nanoparticles with a monodisperse size of about 100 nm for the synthesis of a colloidal shell *via* a water-in-butanol emulsion. The micron-sized capsules display a plasmonic coupling effect, evidenced in a shift of the LSPR peak (Fig. 10).[235] Besides gold colloids, Anandhakumar *et al.*[236] and Radziuk *et al.*[237] created colloidal capsules from silver nanoparticles, synthesizing the capsules *via* the classical LbL colloidal templating approach.

3.3 Capsules with proteins as shell-forming building blocks

Besides these aforementioned capsules based on hard colloidal particles, proteins have been utilized as modular building blocks for micron-sized shell formation, as well. In this respect, viruses – bionanoparticles constructed from proteins – were investigated[42,238] by Russel *et al.* and reviewed[239] by Böker *et al.* for their ability to assemble to colloidal capsules. First reports on albumin-based LbL-based microspheres date back several decades.[240–242] However, the above discussed techniques were only recently implemented to prepare protein capsules with sophisticated shell properties. In first works, various groups combined proteins and a second component for electrostatic interactions in LbL synthesis routes to create protein shells.[243–246] LbL-templating of proteins, which were subsequently cross-linked to form an intrinsically stable shell, were employed by Möhwald and co-workers. The authors first templated against $MnCO_3$ particles and then added the dispersion to a glutaraldehyde solution to induce a reaction of its aldehyde groups with BSA amine groups. Cores could be dissolved by incubation in low molar HCl leading to hollow and 5 μm-sized capsules with BSA shells.[247] Glutaraldehyde induced cross-linking was also employed for hemoglobin[248] and glucose oxidase based capsules.[249] A non-covalent linking method based on physical adsorption was later on developed by Mertz and Caruso *et al.*, by first functionalizing silica templates with bromoisobutyramide, which subsequently acts as an intermolecular linker of adsorbed human serum albumin (HSA).[250] HSA was further used in a follow-up study by the authors for the creation of protein shells (Fig. 11) and their biofunctionalization for cell viability experiments.[127]

Besides these LbL approaches, which are mainly derived from polymer chemistry, capsules with proteins as shell-forming building blocks were also created by various emulsion-based routes using proteins that more strongly resemble nanoparticles. For instance, ferritin was employed as a Pickering-emulsifier by Fujii *et al.*,[251] and besides their work on bionanoparticles, Böker *et al.* also investigated ferritin–PNIPAAm conjugates as shell forming conjugates.[252] Furthermore, 'protein particles' were also investigated for the stabilization of dextran/PEO-based water-in-water emulsions.[253] Also by stabilizing all-aqueous emulsions, colloidal capsule-like structures were assembled from protein

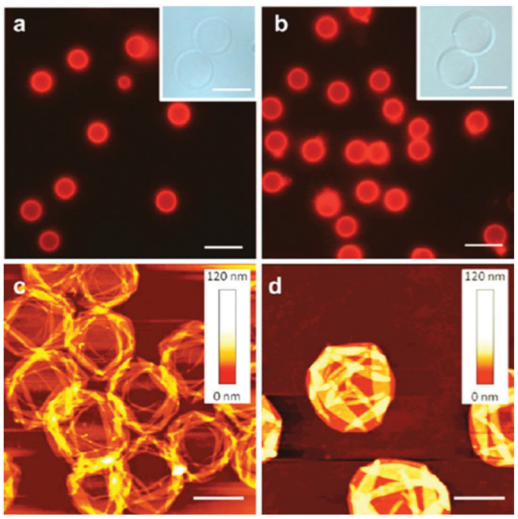

Fig. 11 Fluorescence microscopy (a and b), bright field microscopy (insets) and AFM micrographs of template-based HSA-shelled capsules. (Scale bars: (a and b) 10 μm, (insets), 5 μm, (c and d) 2 μm). (Adapted with permission from ref. 127. Copyright (2012) American Chemical Society.)

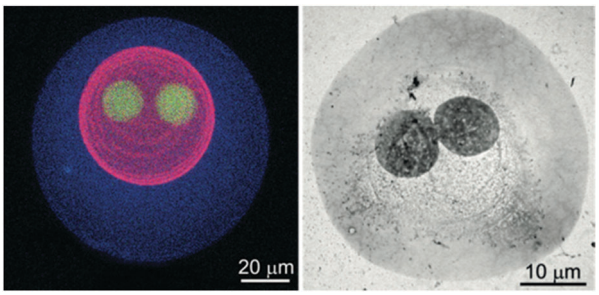

Fig. 12 Proteinosomes-in-proteinosome: (left) proteinosome three levels of organization visualized with different fluorescent markers in a fluorescent microscope (right) TEM micrograph of a proteinosome with two levels of organization. (Reproduced with permission from ref. 256. Copyright 2016, Wiley-VCH Verlag GmbH & Co. KGaA.)

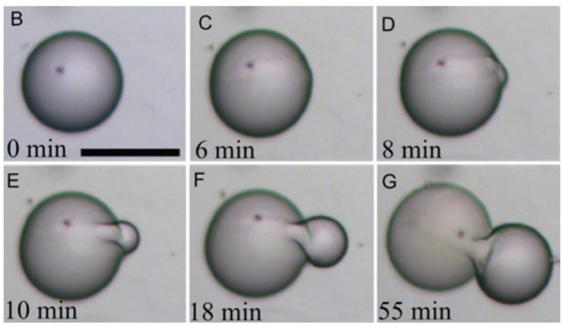

Fig. 13 Self-reproducing colloidal capsule (inorganic protocell) based on silica nanoparticles. (Reproduced with permission from ref. 261. Copyright 2014, Wiley-VCH Verlag GmbH & Co. KGaA.)

nanofibrils and termed as 'fibrillosomes'.[254] Another exceptional report was recently made by Mann *et al.* on protein–polymer based protocells. Here, the protein shells, termed as 'proteinosomes', were assembled from PNIPAAm-conjugated BSA at water-in-oil emulsion droplets prior to shell cross-linking.[43] These proteinosome structures were further advanced in subsequent studies to feature enhanced shell functionality through a multivalent enzyme-based membrane[255] that exhibits higher-order structure and function,[48] and that possesses multiple subcompartments.[256] In the latter report, the authors were able to create host–guest proteinosomes-in-proteinosomes (Fig. 12). Here, the release of encapsulated dextran and DNA from subcompartments was demonstrated. Some of these protein-based capsules represent a distinct class of protocells, which have also been created from inorganic particles in previous reports.

3.4 Inorganic protocells

Prior to their work on utilizing proteins as building blocks for the creation of structures with cell-precursive morphologies and functionalities (protocells),[257] Mann *et al.* also published pioneering works on such structures based on inorganic nanoparticles.[45,258] Initially, Li *et al.* encapsulated a wide variety of biomolecules in silica nanoparticle-based capsules. The resulting protocells were then used for *in vitro* protein synthesis. Beyond this, silica protocells with enhanced membrane functionality were created by grafting a pH-susceptible copolymer onto the membrane, giving rise to electrostatically gated permeability. In contrast to previous emulsion-based colloidal capsules which were usually solely able to inhibit diffusion of larger biomolecules out or into the protocells, these structures were able to preserve this functionality also for smaller molecules. This internal protocell functionality was then investigated for the performance of enzymatic dephosphorylation reactions.[44] In a further study, cytoskeletal structural components were further mimicked with inorganic colloidal capsules *via* the integration of a supramolecular hydrogel within a protocell. The hydrogelation reaction was achieved by encapsulating a gel precursor (*N*-fluorenylmethylcarbonyl-tyrosine-(*O*)-phosphate) within the aqueous core of the capsules and a subsequent performance of an ALP-mediated removal of phosphate groups from the precursor.[259] The authors also observed the formation of nanofilaments from the hydrogels which were further investigated in a subsequent study.[260] A primitive cell-like division process of silica protocells was also invented by Mann and co-workers. Here, colloidal capsules containing a sodium phosphate buffer solution in a continuous oil phase were produced. Upon the addition of tetramethoxysilane (TMOS) a swelling inside the shells was induced due to methanol formation, leading to bud formation on the protocell surface. Auxiliary silica nanoparticles then assembled on the newly formed bud and a second generation micro-compartment was created (Fig. 13).[261] Clay-based (montmorillonite) protocells with a temperature-responsive PNIPAM-based membrane were recently used for the establishment of simple cell-like signaling pathways,[46] which resembles some similarities to works by Tamate *et al.* who used temperature responsive microgel particles to induce shape oscillation in protocells.[47]

3.5 Conclusions for micron-sized colloidal capsules

In summary, the use of particles with distinct morphological or physical properties in the shell of colloidal capsules may be effectively utilized to tailor the capsule's properties. However, the analysis of the capsules often tends to be qualitative and has therefore partially earned this field the rather negative tag of 'pretty picture science'. Numerous standard colloid properties of the capsules are often only marginally discussed and their thorough characterization should be established as good practice in future studies within this field. These include, among others, the polydispersity and long-time colloidal stability of the capsules in relevant media, the interior build-up as well as thickness and number of monolayers of particles in the capsule's shell (*e.g.* by scanning TEM), membrane permeability, mechanical properties of the capsules (*e.g. via* AFM analysis), or the surface chemistry of the capsules itself as well as the shell-forming building blocks (*e.g. via* assays for quantification of functional surface groups).

4. Nano-scaled colloidal capsules

Miniaturization of encapsulation structures plays a pivotal role in their potential transfer from fundamental research objects to competitive products in technical, end-consumer or biological applications. All synthesis routes described in Section 2 have

been utilized by various groups for the synthesis of nano-scaled capsules. However, whilst for micron-sized colloidal capsules we found a great majority of emulsion-based structures, for submicron-sized capsules only a few emulsion-based capsules haven been reported so far.

A decrease in capsule size inherently demands the employment of small or ultrasmall (<10 nm) nanoparticle building blocks. This specifically changes some circumstances for colloidal capsules aimed to be formed *via* the emulsion route. As described above, for the emulsion-route, the adsorption enthalpy of the particles is lowered with a decrease in particle size and tends to be lower compared to thermal particle motion, which might lead to the detachment of particles from the liquid–liquid interfaces of emulsion droplets.[78] Additionally, several groups discuss the occurrence of so-called 'image charge effects' that prevent hydrophilic particles to absorb at the droplet interface, even though the net adsorption enthalpy is favourable.[83,262,263] Furthermore, as recently described by Rotello *et al.*,[16] a decrease of the emulsion droplet/capsule radius (r), which eventually leads to the formation of a nanoemulsion,[264] goes along with an increase in Laplace pressure (ΔP) – the pressure difference between inside and outside the droplet – that is exercised onto the droplet interface:

$$\Delta P = 2\gamma_{O/W}/r$$

As a result, nanoemulsion droplets tend to coalesce much faster. Hence, in contrast to larger emulsion-based colloidal capsules, where a structural stabilization can be more easily performed after the particles have adsorbed at the emulsion droplet interface, nano-scaled colloidal capsules require some form of accompanying *in situ* stabilization of the particles at the interface. However, a general theoretical description of the forces that influence the self-assembly of colloids at the nanoscale are more complex in comparison to the micron-scale as the interactions are not linearly additive and classical DLVO theory does not apply.[265,266]

Only a limited number of reports of emulsion-based colloidal capsules with sizes below 1 μm exist so far, including works by our group. We exploited a synergistic effect stemming from oil-soluble surfactants to decrease the capsule size, combined with a simultaneously occurring shell stabilization. Utilizing ultrasound homogenization, we created a water-in-oil emulsion, with the water phase containing the shell-forming particles and the continuous oil phase containing oil-soluble surfactants (lipids). The lipids synergistically decreased the surface tension of the oil–water interface leading to nano-scaled droplet sizes and concurrently drove the nanoparticles to adsorb and to agglomerate at the interface. This synthesis route was based on previous observations of the formation of nanoparticle lipid thin films studied by us using interfacial shear rheology[86] and by other groups using additional characterization methods.[262,267] We performed the capsule synthesis with SiO_2, Al_2O_3 and Al_2O_3-coated SiO_2 core–shell nanoparticles[268] (Fig. 14) as well as nanodiamonds[35] in combination with either stearic acid or stearyl amine. Utilizing the same approach, we also formed submicron colloidal capsules from rhodamine fluorescent core–shell silica particles.[30] Also using silica particles and surfactants, *i.e.* lecithin or oleylamine, Eskandar *et al.* prepared submicron-sized Pickering-emulsions. Inverse Pickering-emulsions with sizes below 500 nm and exceptional stability were also prepared by Ziener *et al.* by employing silica particles and *in situ* hydrophobizing the particles with oil-soluble surfactants.[269] Earlier, Ziener and co-workers investigated another approach for the preparation of emulsion-based colloidal capsules. This was achieved by templating monomer droplets with silica particles followed by a temperature-induced polymerization of the core.[17] Similarly, a combination of Pickering-emulsification and solvent displacement technique was performed for the synthesis of colloidal capsules. Here, silica particles were adsorbed on hexane droplets comprising poly(styrene-*co*-4-vinyl pyridine) copolymers, which phase-separated prior to the polymerization of the capsule's core.[270] Khashab *et al.* adsorbed negatively and positively charged nitrophenylene-doped silica nanoparticles on the droplets of an oil-in-water emulsion leading to electrostatically stabilized Pickering-emulsions. Upon light-irradiation the charge of the positively charged particles could be reversed, leading to a destabilization of the shell and an eventual disassembly of the capsules, which could be combined with a time-dependent cargo release.[271]

Another Pickering-emulsion approach combining a set of two types of particles (SiO_2 and TiO_2) was adopted by Wu and co-workers, where the core of the colloidal capsules was polymerized prior to dispersing the capsules in waterborne polysiloxane.[272] In addition to these Pickering-emulsion-based colloidal silica shells,

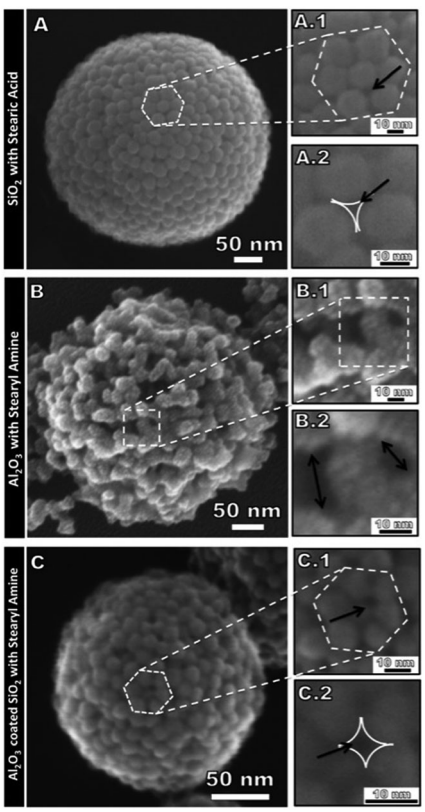

Fig. 14 Submicron-sized colloidal capsules with SiO_2, Al_2O_3, Al_2O_3-coated SiO_2 particles based colloidal shells (Reprinted with permission from ref. 268. Copyright (2013) American Chemical Society.).

capsules from gold nanoparticles have been reported as well. As already introduced above, Rotello and co-workers used 2 nm sized gold nanoparticles for an oil-in-water emulsion based nanocapsule synthesis. Here, arginine-functionalized gold colloids adsorbed on linoleic acid droplets leading to a primary shell stabilization based on a distinct arginine–carboxylate interaction. Secondly, transferrin was introduced to the system leading to a further lateral stabilization of the colloidal shell through electrostatic attraction (see also Fig. 25 for an illustration of shell stabilization of a follow-up study).[16]

Non-emulsion based colloidal silica shells were also reported by various groups. In their early works Caruso *et al.* utilized their templating approach with polyelectrolytes and colloids in combination with silica and other inorganic nanoparticles.[19,273–275] Herz *et al.* templated ZnS particles with fluorescent core–shell silica particles to reduce the fluorescent proximity quenching stemming from the energy transfer of closely neighboring fluorescent particles.[29] Wu *et al.* created PMMA@SiO_2 hybrid particles by templating silica sols on monomer templates prior to a polymerization step.[276,277] Armes *et al.* synthesized various colloidal shells by templating silica sols against preformed monomer droplets with a subsequent core polymerization step.[71,278–280] The packing patterns of silica and other particles templated against PS particles and polymersomes were analyzed by Bon and co-workers.[281,282] Ritter *et al.* formed capsules from β-cyclodextrin and adamantyl-modified particles in an aqueous solution, which is assumed by the authors to occur due to supramolecular complexation.[283] Zhou *et al.* assembled vesicles by physisorption of triblock copolymers on 15 nm silica particles, which showed surface reconstruction characteristics from a raspberry-like to a brain coral-like topography.[284] Additionally, Guan *et al.* recently described colloidal capsules with varying morphologies using a templating approach.[285]

4.1 Distinct physical properties of building blocks and resulting nano-sized colloidal capsules

4.1.1 Nano-scaled colloidal capsules assembled from magnetic nanoparticles. Based on their original templating approach, Caruso *et al.* adsorbed Fe_3O_4 nanoparticles and polyelectrolytes on PS-core templates, with that pioneering the field of nano-scaled magnetic colloidal capsules.[286] By varying the number of coating layers from one to five, after subsequent etching of the PS core, the diameters of the hollow capsules could be adjusted to be between 650 and 960 nm.[287] Maceira and co-workers also used a templating approach with polyelectrolytes, although they templated against SiO_2 particles and formed the magnetic colloidal shell (cobalt nanoparticles) by an *in situ* seed formation process.[288] Based on our previously discussed Pickering-emulsion approach in combination with lipids, we likewise synthesized colloidal capsules from iron oxide nanoparticle with submicron sizes. Characterization of the structures with an alternating gradient magnetometer revealed that the capsules maintained their superparamagnetic properties. The capsules could be affected by an external magnetic field (Fig. 15).[30] Another emulsion-based method to stabilize the shell of magnetic particle enclosed capsules was employed by Shen *et al.* who silanized a Fe_3O_4 Pickering-emulsion. The final structures also maintained their superparamagnetic properties.[289]

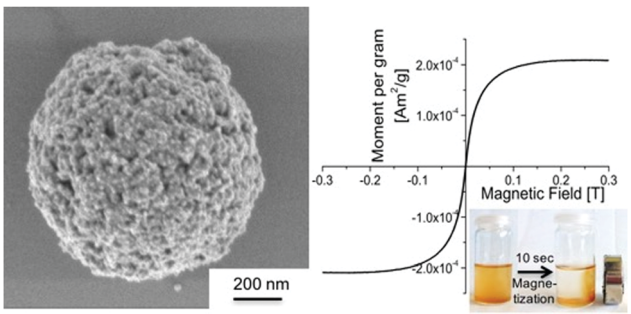

Fig. 15 Submicron-sized colloidal capsule formed from iron oxide nanoparticles featuring superparamagnetic properties. (Reproduced with permission from ref. 30. Copyright 2015, Wiley-VCH Verlag GmbH & Co. KGaA.)

We already briefly discussed some magneto-liposome/polymersome structures in Section 2.4. Recent work by Park *et al.* is worth further noticing, describing the size control of magneto-polymersomes. The authors loaded magneto-polymersomes with iron oxide particles of different sizes through which they were able to control the size of the resulting submicrometer polymersomes. The vesicles were formed by first mixing poly(acrylic acid)–polystyrene block copolymers with iron oxide particles in a dioxane and THF mixture and subsequently adding water to induce vesicle formation. TEM-tomography was utilized for a detailed morphological characterization of the polymersomes (Fig. 16).[199] The structures reportedly featured high transverse relaxation rates in analogy to a previous report about magneto-polymersomes by Sandre and co-workers.[290]

4.1.2 Nano-scaled colloidal capsules assembled from gold nanoparticles. In the past years, an especially strong focus on the utilization of gold nanoparticles to study interparticle surface plasmon interactions has emerged.[291,292] The surface plasmon resonance of gold nanoparticles is extremely sensitive to changes in the local environment surrounding the particles and to the interparticle distances, making gold particles specifically interesting for nano-scaled colloidal capsule formation.[293] Again, based on a hard templating approach with PS particle cores, Caruso *et al.* were the first to report submicron colloidal capsules formed from Au nanoparticles and with that pioneered the field of plasmonic coupling in colloidal submicron capsules. UV-visible spectra of the capsules displayed a plasmon resonance peak of 655 nm in comparison to the gold nanoparticle dispersion of 517 nm.[294]

Following up on this report, more templating approaches have been used to further tailor the resulting capsule properties. After earlier reports of densely[13] nanoparticle-coated micron-sized and loosely[295] coated submicron-sized microgels, Karg *et al.* reported a high density colloidal gold shell adsorbed on a thermoresponsive poly-(NIPAM-*co*-allylacetic acid) microgel. Based on electrostatic interactions a swollen microgel template was covered with PSS/PAH coated gold nanorods (57 nm in length and 15 nm in diameter). Upon a temperature increase the microgel template shrunk from approx. 700 nm at 15 °C to 270 nm at 60 °C, leading to dense colloidal particle surface coverage. The decrease in microgel size inherently led to a

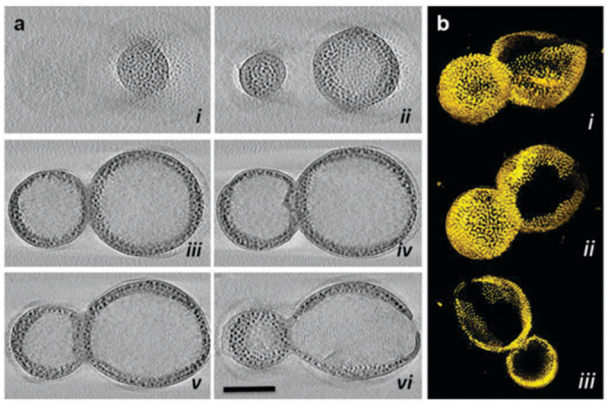

Fig. 16 Magneto-polymersome (a) TEM tomography micrographs and (b) surface renderings (Adapted with permission from ref. 199. Copyright (2014) American Chemical Society.).

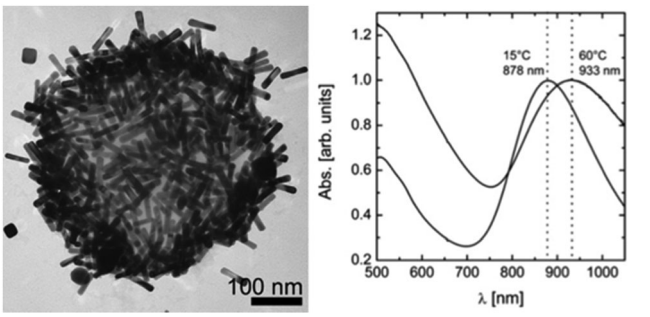

Fig. 17 Left: Micrograph of a gold nanorod-covered PNIPAm microgel particle; right: UV-vis spectra of a swollen (15 °C) and collapsed microgel (60 °C) (Adapted with permission from ref. 37. Copyright (2009) American Chemical Society.).

decrease of the separation distances of the nanorods, causing a red-shift of the UV-vis spectra band induced by surface plasmon interaction (Fig. 17).[37] Another report utilizing gold colloids and a hard template without the use of polyelectrolytes was recently made by Landon *et al.* designing 'hollow golf nano balls'. The authors first attached 100 nm PS particles to a larger SiO_2 template and subsequently adsorbed 3 nm gold particles on the SiO_2@PS template. Followed by a plating process of the gold particles and removal of the SiO_2@PS template resulted in the formation of a partially fused gold colloid surface with a morphology resembling a golf ball.[296] Another distinct linking approach of a colloidal particle gold shell template on silica particles was reported by Liu and co-workers. The authors adsorbed negatively charged bis(*p*-sulfonatophenyl)phenyl phosphine capped 14 nm gold particles on an aminated SiO_2 template. A subsequent treatment of the structures with Ag^+ led to covalent interconnections between the gold particles, which was performed prior to HF etching of the silica core.[14] Besides the works of Rotello *et al.*, which we will discuss in more detail in Section 5, only a few reports of emulsion-based submicron-sized colloidal gold particle shells could be found, including a report by Tian *et al.* who assembled amphiphilic gold particles on the droplet interface of a toluene-in-water emulsion.[297]

4.1.2.1 Nano-scaled colloidal capsules assembled from polymer-grafted gold nanoparticles. As already mentioned above, a great number of reports of capsules built from colloidal gold particles are based on the amphiphilicity-driven self-assembly of polymer-brush-conjugated gold particles. In advance to the first works on the vesicle forming capabilities of gold colloids with a mixed homopolymer architecture, Duan *et al.* investigated the adsorption kinetics of PEG and PMMA conjugated nanoparticles at the oil–water interface and were able to reversibly tune the assembly of the particles at the interface by the addition of different solvents to the system.[298] The nanoparticles were synthesized *via* a dual grafting-"To" and -"From" route, by first simultaneously bonding the hydrophilic polymers to the particle, in combination with an initiator species for a subsequent grafting-"From" step performed by atomic transfer radical polymerization (ATRP). On a side-note, polymer brush growth from various types of nanoparticles was recently reviewed by Böker and co-workers.[299]

Based on 14 nm gold particles grafted with a dual homopolymer architecture consisting of PEG and PMMA brushes (Au@PEG/PMMA) Song *et al.* created approx. 200 nm sized nanoparticle vesicles *via* a film rehydration method (Fig. 18). UV-vis spectra showed a 30 nm red shift of the vesicles in comparison to the individually dispersed Au@PEG/PMMA particles, indicating a surface plasmon coupling of the gold particles. The authors also studied the pH-responsive disassembly of the vesicles by introducing 25% 4-vinylpyridine (4VP) into the PMMA chain, allowing a controlled degradation of the vesicles upon shifting the pH from 7 to 5.[49] The intracellular drug delivery potential of these Au@PEG/PMMAVP[152] and photo-regulated Au@PEG/PNBA[153] vesicles were investigated in follow-up studies, as reviewed in Section 5. The vesicles were further advanced by the substitution of the spherical particles with nanorod gold colloids. By changing the initiator species, Song *et al.* were able to conduct an organocatalytic surface-initiated ring-opening polymerization of lactic acid to retrieve PEG and polylactide mediated gold nanorods (AuNR@PEG/PLA). After vesicle formation, the PLA allowed for an enzymatic disruption of the shell *via* treatment with proteinase K as well as a rupturing by heating the vesicles, which was induced by a 808 nm laser.[154] Recently, Song *et al.* simplified the gold particle functionalization by solely applying a grafting-"To" step for the fixation of mixed homopolymers on the particles. Individual PEG and PLGA polymer-chains with thiol end-capping were simultaneously reacted with CTAB-stabilized gold nanorods, eliminating the need for the rather laborious combination of grafting-"To" and grafting-"From" steps. The resulting Au@PEG/PLGA particles could be combined with reduced graphene oxide for an w/o/w-based synthesis of approx. 65 nm sized NP vesicles.[155] In a follow-up study, also based on an emulsion-route and employing polyvinyl alcohol as an emulsion stabilizer, the sizes of the Au@PEG/PLGA based vesicles were adjusted to ~60 nm.[52] Deng an co-workers applied a similar approach and conjugated 14 nm Au NP with pre-synthesized PCL-SH and $PMEO_2MA$-SH grafts.[300] The further miniaturization of these NP vesicles with the combination of biodegradable polymers makes these structures of specific interest for biomedical applications which will be discussed in more detail in Section 5.

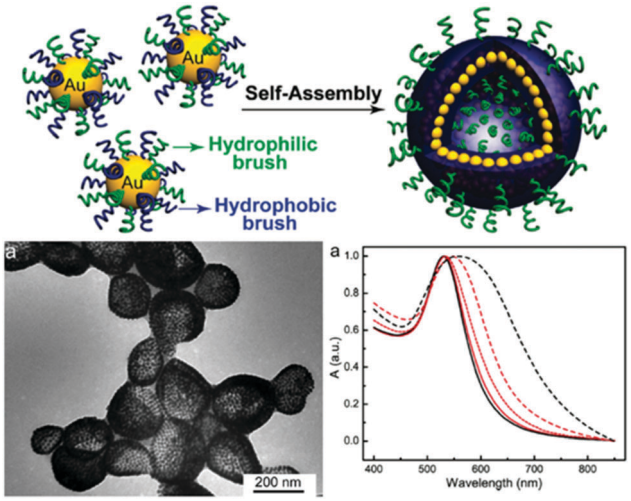

Fig. 18 (top) Mixed PEG-PMMA grafting architecture on gold nanoparticles and resulting nanoparticle vesicle; (bottom-left) TEM micrograph of vesicles; (bottom-right) UV-vis spectra of Au@PEG/PMMA dispersion and respective colloidal capsules (native Au@PEG/PMMA dispersion in $CHCl_3$ (black solid line), in H_2O: vesicles of Au@PEG/PMMA (black dashed line), Au@PEG/PMMAVP with 25% 4VP (red solid line), vesicles at pH 7.0 (red dashed line), disassembled vesicles (red dot line)) (Adapted with permission from ref. 49. Copyright (2011) American Chemical Society.).

As mentioned in Section 2.3, Nie *et al.* utilized a BCP polymer-brush architecture for colloidal capsule synthesis. In their initial work, the authors reported a strong dependence of the possibility to form NP vesicles on the hydrophobic block length and particle size. Larger particles featuring a diameter of 8 nm or larger only formed vesicles if the PS block length had a mass of 10 000 g mol^{-1} or more. In other words, vesicle assembly can only be achieved if the chain length of the polymer is at least in the size range of the nanoparticle diameter. The resulting vesicles featured distinct interparticle spacings between the gold particles which are determined by the polymer block length (Fig. 19).[15] These and further vesicles based on nanoflower-shaped Au particles[145] influenced the resulting UV-vis absorption spectra. Au NP designed with different lengths of the PS block were further probed for the assembly in THF:water mixtures with different volumetric ratios.[144] In another study, the photosensitizer chlorine e6 (Ce6) was loaded into PEO_{45}-*b*-PS_{245} grafted Au NP Vesicles with final sizes of $\sim$280 nm. Furthermore, NP vesicles with enhanced biocompatibility featuring PCL as the hydrophobic block and a high photothermal conversion efficiency were assembled from 26 nm sized Au NPs grafted with PEO_{45}-*b*-PCL_{270} BCPs. The resulting vesicles featured narrow size distributions of 192.6 $\pm$ 11.8 nm or 207.3 $\pm$ 15.7 nm, depending on the Au@PEO-*b*-PCL concentration at the start of the synthesis. Degradation of the vesicles could be observed by either increasing the temperature or after a prolonged period of time of 8 weeks at a constant temperature of 37 °C.[50] The surfactant-like characteristics of amphiphilic polymer-tethered nanoparticles were recently reviewed by Zhang and Zhao.[301]

Vesicles from block-oligomer-tethered gold nanoparticles with shorter hydrophilic and hydrophobic units were reported by Niikura and co-workers. Here, gold nanoparticles with a citric acid coating were functionalized with a ligand of intermediate length, comprising an oligo(ethylene glycol) (OEG) group, a fluorinated tetraethylene glycol (FG) group, and a 11-carbon alkyl subunit. The resulting 60 nm sized vesicles exhibited surface plasmon coupling characteristics, which was expressed in a 30 nm red shift in the UV-vis adsorption spectra.[302] In a follow-up study, the sub-100 nm vesicles were probed for drug-encapsulation and light-triggered release applications.[303] An unprecedented 'entropy-driven size segregation effect' was reported by Niikura *et al.* when combining citric-acid coated gold nanoparticles with different sizes with a glucose-terminated FG-11-carbon alkyl ligand. The particles of different sizes first aggregated and then transferred to a yolk/shell build-up (Fig. 20).[304] Another phase separation effect was also reported by Nie *et al.*, observed during the coassembly of BCP-tethered Au NPs with free BCPs, leading to Janus-like colloidal shells. Au NP tethered with BCPs with different PS and PEO block lengths were concurrently assembled with 'free' BCPs, which also comprised different PS and PEO lengths. The Janus-like vesicles included spherical, hemispherical and disk-like shapes (Fig. 21).[201] Rasch *et al.* observed an analogous phase separation effect in their nanoparticle–liposome hybrids utilizing dodecanethiol-coated Au colloids, which we already briefly discussed in Section 2.4. The authors reported the assembly of spherical Janus-like nanoparticle-loaded liposomes based on a dialysis route (Fig. 22A and B). Here, the formation of a Janus-like vesicle morphology is associated with a clustering of the hydrophobic particles in the lipid bilayer. When the particles are confined, the bilayer must first 'unzip' which creates small gaps around the particles, which are eventually reduced upon clustering of particles.[186] Other liposomes with gold nanoparticles that were packed rather sparsely inside the bilayer were reported by An and co-workers. Here, the liposomes were probed for a photo-induced drug release by local membrane heating which changed the membrane permeability.[305] A different approach was recently reported by Nakamura *et al.* who adsorbed gold nanoparticles on a vesicle based on fullerene amphiphiles

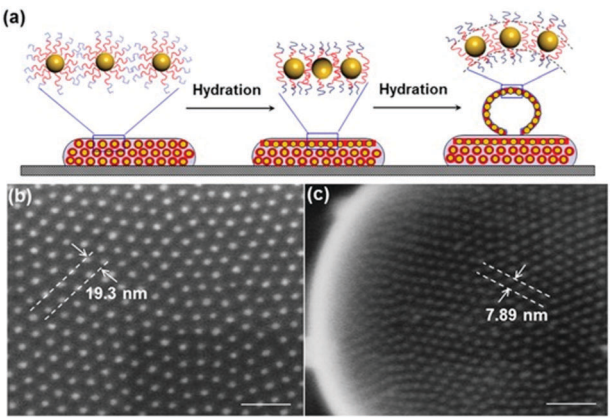

Fig. 19 (a) Scheme of the association of the hydrophobic block of BCPs during vesicle self-assembly; (b and c) SEM images of discrete spacings between AuNP on vesicle surface. scale bars, 100 nm. (Copied with permission from ref. 15. Copyright (2012) American Chemical Society.)

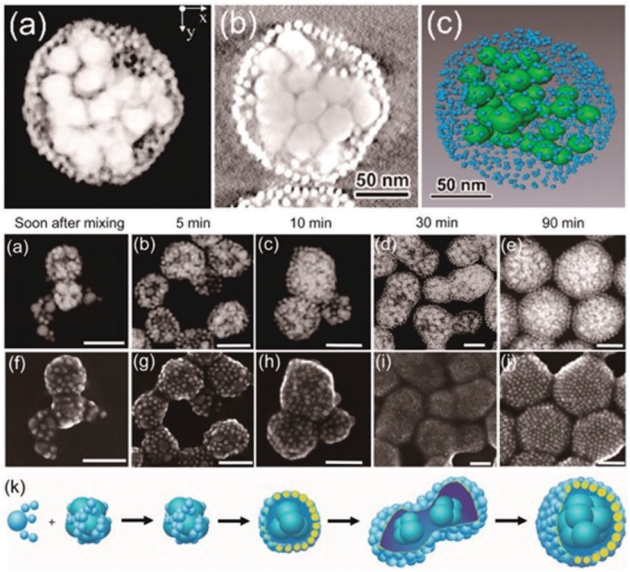

Fig. 20 Egg/yolk like size-segregated core–shell Au nanoparticle vesicles. Top: STEM tomography images of a 5 nm NP based shell and 30 nm Np based core (a) 3D reconstruction; (b) sliced XY image; (c) 3D representation. Bottom: Time evolution segregation of differently sized Au nanoparticles (Adapted with permission from ref. 304. Copyright (2016) American Chemical Society.).

($R_5C_{60}^-K^+$). Au NP approx. sized 3.5 nm and comprising (11-mercaptoundecyl)tetra(ethylene glycol) ligands were conjugated to potassium ions on the surface of the fullerenes. The Au NP served a seed and could be further grown to sizes of approx. 7 nm leading to an increased surface coverage.[306]

4.1.3 Nano-scaled colloidal capsules assembled from multiple modular building blocks. Based on our above discussed lipid-employing emulsion route for concurrent shell stabilization and reduction of capsule size, we reported the co-assembly of different nanoparticle types to create multivalent submicron-sized capsules. We used fluorophore-doped (rhodamine B) silica and superparamagnetic iron oxide nanoparticles in combination with stearic acid for our water-in-oil submicron capsule synthesis. The resulting colloidal shells maintained the distinct physical properties of the modular building blocks (Fig. 23).[30] Similarly, so-called supernanoparticles featuring magneto-fluorescent properties were described by Chen *et al.* who were able to create core–shell clusters featuring a core of magnetic nanoparticles and a shell with a monolayer of quantum dots.[31]

Rotello *et al.* synthesized multivalent colloidal capsules based on a delicate interplay of electrostatically and covalently interconnected modular building blocks adsorbed on fatty acid templates dispersed in water. The so-called nanoparticle-stabilized capsules were used for fluorescence resonance energy transfer (FRET) studies, by the incorporation of quantum dots (QD) and fluorescent proteins in the capsule's shell. Green-emitting QDs (CdSe/ZnS core–shell particles) were first surface-grafted with dihydrolipoic acid and then functionalized with a polyhistidine-conjugated red fluorescent protein *via* metal affinity coordination chemistry. These protein–QD conjugates were then adsorbed onto the surface of Au NP containing fatty acid droplets (linoleic acid and decanoic acid) leading to final capsule sizes of 120 ± 50 nm. The capsules further featured stimuli-responsive release of the hexahistidine-tagged red fluorescent protein which will be further discussed in Section 5.2.[307] As briefly mentioned in Section 2.4.2 Nie *et al.* combined free PS_{107}-*b*-PAA_4 BCPs with 20, 30, or 50 nm-sized PS_{490}-*b*-PEO_{45}-grafted Au NP and 15 or 25 nm-sized oleic acid-capped Fe_3O_4 NP for the synthesis of multivalent janus vesicles which featured sizes of approx. 570 nm. The authors reported the formation of vesicles with either spherical or hemispherical morphology, similar to their previously described structures illustrated in Fig. 21. These so-called 'magneto plasmonic janus vesicles' exhibited strong near-infrared

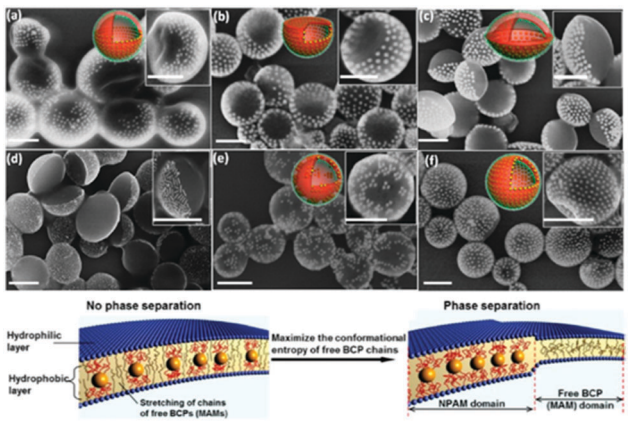

Fig. 21 Top: SEM micrographs of Janus-like nanoparticle vesicles observed in the concurrent assembly of PEO-*b*-PS BCP tethered Au NP with "free" PEO-*b*-PS BCPs with (a) spherical, (b) hemispherical, (c and d) disk-like shapes; and non-Janus-like vesicles with (e) patchy and (f) heterogenous morphology. Bottom: Representation of the phase separation effect within the free BCP bilayer attributed to an entropy-driven attraction of the BCP-tethered Au Np (Adapted with permission from ref. 201. Copyright (2014) American Chemical Society.).

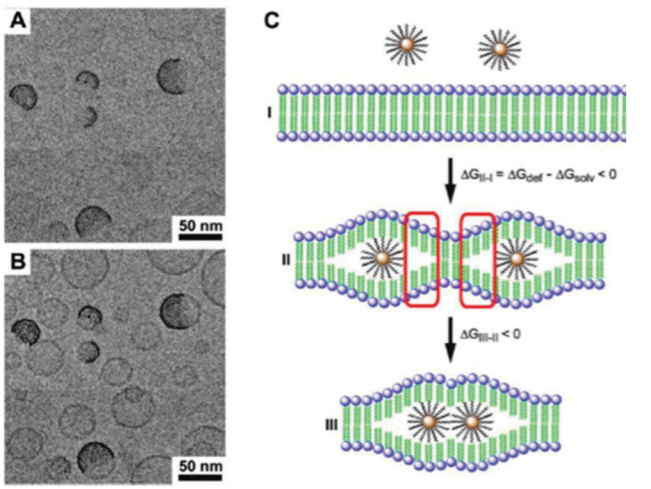

Fig. 22 (A and B) TEM images of spherical Janus-like liposome–nanoparticle hybrids. (C) The gold colloids are confined in the hydrophobic part of the liposome by first "unzipping" the bilayer membrane and secondly clustering to reduce the sizes of so-called "strained regions". (Adapted with permission from ref. 186. Copyright (2010) American Chemical Society.)

absorption, as well as an enhanced transverse relaxation (T_2) contrast effect due to the dense confinement of the particles in the vesicle membrane. The authors examined the structures as light- and magnetic field-responsive containers for triggered release of a model drug and as contrast agents for different bioimaging techniques (see Section 5.3 for more details on their *in vivo* experiments).[202]

4.2 Nano-scaled colloidal capsules assembled from proteins or bionanoparticles as building blocks

In 1999, Caruso and Möhwald published the first work of protein (BSA and IgG) and polymer-templated PS submicron-sized particles,[308] followed by further reports utilizing different enzymes, *i.e.* horseradish peroxidase, β-glucosidase, or urease for the templating process.[309–312] Following these initial reports and their above described template-based synthesis of micron-sized capsules with a protein shell, Caruso and Mertz *et al.* further adjusted their route for the synthesis of capsules with diameters between 50 and 150 nm with a human serum albumin (HSA) shell. The HSA proteins were templated against siRNA loaded isobutyramide-mediated mesoporous silica particles (MSNP) (Fig. 24) and subsequently the MSNP core could be removed by incubating the structures in a buffered HF solution.[129] Viruses, which can be interpreted as protein-based bionanoparticles, were used by Wang *et al.* in combination with poly(4-vinyl-pyridine) (P4VP) for the synthesis of colloidal capsules. P4VP in DMF was slowly added to an aqueous solution of spherically shaped cowpea mosaic viruses (CPMV) or rod-like tobacco mosaic viruses (TMV), leading to a solvent change induced assembly of close-packed virus-enclosed capsules.[313]

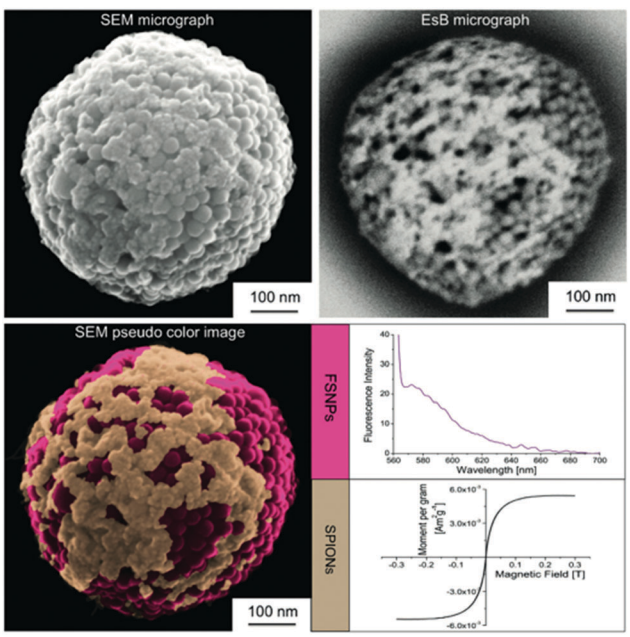

Fig. 23 Bifunctional submicron colloidal capsule concurrently assembled from fluorescent silica and iron oxide particles, comprising fluorescent and superparamagnetic properties. (Reproduced with permission ref. 30. Copyright 2015, Wiley-VCH Verlag GmbH & Co. KGaA.)

4.3 Conclusions for nano-scaled colloidal capsules

In the last decade a number of novel and promising nano-scaled colloidal capsules have been reported. However, similar conclusions for nano-scaled colloidal capsules hold true as the ones briefly discussed above for micron-sized capsules (Section 3.5). Here, likewise, a good practice of the characterization of the capsules needs to be established, even though visualization of the nano-scaled capsules can so far only be performed *ex situ* after their preparation for electron microscopy studies. Additionally, a complete mechanistic understanding of the varying assembly phenomena that occur at the nano-scale remain not fully investigated; such as the kinetics of formation of colloid thin-films on nano-emulsion droplets and their mechanical and rheological properties, deeper knowledge of the delicate interplay of colloid size, length of the hydrophilic and hydrophobic units, grafting density, and the resulting tendency of polymer-grafted particles to form capsules with defined sizes, notwithstanding the often unintuitive and poorly understood colloidal behaviour of small and ultrasmall nanoparticles.[265] Detailed knowledge of these and other factors could allow for the phrasing of simple design rules which could then lead this field closer to a knowledge-based design of these structures. Furthermore, the establishment of a gold standard synthesis route that would allow a reproducible formation of highly monodisperse samples with a high yield, analogous to the now ubiquitous microfluidic based synthesis of micron-sized capsules, is needed to advance nano-scaled colloidal capsules into a mature field of science in the near future.

5. Colloidal capsules for biological applications

A great number of the above described colloidal capsules are developed to be used in bionanotechnology, like biosensing, bioimaging or targeted drug delivery. With silica[314–317] (*e.g.* C·spec®), quantum dots[318,319] (*e.g.* EviTag®), gold[320] (*e.g.* Aurimmune, AuroVist™), iron oxide[321–324] (*e.g.* Feraheme™, NanoTherm®, Combidex®, Feridex®/Endorem®, Resovist®/Ferucarbotran) and other (ultrasmall[325]) nanoparticles either being in (pre-)clinical trials or FDA-approved and (temporarily) in clinical use, utilization of these material classes, as modular building blocks for colloidal capsule self-assembly, could open new design routes in the synthesis of multivalent nanomedical agents.[326] First *in vitro* studies in different cell lines and *in vivo* experiments in rodent models have very recently been performed with colloidal capsules and represent promising approaches and possible competitors to *e.g.* amphiphile-based vesicles. Numerous guidelines and considerations need to be taken into account for drug-carrier design, which makes the synthesis of colloidal capsules formed from the above mentioned inorganic particles significantly more complex in comparison to their organic vesicle counterparts, *i.e.* liposomes and polymersomes. These considerations include a thorough and standardized nanosafety assessment of the individual nanoparticle building blocks and the assemblies as a whole.[327–329] In many of the studies discussed in the following paragraphs, considerations for the design of nanomedical agents have been

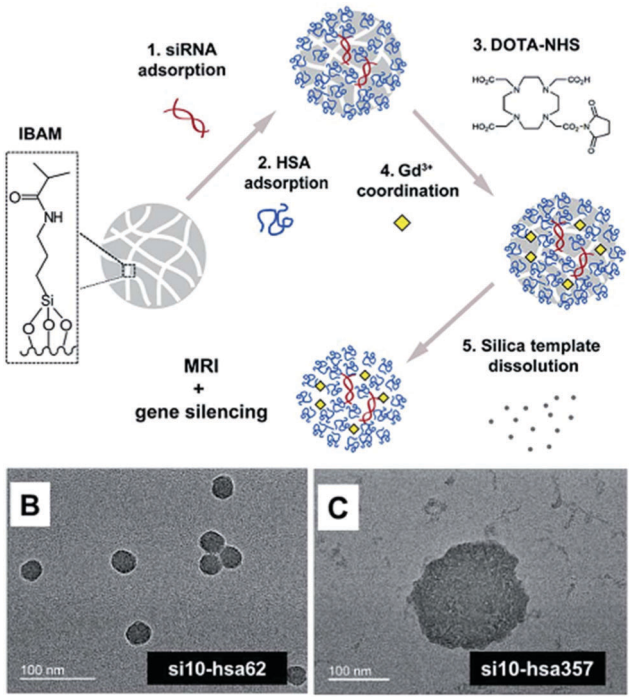

Fig. 24 Top: Synthesis route of gadolinium-mediated and siRNA loaded human serum albumin capsules; bottom: TEM micrographs of differently sized HSA capsules. (From ref. 129. Reproduced with permission from The Royal Society of Chemistry.)

applied in the synthesis of colloidal capsules for *in vivo* experiments in varying degrees. Aspects of the biological fate of colloidal capsules have been characterized as well in some studies. However, this novel field of bionanotechnology is far from presenting a unified approach towards nanosafety or biomedical design rules which would greatly facilitate the development of advanced nanocarrier systems.

Nevertheless, the self-assembly of nanoparticles to colloidal capsules enables the synthesis of novel nanoprobes whose functionalities can be tailored through the collective properties of the shell-forming particles. The integration of superparamagnetic, plasmonic, fluorescent or further functional colloids with distinct physical properties into the shell of colloidal capsules allows the creation of synergies for applications such as multimodal imaging, photo-/hyperthermal treatments, or targeted drug delivery.[326] Furthermore, such capsules may solve some of the problems larger individual inorganic nanoparticles face in bionanotechnology. The potential to design colloidal capsules with the ability to extra- or intra-cellularly erode into their individual building blocks and then follow distinct clearance pathways[330,331] (*e.g.* renal clearance) imparts them with a great advantage over non-degradable larger inorganic nanoparticles which the human organism is not capable to metabolize and consequently cause great concern regarding long-term toxicity.[332] Additionally, by using ultrasmall nanoparticles to create colloidal capsules with diameters of approx. 100 nm or smaller they can synergistically inhibit accumulation within the mononuclear phagocyte system and passively target tumors by utilizing the enhanced permeability and retention (EPR) effect.[333] Another benefit of the degradable shell of colloidal capsules is their potential ability to deliver active pharmaceutical agents (*i.e.* chemotherapeutics, siRNA, *etc.*) directly to the cytosol by membrane fusion and by avoiding endosomal sequestration. Hence, precise combinations of size, surface moieties and controlled degradation behavior into their shell-forming individual building blocks with complete clearance will be central for the potential bench-to-bedside translation of colloidal capsules for parenteral/intravenous administration.

As briefly described above, gold NP are of high interest for colloidal capsule formation as the architectural build-up of the shell can have significant impact on their surface plasmon resonance (SPR), which can be tailored through particle size and interparticle spacing. Interparticle plasmonic coupling results in a shift of the SPR band towards longer wavelengths (red shift) of the near-infrared range (NIR). This is highly desirable for *in vivo* applications, as NIR light is attenuated less by biological tissues than visible light.[334] This can be efficiently exploited for imaging and therapy applications as plasmonic (supra)particles convert light strongly at SPR wavelengths.[293] As discussed throughout the following sections, colloidal capsules assembled from Au NP can specifically be used in photothermal and photodynamic therapy,[335] photothermal and photoacoustic imaging,[336] as well as remote controlled release of encapsulated drugs.[326] Similarly, colloidal capsules and other supraparticles assembled from superparamagnetic nanoparticles can potentially be tailored to feature distinct magnetic properties that distinguish them from larger individual iron oxide nanoparticles. Here, high r_2 transverse relaxivity values to potentially enhance the image contrast in T_2-weighted magnetic resonance imaging (MRI), a high specific absorption rate (SAR) for heat generation, and high magnetic responsiveness to allow such colloidal structures to be moved *via* an external magnetic field, are desired.[54] These properties would allow colloidal capsules formed from superparamagnetic colloids to be utilized in applications such as magnetic fluid hyperthermia[337] and hyperthermic drug release, magnetic particle imaging,[338,339] and magnetic resonance imaging.[340]

We will first briefly review micron-sized colloidal capsules that were designed for biological applications. Subsequently, *in vitro* and *in vivo* studies will be reviewed in detail, describing the unique properties of colloidal capsules within this field. Finally, we will close this section with a critical discussion on whether the here described capsules should be considered for *in vivo* applications in the near future.

5.1 Micron-sized colloidal capsules for biological applications

A certain number of micron-sized colloidal capsules have been reported which do not have to deal with the hassles that are faced in the design of nanocarriers as they are almost solely aiming at non-human *ex vivo* applications. For instance, micron-sized colloidal capsules have been investigated to retain enzyme activity for improved enzymatic catalytic performance, including reports for amylase,[341] laccase,[342] CalB,[40] lipase A, or benzaldehyde lyase.[22] Furthermore, colloidal capsules were investigated to incorporate various different hydrophobic cores.[343]

For example, Porta and Kros examined mesoporous silica nanoparticle-based capsules with a polyacrylamide core for the local delivery of hydrophobic all-*trans* retinoic acid (ATRA), also called tretinoin, in zebrafish. The large colloidal capsules with diameters of approx. 100 μm could be handled with tweezers and were implanted into the caudal fin of the zebrafish. The authors observed a delay in tail regeneration from the zebra fish due to the release of ATRA from the capsules.[344]

5.2 *In vitro* studies of nano-scaled colloidal capsules

We will start discussing nano-scaled colloidal capsules for bionanotechnology with reports on *in vitro* studies. As mentioned above, Rotello and co-workers have published a series of reports of colloidal capsules for biological applications. In their initial report, the authors encapsulated paclitaxel in the hydrophobic linoleic acid core of transferrin and arginine–Au NP stabilized nanocapsules. The drug-delivery capabilities of these paclitaxel-loaded capsules were probed on HeLa cells and proved to be effective by exhibiting a half-maximal inhibitory concentration (IC_{50}) of 13.5 ng mL^{-1} after 24 h of incubation. Control experiments showed no carrier toxicity.[16] Nanocapsules formed from a combination of His-Lys-Arg-Lys-capped gold nanoparticles ("Au_HKRK" NP), histidine$_6$-tagged red fluorescent protein "mCherry" and dihydrolipoic acid-capped CdSe/ZnS core–shell particles ("DHLA_QD") were used for cellular studies, as well. The emission–adsorption overlap of the QD and mCherry spectra enabled FRET studies. The nanocapsules formed from the aforementioned components were incubated with HeLa cells and were taken up by the respective cells *via* endocytosis. Here, histidine and chloroquine could be utilized as disrupting and releasing agents of the mCherry proteins from the endosomes/lysosomes into the cytosol.[307] A process resembling cell membrane fusion for the delivery of proteins and small molecule drugs was investigated in several studies as well by Rotello and co-workers. Au NP-stabilized nanocapsules were utilized for the delivery of protein (GFP, green fluorescent protein) and enzyme (caspase-3) into the cytosol of HeLa cells (Fig. 25). With GFP being a protein imaging agent and caspase-3 a therapeutic enzyme, the protein stabilized NP capsules exhibited multivalent functionality. Caspase-3 was reported to be effectively delivered, leading to the induction of apoptosis, whilst the GFP allowed for a monitoring of its intracellular delivery.[21] In another report, again avoiding endosomal sequestration, the proposed cell-membrane fusion process was used for the delivery of small interfering RNA (siRNA) directly to the cytosol, which can be favorable over endocytic routes which were previously described for other nanocarriers. Electrostatically stabilized complexes consisting of siRNA and arginine-functionalized Au NP were again confined on the surface of linoleic acid oil-in-water emulsion droplets. The transfected siRNA allowed for a very high knockdown of green fluorescence protein (deGFP) in deGFP-HEK293 cells. Furthermore, the delivery of a different siRNA type allowed for silencing of polo-like kinase 1 (PLK1), a kinase enzyme, possessing cell cycle regulation properties and often overexpressed in tumor cells. The siRNA was efficiently protected against nuclease degradation. The membrane fusion mediated cytosolic release of siRNA was evidenced in various control experiments.[51] In a subsequent report, Rotello *et al.* developed a novel method to monitor the trafficking of proteins from nanocapsules to the nucleus. Different nuclear localization signal (NLS) sequences were reportedly used to track the transfer to the nucleus. Enhanced green fluorescent proteins (eGFP) were utilized to function as a fluorescent reporter protein, which was again delivered *via* the membrane-fusion route (Fig. 26a). Among the different NLS sequences, listed in Fig. 26b, $NLS^{c\text{-}Myc}$-eGFP exhibited the most significant nuclear accumulation ability (Fig. 26c and d). Furthermore, the cytosol delivery of $NLS^{c\text{-}Myc}$-eGFP was monitored *via* live cell video imaging, revealing a significant delivery to the cytosol after 60 s and laser scanning confocal microscopy reportedly showed the establishment within the nucleus after 6 min.[345] The co-delivery of nanocapsules containing both a proapoptotic protein and paclitaxel as a antimitotic agent was reported as well. Here, paclitaxel was first incorporated in linoleic acid emulsion droplets, followed by the adsorption of arginine-conjugated Au NP on the droplet surface and by an adsorption of negatively charged proteins on the surface of the nanocapsules. The utilized proteins, transferrin and CASP3, were used as non-active control and therapeutic agents. HeLa cell viability was measured by incubation with "NPSC-PTX-CASP3" nanocapsules. These dual-cargo containing nanocapsules exhibited substantially higher efficiency to induce apoptosis in comparison to free paclitaxel and unloaded capsules, consisting of Au NP with either paclitaxel or one of the proteins.[346] Dual-cargo siRNA and tamoxifen loaded colloidal capsules[347] as well as colloidal capsules for the direct cytosolic delivery of larger proteins, again avoiding

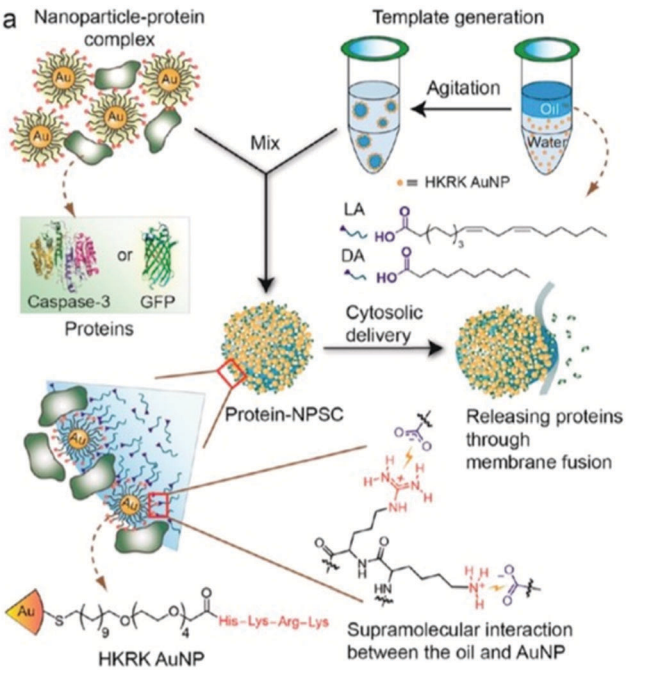

Fig. 25 Scheme of Au NP and protein stabilized colloidal nano-capsules, which were utilized for a membrane fusion based release of proteins directly into a cell's cytosol. (Adapted with permission from ref. 21. Copyright (2013) American Chemical Society.)

endosomal entrapment,[348] were also investigated by Rotello *et al.* in other studies. A recent report by Rotello *et al.* of dendrimer–Au NP based colloidal capsules will be discussed in the following *in vivo* section.

Song *et al.* also performed various *in vitro* studies with colloidal capsules formed from Au nanoparticles with a mixed homopolymer architecture. These colloidal capsules with enhanced biocompatibility were synthesized *via* conjugation with a cell-membrane targeting antibody (HER2 protein), and a pH-susceptible dissolution trigger, that makes use of the acidic environment of intracellular compartments (Fig. 27). The nanoparticle vesicles formed from PEG- and PMMAVP-grafted 14 nm gold particles could be loaded with doxorubicin and were aimed at drug-delivery *via* an endocytic pathway. Additionally, the capsules were conjugated with a Raman reporter (BGLA), which enabled the identification of the disassembly of the capsules by monitoring the surface enhanced Raman scattering (SERS) signal *via* Raman spectroscopy. The authors successfully targeted HER2-positive SKBR-3 breast cancer cells with the antibody-tagged capsules, whilst this receptor-mediated targeting was evidenced in control experiments with HER2-negative MCF-7 breast cancer cells, which showed no specific binding of the capsules. Additionally, doxorubicin, deprotonated with triethylamine, was encapsulated by first forming a hybrid thin-film of doxorubicin and Au@PEG/PMMAVP4 particles on the wall of a small vial, and then rehydrating the film and by that inducing the nanoparticle vesicle formation. The release of doxorubicin from the capsules showed a strong pH-dependence.[152] Very similar nanoparticle vesicles featuring a photo-responsive disassembly trigger were synthesized by utilizing poly(2-nitrobenzyl acrylate) (PNBA) as the hydrophobic brush which can be reacted to water-soluble poly(acrylic acid) after light irradiation, inducing capsule erosion to single particles. In accordance to the aforementioned Au@PEG/PMMAVP4 based vesicles, the capsules also featured a plasmon coupling red-shift, which could be further controlled by varying the PEG/PNBA ratio to 1 : 1, 1 : 2, and 1 : 4, leading to localized surface plasmonic resonance peaks of 550, 630, and 745 nm respectively. Folate was conjugated to the capsules as well, to serve as a moiety to target the folate receptor, which is overexpressed in numerous cancer types, including MDA-MB-435 breast cancer cells. In comparison to nanoparticle vesicles without folate ligands, the conjugated vesicles reportedly showed greatly enhanced binding to the cells, which was qualitatively observed by the authors via dark-field microscopy imaging. The encapsulation and release of doxorubicin was also investigated for the capsules on MDA-MB-435 cells.[153] Nanoparticle vesicles from PLA and PEG conjugated gold nanorods were also investigated by Song and co-workers. The Raman reporter carrying colloidal capsules featured distinct SERS signals, potentially enabling their use for Raman imaging and spectroscopy. Proteinase K, a protein used for the enzymatic degradation of PLA, was used for the degradation and controlled erosion of the PLA capsules, leading to the release of encapsulated doxorubicin. The capsules were further investigated in *in vitro* studies by demonstrating the targeting of EpCAM-positive Hep3B cancer cells with monoclonal antibodies, in comparison to antibody-free capsules and EpCAM-negative PLC/PRF/5 cells. The capsules were thoroughly characterized *via* dark-field and fluorescence imaging, inductively coupled plasma mass spectroscopy, and Raman spectroscopy (Fig. 28). The nanocarriers were also investigated as potential

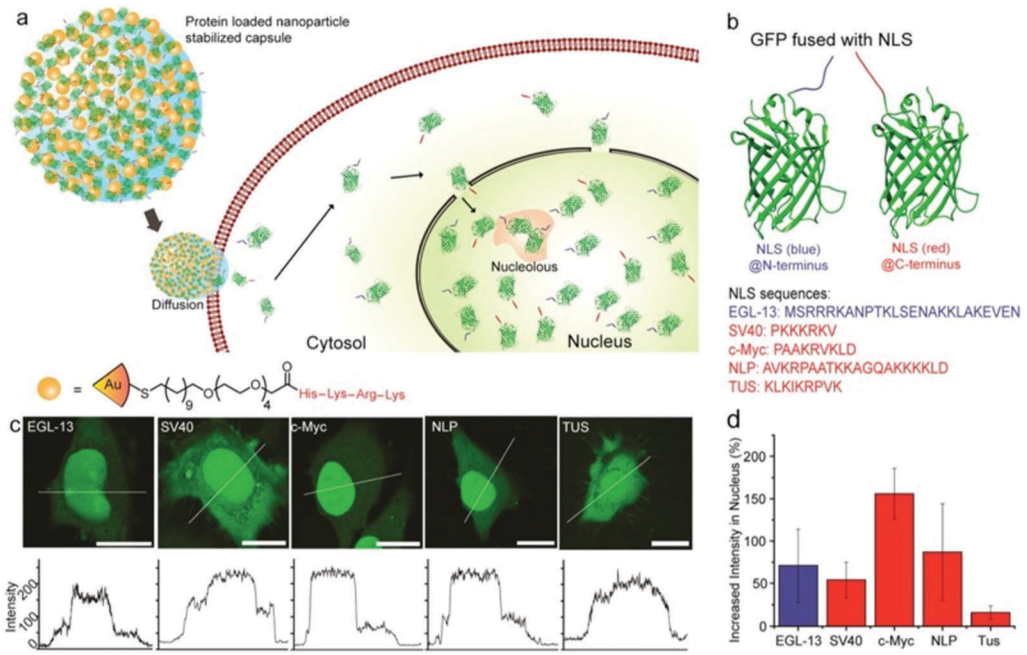

Fig. 26 (a) Scheme of Au NP and eGFP stabilized nanocapsules and their membrane fusion based Protein release; (b) eGFP structure with nuclear localization signal sequences; (c) different cell images fused with eGFP (scale bar: 20 μm); (d) increase of nuclear intensities of different NLS-eGFPs (Copied with permission from ref. 346. Copyright (2015) American Chemical Society.).

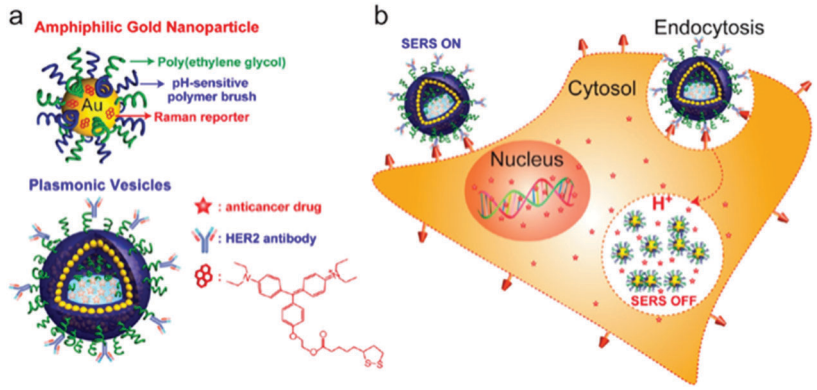

Fig. 27 (a) Scheme NP Vesicle formed from PEG/PMMAVP@AuNPs conjugated with a Raman reporter, HER2 antibody and loaded with DOX; (b) scheme of cellular internalization and erosion process of the vesicles (Copied with permission from ref. 152. Copyright (2012) American Chemical Society.).

structures for theranostic nanomedicine by utilizing their chemo-photothermal properties. After antibody-based cell targeting, the capsules were heated and triggered to release encapsulated doxorubicin *via* laser-light irridation.[154] Further nanoparticle vesicles from polymer-grafted gold colloids from Song *et al.* as well as from Nie *et al.*, will be discussed in the subsequent *in vivo* studies section.

Nanoparticle membrane loaded liposomes and polymersomes have also been investigated intensely in *in vitro* studies. Wei *et al.* for example used biocompatible PEG–PLA BCPs in the combination with hydrophobic Fe_3O_4 particles for the formation of nanoparticle loaded polymersomes. By conjugating the polymersomes with a secondary antibody, the structures gained immunolabeling properties, which were probed by the authors on a prostate specific antigen, potentially allowing for their use for the detection of different cancer biomarkers. The polymersome immunosensor's effectiveness was investigated for the detection of different prostate-specific antigen (PSA) concentrations (Fig. 29) and compared well an established enzyme-linked immunosorbent assay (ELISA) method.[195] Based on ultra-small superparamagnetic iron oxide nanoparticles (USPION) bilayer loaded poly(trimethylene carbonate)-*b*-poly(L-glutamic acid) (PTMC-*b*-PGA) polymersomes, Lecommandoux *et al.* created doxorubicin loaded vesicles, which may also serve as magnetic resonance imaging (MRI) contrast agents. The nanoparticle–polymersome hybrid's morphological properties were visualized *via* (cryo-)TEM (Fig. 30 – top-left), AFM and small angle neutron scattering (SANS), while the magnetic properties were analyzed *via* magnetophoresis and with a magnetometer. Furthermore, MRI properties were investigated by measuring the T_1 and T_2 relaxation times of the Fe_3O_4 particles in the bilayer. After loading the polymersomes with doxorubicin, the drug could be released *in vitro* from the vesicles by heating the UPSIONs *via* an oscillating magnetic field.[196] In a follow-up study, Lecommandoux *et al.* investigated the ability of doxorubicin release after the internalization of the magneto-polymersomes in HeLa cells.[197] Besides this, liposomes decorated with a magnetic-hydroxyapatite layer were investigated by Liu *et al.* for ultrasound-triggered drug release.[349] Similarly, and as briefly mentioned in Section 2.4.1, Amstad *et al.*[191] and Qui *et al.*[193] utilized iron oxide particles loaded into the bilayer of

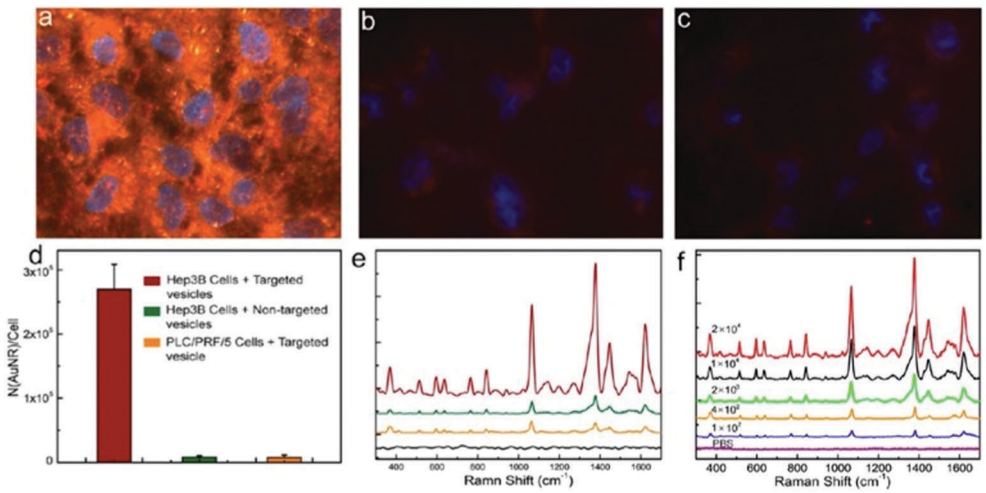

Fig. 28 Hep3B cells cultured with (a) targeted, (b) native and (c) live PLC/PRF/5 cells all incubated with Au@PEG/PLA based colloidal capsules. (d) Vesicles taken up the cells; (e) SERS signals and (f) SERS spectra of Hep3B cells cultured with different vesicles. (Copied with permission from ref. 154. Copyright (2013) American Chemical Society.)

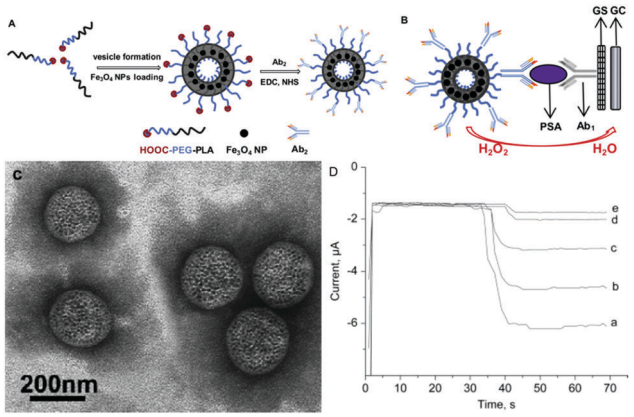

Fig. 29 (A) Scheme of loading process of magneto-polymersomes and (B) immunosensor capabilities; (C) TEM micrograph; (D) immunosensor effectiveness for the detection of PSA (Reprinted from ref. 195, Copyright (2010), with permission from Elsevier.).

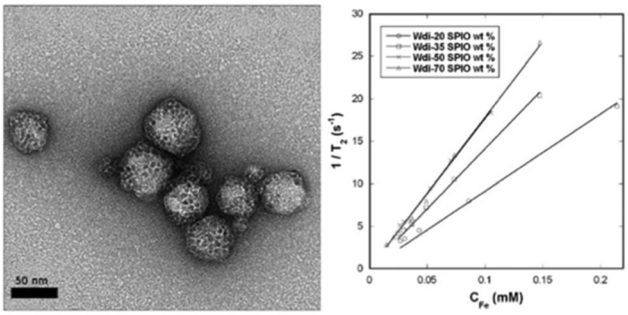

MRI grey level (%)	100	73	54	40	18	2
[Fe] (μM)	0	21	37	49	74	148
C_{weigth} (μg/mL)	0	2.9	5	6.7	10	20
$C_{vesicle}$ (nM)	0	0.25	0.42	0.57	0.85	1.7

Fig. 30 (top-left) TEM micrograph of PTMC-*b*-PGA based polymersomes loaded with iron oxide particles; (top-right) transverse relaxation rates *vs.* iron conc. of magneto-polymersomes loaded with varying iron oxide weight percentages; (bottom) T_2-weighted MRI images and values for concentrations of iron ions in different samples. (Adapted with permission from ref. 196. Copyright (2013) American Chemical Society.)

liposomes, and were able to control the membrane permeability also *via* heating of the iron oxide particles within the bilayer. Both groups used calcein as a model drug to study the release from the magneto-liposomes. Design strategies and functional properties of smart vesicles, including nanoparticle equipped polymersomes, were recently reviewed by Lecommandoux and co-workers.[350]

Further *in vitro* studies for the use of capsules based on protein building blocks, were performed by Mertz and co-workers. Here, as briefly mentioned above, HSA-based capsules were formed on mesoporous silica templates (see Fig. 24 in Section 4.2) and modified with macrocyclic gadolinium (DOTA–Gd) complexes and were investigated for their potential use as MRI contrast agent. T_1-weighted MR imaging showed MRI contrast enhancements for HSA capsules modified with and without siRNA (Fig. 31 – left A and B), which compared well to regulatory approved Gd-based MRI contrast agents. Furthermore, the authors reported investigations on the gene silencing abilities of the HSA capsules, which were probed on A549luc lung carcinoma cell lines *via* quantification of luciferase activity. Depending on the initial siRNA amount throughout the HSA capsules, the gene reporter expression within the A549luc cells could be inhibited up to 80% without Gd-modification and up to 50% with Gd-modification.[129]

5.3 *In vivo* studies of nano-scaled colloidal capsules

Recently, initial preclinical studies to assess a potential future bench-to-bedside translation of colloidal capsules were performed in *in vivo* experiments in various rodent models. As mentioned above, Nie *et al.*[27,150,326] and Song *et al.*[26,151] have both recently published reviews about colloidal capsules from polymer-grafted Au particles, including summaries about recent *in vivo* studies. We recommend these reviews for secondary references and will only marginally discuss the therein reviewed reports. We will start the discussion on *in vivo* studies with recent reports from Song and co-workers, who utilized the EPR effect for passive tumor targeting. Here, for the formation of colloidal capsules, the authors used 8 × 2 nm-sized gold nanorods, which, due to their small size, potentially possess renal clearance capabilities.[331] The resulting capsules featured sizes between 60 and 100 nm, which is theoretically small enough to prevent an accumulation in the reticuloendothelial system, which usually occurs for such structures featuring sizes above 100 nm. The size of these colloidal capsules stand in good accordance to a recent liposome-based study for the ideal size of 50 nm for vesicles with the highest tumor tissue retention.[351] The nanorods were functionalized with PLGA and PEG grafts to form emulsion-based biocompatible colloidal capsules. As PLGA is prone to degrade in an aqueous environment through de-esterification, the capsules were able to nearly completely dissociate to their individual units after 11 days. Resulting from the efficient plasmonic coupling of the nanorods, the vesicles were also investigated for their potential use as photothermal therapy (PTT) vehicles through laser-induced heating, and could further be monitored *in vivo via* photoacoustic (PA) imaging as well as with positron emission tomography (PET) after ^{64}Cu-labeling of the vesicles (Fig. 32). *In vitro* experiments were performed on U87MG human glioma cell lines and all *in vivo* experiments were conducted using glioblastomar carrying U87MG mice. After intraveneous injection of the vesicles, control experiments, using photoacoutic imaging, vesicles showed a higher accumulation in the tumor region in comparison to the individual vesicle-forming gold nanorods. PET imaging revealed a vesicle uptake in the tumors of approx. 9.5% ID g^{-1} after 24 h and a blood half-life of approx. 18 h of vesicles, and the authors conclusively report a major clearance of the vesicles after 10 days of their administration. However, it needs to be noted, that after 10 days, vesicle ID g^{-1} values still reached at least 2.5% in most organs, and a critical value of 5% in the liver. Furthermore, the

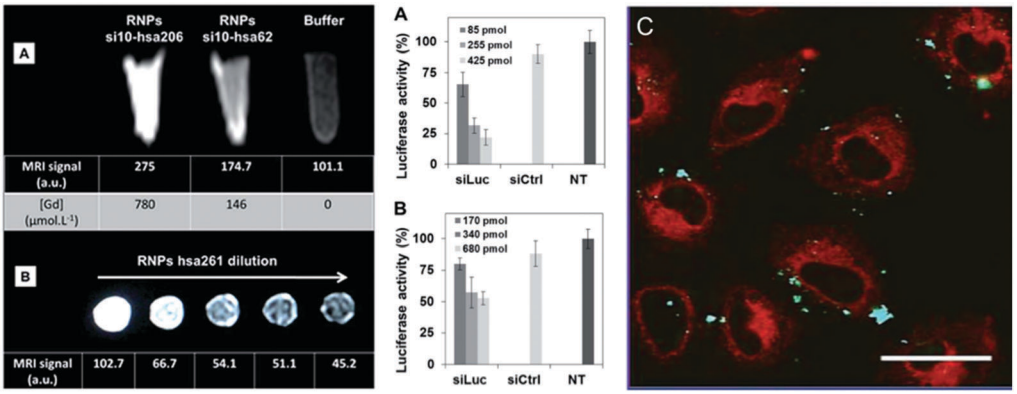

Fig. 31 Left (A) T_1-weighted MRI images of HSA capsules modified with Gd and siRNA (B) T_1-weighted MRI images of HSA capsules modified solely with Gd. Biological *in vitro* tests. Right luciferase activity indicating the gene silencing ability of the siRNA/HSA capsules (A) without and (B) with Gd. (C) Images of A549 cells incubated with Gd and siRNA HSA capsules. (From ref. 129. Reproduced with permission from The Royal Society of Chemistry.)

authors studied photothermal therapy efficiency on xenografted tumor-bearing mice, and were able to reach heat-induced tissue damage within the vesicle containing tumors. However, all tumor-bearing mice reportedly died after 40 to 50 days, due to reoccurrence of the tumor.[52]

In a similar recent study by Song *et al.*, Au-nanorod@PEG/PLGA based vesicles were further equipped with doxorubicin-loaded and PEGylated reduced graphene oxide. Here, the interplay of the plasmonic Au nanorod capsules and the reduced graphene oxide led to enhanced photothermal performance of this hybrid vesicle-like structure. The vesicles featured sizes of approx. 65 nm and in accordance to the study above, the vesicles impact could be monitored *via* PA imaging and *via* PET imaging after ^{64}Cu-labeling. Fig. 33a shows 2D and 3D ultrasound photoacoustic images of U87MG tumor-bearing mice, and Fig. 33b the different PA intensities of the vesicles with and without graphene oxide. Vesicles labeled with ^{64}Cu allowed for PET imaging, reportedly showing a blood half-life of approx. 19.6 h of the vesicles (Fig. 33c) and a corresponding tumor uptake which increased from 0.79% after 1 h to approx. 9.7% ID g^{-1} after 24 h (Fig. 33d and e). Furthermore, using 808 nm, 0.25 W cm^{-2} laser light irradiation, the authors reported to be able to utilize the photothermal abilities of the vesicles to increase the tumor temperature, causing the vesicles to disrupt and leading to a controlled release of the encapsulated doxorubicin. These chemo-photothermal therapy properties of vesicles were assessed using thermographic imaging and monitoring the temperature change in the tumor region (Fig. 34a and b). The authors observed no difference in therapeutic efficiency for vesicles with and without doxorubicin for the first 5 days. Over a longer time span, the tumor growth in mice treated with doxorubicin loaded vesicles was delayed in comparison to DOX-free vesicles. This led to an increased life-span of the Au-vesicle-dox treated mice (>40 d) in comparison to free DOX and native Au-vesicles (20–26 d) (Fig. 34d). Additionally, tissue sections of differently treated tumors showed most severe cancer necrosis and least cancer cells for the DOX-loaded Au-vesicles in comparison to the other samples (Fig. 34e).[155] In conclusion, these two studies by Song *et al.* represent seminal approaches for further *in vivo* studies of similar kind, where good practice is applied and guidelines for the synthesis for nanomedicine structures are followed. Their use of gold nanorods as the shell-forming building blocks, which potentially possess favourable clearance properties in comparison to larger particles or spherical gold colloids, builds a fundament for future studies in this field. However, besides the beneficial short-term therapeutic effects the potential negative long-term consequences of the gold nanoparticles should be investigated in more detail in future studies.[352,353]

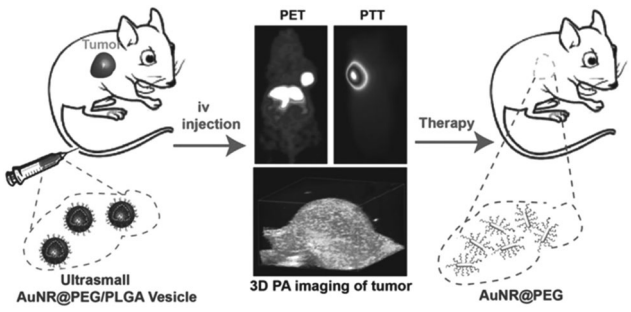

Fig. 32 Scheme of vesicle administration to mice and their subsequent erosion to individual building blocks after PET and PA imaging was applied (Reproduced with permission from ref. 52. Copyright 2015, Wiley-VCH Verlag GmbH & Co. KGaA.).

Nie *et al.* also performed *in vivo* experiments utilizing vesicles formed from BCP-tethered gold colloids. In initial *in vivo* experiments Nie *et al.* used a xenograft model of mice bearing 4T1 tumors. Vesicles formed from PEG–PS–BCP coated 40 nm sized Au NP were intratumorally injected and heated *via* 808 nm laser irradiation. The authors reported good therapeutic efficacy, as the tumors were ablated and showed no reoccurrence.[144] Following this report, Nie and co-workers synthesized Au NP based vesicles, encapsulating a photosensitizer chlorine e6 (Ce6) within their hollow interior (Fig. 35 – left). The vesicles were assembled from PEO_{45}-*b*-PS_{245} mediated 26 nm sized Au core-NP and featured average diameters of approx. 280 nm. The vesicles possessed intrinsic fluorescent, thermal, and photoacoustic properties which could reportedly be utilized for photothermal treatment by heating the vesicular Au NP membrane

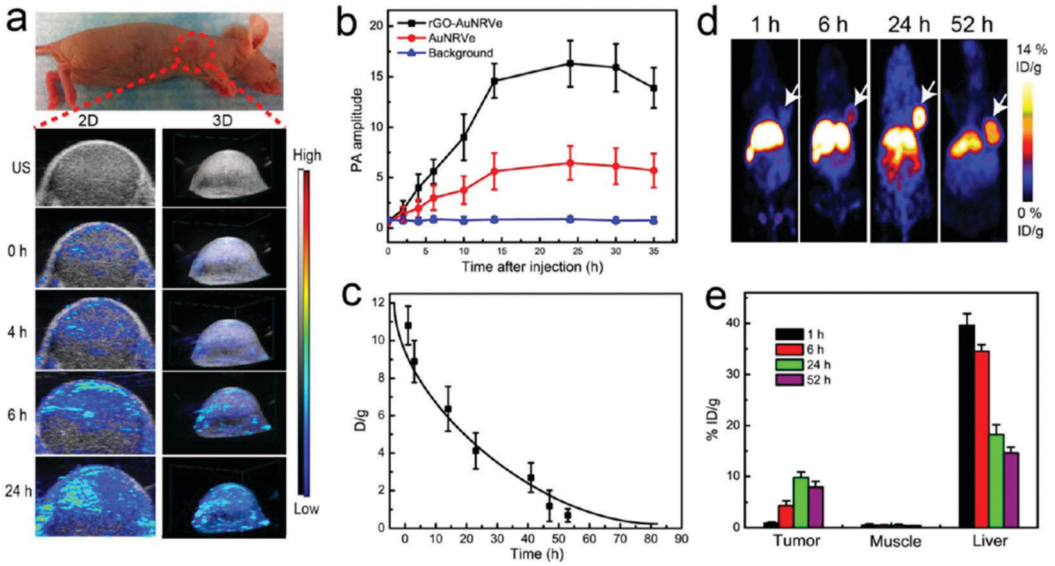

Fig. 33 (a) *In vivo* images acquired *via* ultrasound and photoacoustic measurements; (b) PA values of tumor region; (c) biodistribution of 64Cu labeled colloidal capsules; (d) coronal PET images after administration of vesicles; (e) biodistribution of vesicles in different organs (Adapted with permission from ref. 155. Copyright (2015) American Chemical Society.).

and photodynamic therapy (PDT)[354] by using the singlet oxygen ($^1O_2$) species produced by the Ce6 photosensitizer upon light irradiation, to treat malignant cells. *In vitro* in a MDA-MB-435 human breast cancer cell line, the authors were able to dissociate the Au NP vesicles through photothermal activation, causing the Ce6 to be released. This was quantified by measuring the fluorescent signal of singlet oxygen sensor green (SOSG), which is reportedly altered by reacting with the singlet oxygen created by the Ce6. The vesicles were taken up by the cells *via* an endocytic-pathway and were mainly found within lysosomes of the cells. Furthermore, the cell experiments showed decreased cell viability for cells incubated with Ce6-functionalized Au NP vesicles and treated via PDT/PTT in comparison to free Ce6 and unloaded Au NP vesicles. For *in vivo* experiments, the authors used mice with MDA-MB-435 breast cancer xenografts, and Ce6 loaded vesicles were again intratumorally administered. The authors then used *in vivo* fluorescence, thermal, and photoacoustic imaging to track the tumor (Fig. 35a, b and d). The PTT effectiveness was investigated by increasing the temperature of the tumor to above 42 °C *via* laser irradiation (Fig. 35c), whilst tissue in close proximity to the tumor was barely affected. The Ce6 mediated Au NP vesicles exhibited the highest therapeutic efficacy in comparison to control experiments, indicating promising theranostic abilities of these structures.[159]

In another report from Nie and co-workers, the PS block was substituted with polycaprolactone (PCL), to increase the biocompatibility of the used BCPs and the resulting vesicles. PCL reportedly features a melting of approx. 60 °C enabling its degradation through thermal heating of the Au NP vesicles. The vesicles featured a strong plasmonic coupling effect, shifting the LSPR peaks to NIR wavelengths. This shift was again used for *in vivo* PTT experiments in combination with rapid clearance of the individual Au NP after vesicle dissociation. The *in vivo* experiments were again performed by intratumorally injecting the vesicles in mice bearing MDA-MB-435 tumor xenografts. Experimental methodology was applied in accordance to the above discussed paper by Song and co-workers. PA and PT imaging was applied and the PTT effectiveness was assessed for Au NP vesicles. Tumor growth could be efficiently slowed and no reoccurrence was observed in mice treated with vesicles, in comparison to a control group. The overall therapeutic efficacy was the highest for the PCL based vesicles, in comparison to free gold nanorods or PS based vesicles. The life span of the mice treated with PCL vesicles was greater than 30 days, whilst the average life span of the other groups was between 14 and 20 days. Due to their size, the vesicles were mainly taken up by the RES system, *i.e.* mainly in the liver and spleen, which were cleared 8 days post injection.[50] Nie *et al.* were also able to further tailor the build-up of nanoparticles within a Au NP-PS-*b*-PEO vesicle membrane, leading to string-like arrangements. These NP 'chain vesicles' posses an eightfold increased PA imaging efficiency over non-chained vesicles and also allow for a NIR induced release of an encapsulated model drug (Rhodamine B). Nude mice were subcutaneously injected with the vesicles and irradiated with NIR laser light. The increased efficiency of the chain vesicles was then visualized *via* PA imaging.[162] Further *in vivo* studies were performed by Nie *et al.* with magnetic and plasmonic janus vesicles comprising a densely loaded membrane of gold NP and Fe_3O_4 NP. Due to plasmonic coupling and ordering of the particles, the structures featured shifted NIR peaks towards higher wavelengths and also exhibited an enhanced transverse relaxation effect, allowing the structures to be utilized as contrast agents in PA and T_2-weighted MR imaging. The authors also demonstrated the controlled destruction of the structures triggered by NIR light in combination with a controlled release of a model drug through a magnetic field.

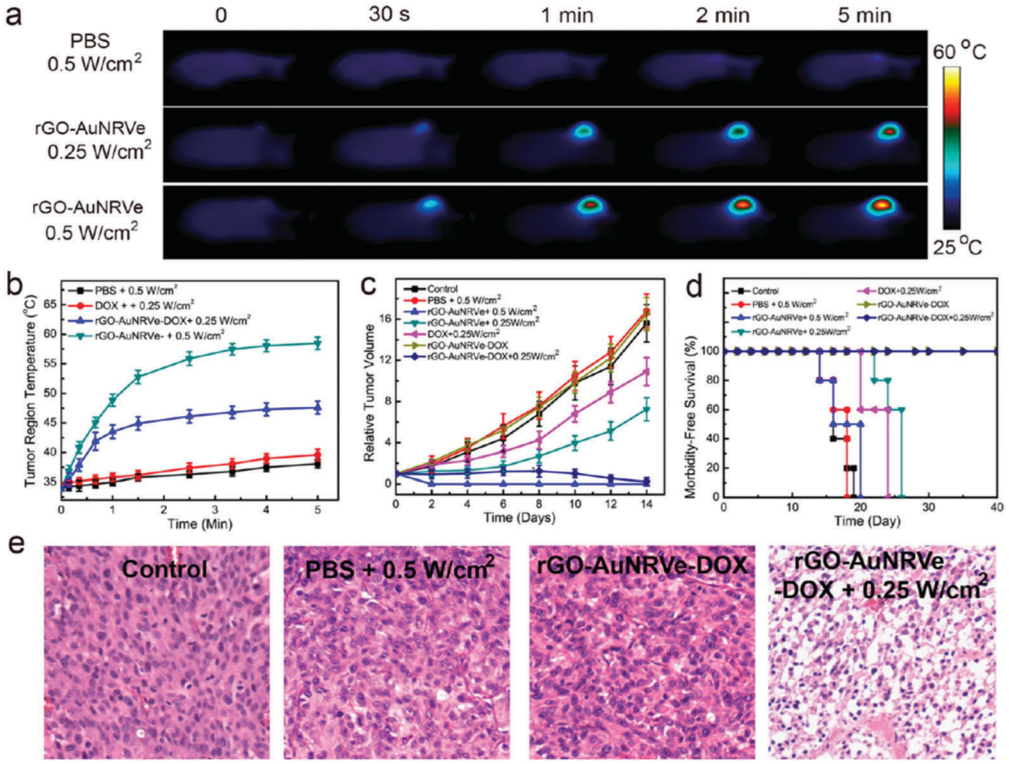

Fig. 34 (a) Thermal images of the tumor region injected with Au NP vesicles and (b) resulting temperature change after irradiation with a 808 nm laser. (c) Relative tumor volume of the tumor-bearing mice and (d) comparison of survival curves of mice receiving varying treatments. (e) Comparison of tumor tissue sections, showing a more severe cancer necrosis and fewer cancer cells for treatment with DOX-loaded Au NP vesicles. (Adapted with permission from ref. 155. Copyright (2015) American Chemical Society.)

For the *in vivo* studies U87MG tumor-bearing athymic nude mice were intravenously injected with hemispherical janus. Targeting towards the tumors was performed with an external magnet and identified *via* MR and PA imaging.[202]

The possibility to combine various types of materials with exploitable properties to create synergies for combined drug targeting and bioimaging is one of the central characteristic colloidal capsules possess and which sets them apart from most other vesicles and nanocapsules. The studies provided by Nie *et al.* describe pioneering works for the use of multifunctional colloidal capsules for bionanotechnology, which aim to utilize the full potentials of the colloidal capsule building block system. In future studies, it would be particularly interesting to further miniaturize the capsules towards diameters below 100 nm for the utilization of size-depended clearance pathways[330,355] after capsule erosion.

In a report from another group, Deng *et al.* applied a grafting-TO approach, similar to previously reported works from Song *et al.*, to functionalize 14 nm Au NP with hydrophilic poly-2-(2-methoxyethoxy) ethyl methacrylate ($PMEO_2MA$) and hydrophobic PCL polymer grafts. The authors also observed a shift of the LSPR to (near) infrared wavelengths. PT imaging was applied for *in vivo* experiments of female BALB/c nude mice which, following subcutaneous MCF-7 cell injection, beard MCF-7 tumors. Au NP based vesicles were intratumorally injected into the mice and could be visualized *via* PT imaging. Enhanced PTT characteristics were observed for larger Au NP vesicles, allowing for ablation of the tumors leading to complete tumor regression. The vesicles were also investigated by the authors as X-ray CT contrast agents, owing to their high absorption coefficient. The contrast of the tumor tissue could be greatly enhanced post injection of the Au NP vesicles (Fig. 36A and B) and subsequently allowed for three-dimensional visualization of the tumor (Fig. 36C).[300]

Rotello and co-workers used dendrimers to stabilize the shell of paclitaxel-loaded colloidal nanocapsules, which were formed from 2 nm-sized Au core particles. The authors used poly(amido amine) (PAMAM) dendrimers in combination with dithiocarbamate (DTC) chemistry for the cross-linking of the shell. B16F10 skin melanoma cell lines were incubated with the capsules to investigate their impact on cell viability. The cell lines were monitored via flow cytometry and ICP-MS analysis and reportedly showed good cellular uptake. Unloaded capsules showed low cytotoxicity and paclitaxel loaded capsules were more effective in decreasing cell viability in comparison to free paclitaxel. For *in vivo* studies, the authors used female C57BL6 mice with ages of 8–10 weeks, and weights between 20 and 25 g. B16F10 cells were injected into the mice, which were used for the studies after tumor sizes reached 100 mm^3. Thereafter, 100 nm-sized paclitaxel-loaded capsules were administered intravenously and accumulated in various organs, as well as in the tumors, which the authors attributed to the passive targeting capabilities of the capsules, caused by the EPR effect. The authors observed notable decrease of tumor growth in mice treated with

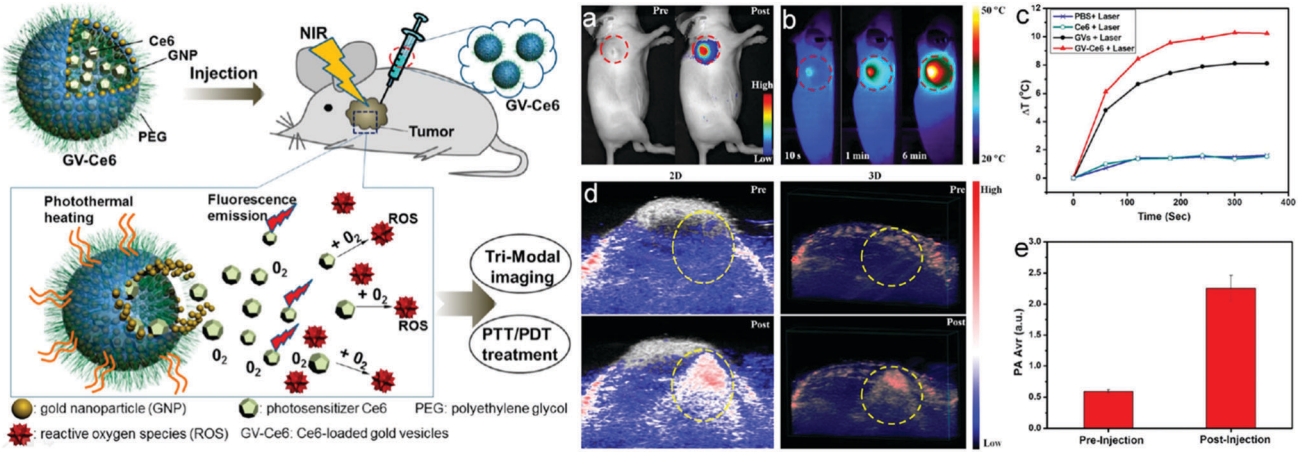

Fig. 35 Left: Scheme of vesicle injection and Ce6 release; right: (a) NIR fluorescence and (b) thermal images of a tumor-bearing mouse, (c) tumor heat response to laser irradiation; (d) photoacoustic images and; (e) intensities of tumor tissues (Adapted with permission from ref. 159. Copyright (2015) American Chemical Society.).

paclitaxel-loaded capsules, in comparison to paclitaxel-free capsules.[356] For future studies, the elucidation of intra-organ biodistribution as well as clearance properties of the individual particles of the eroded capsules would be of significant interest.

In addition to these Au NP based *in vivo* studies, other groups have performed initial works in rodent models with iron oxide based colloidal capsules. These works focused on the sparely and closely packed integration of iron oxide particles in the shell of polymeric nano-[357] and microbubbles.[358,359] These gas-filled structures which feature a polymer shell, are being extensively explored as contrast agents in ultrasonography, magnetic resonance imaging and in single photon emission computer tomography (SPECT) imaging. The structures usually feature sizes on the border of the micro–nano-scale, with diameters above or slightly below 1 μm. Brismar *et al.* reported initial work in this field by investigating magnetic nanoparticle coated microbubbles for MRI and computer tomography. The structures were prepared by loading 8–10 nm sized aminated SPIONs into the shell or onto the surface of poly(vinyl alcohol) and chitosan based microbubbles. The resulting structures featured sizes of approx. 3.8 μm and exhibited superparamagnetic properties, which was evidenced using vibrating sample magnetometer measurements. The authors performed preliminary proof-of-concept experiments for the use of the structures as visualizing agents in magnetic resonance imaging by administrating the structures to rats.[360] In a follow-up report, microbubbles with enhanced multimodality imaging properties were investigated in male Sprague Dawley rats.[361] Recently, Duan *et al.* templated γ-Fe_2O_3 NP against PVA/PLLA microbubbles and investigated the structures as potential agents in magnetic resonance/ultrasound (MR/US) imaging. The authors were able to tailor the T_2 MR contrast by increasing the amount of particles templated on the surface. *In vivo* studies were performed with tumor bearing female BALB/C nude mice which were beforehand injected with COLO-205 cells. MRI imaging was then applied by the authors after intratumoral injection of the SPION templated microbubbles, which resulted in a decrease of the T_2 signal, overall improving the MR imaging results in comparison to the state prior to injection.[362] Similar structures with decreased sizes of approx. 180–200 nm, *i.e.* SPION mediated nanobubbles, were reported by Huang and co-workers. The nanobubbles were prepared from perfluoropentane and PAA–F127 thermosensitive polymers and approx. 5 nm-sized SPIONs.[28]

5.4 Conclusions for colloidal capsules for biological applications

The above described initial experiments represent promising first approaches for the use of nano-scaled colloidal capsules in nanomedicine. However, besides the positive short-term effects

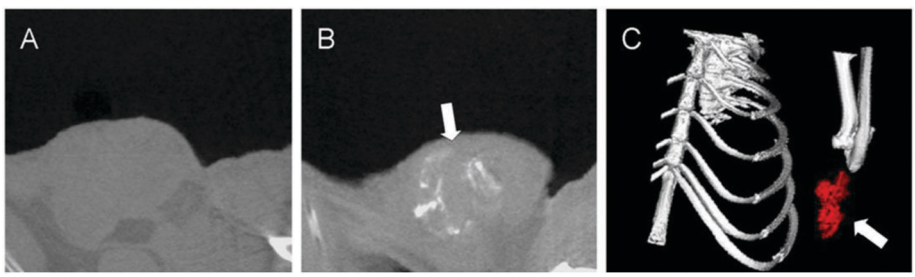

Fig. 36 (A) X-ray computed tomography images of tumor-bearing mice prior, (B) after administration of gold colloid assemblies with diameters of approx. 500 nm leading to an increased Hounsfield Unit value, and (C) 3D CT image of tumor tissue (marked in red) (from ref. 300. Copied with permission from Ivyspring International Publisher (2014)).

these novel nano-pharmaceutical agents show, the mid- and long-term biological fate of the particles, *i.e.* biodistribution and clearance, effects on cell cycling and cell signaling processes, *etc.*, remain greatly unknown. A complete understanding of the individual shell-forming nanoparticles needs to be fully established in future studies before their use in biological applications should be considered.

Generally, the huge and still growing field of nanomedicine[363] with its claim for novel ways to cure diseases has recently raised critical voices and has led to significant debate,[364–369] questioning whether this field will anytime soon return the credit it received in advance. Numerous aspects such as EPA law, FDA law, ethics, environmental health, safety and toxicity[370] along with standardization need to be taken into account for the above nanoparticle types to be considered for in-human use over organic components such as amphiphiles, peptides, proteins or FDA-approved biocompatible polymers (*i.e.* PLGA or PCL). A multitude of factors need to be considered for nanocarrier design,[371] including particle/capsule size and morphology,[351,372–374] surface charge,[375] particle/capsule hardness, potential capsule deformability, complete renal clearance capabilities,[319] active/passive targeting (EPR effect),[333] precise design for biological barrier interaction,[366] pathways for cellular uptake,[376] and surface functionalization with *e.g.* PEG[377] or PEEP[378] for tailored blood half-life (stealthing). Furthermore, a pivotal role is attributed to the formation of a protein corona[379–381] on nanoparticles in biological media which can lead to loss of the receptor targeting ability of protein, antibody or other biomolecule functionalizations on nanoparticles/nanocapsules and which can facilitate rapid macrophage uptake and clearance of the biofunctional colloids.[380] Here, ultrasmall nanoparticles with a zwitterionic coating[382] or certain moieties with tunable hydrophobicity[383] are of increasing interest as they have shown to inhibit biomolecular corona formation effectively and should be considered for new colloidal capsule studies that aim at *in vivo* applications. However, various pharmacokinetic and biodistribution properties, such as intracellular trafficking,[384] organelle targeting, or suborgan biodistribution[385] of (ultrasmall) nanoparticles with distinct surface functionalizations, are still greatly unexplored.[325] These and other short and long-term[352] nanotoxicological[386] factors demand for highly specific designs of studies by all researchers in this field.[327,387] Also, since humans, by nature, are not capable of metabolizing most types of synthetic nanoparticles, the full clearance, *e.g.* by the renal route,[319,330,331] of non-biodegradable particles are an absolute prerequisite for a potential in-human use, especially in consideration of the discontinuation of the clinical use of some previous nanoparticle agents[323] (*i.e.* Ferucarbotran, Ferumoxstran, Ferumoxides). With this said, it will be exciting to see if a general rationale as well as feasible synthetic routes will be found to add colloidal capsules formed from the above described material classes as an alternative to already approved[363] nanomedicial agents formed from natural amphiphile molecules or protein building blocks, like, Doxil® (doxorubicin HCl liposome injection), DaunoXome® (daunorubicin citrate liposome injection) or Abraxane® (albumin-bound paclitaxel). Additionally, the reports of more and more pre-clinical systems tailored for drug-delivery applications of nanocarriers emphasize the need for other nanomedical agents than just tumors[388] in the future, *e.g.* for cancer immunotherapy[389] or the treatment of endothelial disorders[390] and pulmonary diseases.[391]

6. Conclusions and outlook

Great advancements have been achieved in the development of colloidal capsules in the last two decades, including the establishment of a reproducible synthesis route for the fabrication of monodisperse micron-sized capsules, the miniaturization of the capsules combined with the integration of distinct functionalities, and the synthesis of biocompatible nano-scaled capsules with tailored erosion properties as novel nano-pharmaceutical agents. We have reviewed the initial reports and recent literature on colloidal capsules. By reviewing the above described synthesis routes, *i.e.* (1) interfacial colloidal particle self-assembly on emulsion droplets; (2) colloidal templating against hard or soft particles; (3) solvent change induced assembly of polymer-grafted amphiphilic colloids; and (4) dense membrane nanoparticle-loading of liposomes/polymersomes, we aim at unifying the discussion on colloidal capsules and with that, facilitate communication and further progress in this nascent research field.

However, some critical aspects also have to be noted. The characterization of the capsules is often incomplete as repeatedly just one or a few of the following capsule properties are provided in detail, *i.e.*; colloidal stability in various media, erosion kinetics of the capsules, size and polydispersity, topological (*i.e.* membrane permeability), shell (*i.e.* degree of order of particles), and internal structural build-up, mechanical stability in liquid media and dried state, as well as chemical composition (*i.e.* functional groups or ligands). With biomedical applications in mind, it is especially critical to study these material properties in biological environments, as the presence of components from the media/blood, like blood cells, proteins, and salts can drastically alter colloidal stability, surface properties and degradability of the colloidal capsules. As a result, with many reported colloidal capsule systems it is not clear if the production of these capsules can be scaled to allow further development of the capsule system in a biological context.

Furthermore, while the mechanisms of the adsorption and desorption of colloidal particles at planar interfaces are well studied the understanding of the behaviour of nanoparticles at the interface of nano-emulsions is far from complete. A recent study on the organization of colloids at the interface of micron-sized emulsion droplets might be a starting point for future studies.[81] van der Waals, electrostatic double-layer, solvation, and hydrodynamic drag forces as well as Brownian motion, are the driving forces within self-assembly processes,[266,392] though little efforts have been undertaken in most studies to characterize these forces within a respective colloidal capsule synthesis route. A deeper understanding of the pair-wise and multi-component interactions (*i.e.* colloid–colloid, colloid–solvent, colloid–salts and, if present, colloid–template) could provide a better general prediction of the structural outcome of capsules prior to their synthesis. This calls for the development of novel measurement

techniques that can monitor the mentioned properties *in situ* and at the nanoscale as well as fundamental research on thin films at fluid interfaces and the non-trivial interactions during the colloidal assembly of multicomponent nanoparticles. For instance, the recent development of liquid cells for *in situ* liquid TEM may allow the visualization and improved understanding of some colloidal capsule formation and other nanoparticle self-assembly processes in the future.[393,394] Naturally, these experimental techniques should be supplemented with computer simulations at various scales (atomistic modeling of interfaces, coarse grain models for particle interactions, *etc.*) which can provide useful theoretical predictions and support the rational design of colloidal capsules.

Hence, plenty of hard work remains for advancing the broad field of colloidal capsule research which is currently one of the most exciting fields in colloid chemistry. We are looking forward to witness the development of many more sophisticated structures that surpass simple colloidal particles, other nano- and micro-capsules, and vesicles by featuring a range of tailor-made properties for specific advanced applications.

Acknowledgements

We are grateful for funding by the German Research Foundation (DFG) by the grants MA4795/5-1 and /5-2.

References

1 R. Gref, Y. Minamitake, M. T. Peracchia, V. Trubetskoy, V. Torchilin and R. Langer, *Science*, 1994, **263**, 1600–1603.
2 S. Gouin, *Trends Food Sci. Technol.*, 2004, **15**, 330–347.
3 C. S. Peyratout and L. Dähne, *Angew. Chem., Int. Ed.*, 2004, **43**, 3762–3783.
4 R. Akiyama and S. Kobayashi, *Chem. Rev.*, 2009, **109**, 594–642.
5 G. Nelson, *Int. J. Pharm.*, 2002, **242**, 55–62.
6 G. Gregoriadis, *FEBS Lett.*, 1973, **36**, 292–296.
7 V. P. Torchilin, *Nat. Rev. Drug Discovery*, 2005, **4**, 145–160.
8 W. T. Al-Jamal and K. Kostarelos, *Acc. Chem. Res.*, 2011, **44**, 1094–1104.
9 L. Zhang and A. Eisenberg, *Science*, 1995, **268**, 1728–1731.
10 B. M. Discher, Y.-Y. Won, D. S. Ege, J. C.-M. Lee, F. S. Bates, D. E. Discher and D. A. Hammer, *Science*, 1999, **284**, 1143–1146.
11 D. E. Discher and A. Eisenberg, *Science*, 2002, **297**, 967–973.
12 A. D. Dinsmore, M. F. Hsu, M. G. Nikolaides, M. Marquez, A. R. Bausch and D. A. Weitz, *Science*, 2002, **298**, 1006–1009.
13 J.-W. Kim, A. Fernández-Nieves, N. Dan, A. S. Utada, M. Marquez and D. A. Weitz, *Nano Lett.*, 2007, **7**, 2876–2880.
14 M. Liu, Q. Tian, Y. Li, B. You, A. Xu and Z. Deng, *Langmuir*, 2015, **31**, 4589–4592.
15 J. He, Y. Liu, T. Babu, Z. Wei and Z. Nie, *J. Am. Chem. Soc.*, 2012, **134**, 11342–11345.
16 X.-C. Yang, B. Samanta, S. S. Agasti, Y. Jeong, Z.-J. Zhu, S. Rana, O. R. Miranda and V. M. Rotello, *Angew. Chem., Int. Ed.*, 2011, **50**, 477–481.
17 Z. Cao, A. Schrade, K. Landfester and U. Ziener, *J. Polym. Sci., Part A: Polym. Chem.*, 2011, **49**, 2382–2394.
18 D. Patra, A. Sanyal and V. M. Rotello, *Chem. – Asian J.*, 2010, **5**, 2442–2453.
19 F. Caruso, R. A. Caruso and H. Möhwald, *Science*, 1998, **282**, 1111–1114.
20 Z. Nie, D. Fava, E. Kumacheva, S. Zou, G. C. Walker and M. Rubinstein, *Nat. Mater.*, 2007, **6**, 609–614.
21 R. Tang, C. S. Kim, D. J. Solfiell, S. Rana, R. Mout, E. M. Velázquez-Delgado, A. Chompoosor, Y. Jeong, B. Yan, Z.-J. Zhu, C. Kim, J. A. Hardy and V. M. Rotello, *ACS Nano*, 2013, **7**, 6667–6673.
22 C. Wu, S. Bai, M. B. Ansorge-Schumacher and D. Wang, *Adv. Mater.*, 2011, **23**, 5694–5699.
23 A.-M. Cao, J.-S. Hu, H.-P. Liang and L.-J. Wan, *Angew. Chem., Int. Ed.*, 2005, **44**, 4391–4395.
24 A. Rogach, A. Susha, F. Caruso, G. Sukhorukov, A. Kornowski, S. Kershaw, H. Möhwald, A. Eychmüller and H. Weller, *Adv. Mater.*, 2000, **12**, 333–337.
25 N. Vogel, S. Utech, G. T. England, T. Shirman, K. R. Phillips, N. Koay, I. B. Burgess, M. Kolle, D. A. Weitz and J. Aizenberg, *Proc. Natl. Acad. Sci. U. S. A.*, 2015, **112**, 10845–10850.
26 J. Song, P. Huang, H. Duan and X. Chen, *Acc. Chem. Res.*, 2015, **48**, 2506–2515.
27 Y. Liu, Y. Liu, J.-J. Yin and Z. Nie, *Macromol. Rapid Commun.*, 2015, **36**, 711–725.
28 H.-Y. Huang, S.-H. Hu, S.-Y. Hung, C.-S. Chiang, H.-L. Liu, T.-L. Chiu, H.-Y. Lai, Y.-Y. Chen and S.-Y. Chen, *J. Controlled Release*, 2013, **172**, 118–127.
29 E. Herz, A. Burns, S. Lee, P. Sengupta, D. Bonner, H. Ow, C. Liddell, B. Baird and U. Wiesner, *Fluorescent core-shell silica nanoparticles: an alternative radiative materials platform*, 2006, vol. 6096, p. 609605.
30 T. Bollhorst, S. Shahabi, K. Wörz, C. Petters, R. Dringen, M. Maas and K. Rezwan, *Angew. Chem., Int. Ed.*, 2015, **54**, 118–123.
31 O. Chen, L. Riedemann, F. Etoc, H. Herrmann, M. Coppey, M. Barch, C. T. Farrar, J. Zhao, O. T. Bruns, H. Wei, P. Guo, J. Cui, R. Jensen, Y. Chen, D. K. Harris, J. M. Cordero, Z. Wang, A. Jasanoff, D. Fukumura, R. Reimer, M. Dahan, R. K. Jain and M. G. Bawendi, *Nat. Commun.*, 2014, **5**, 5093.
32 M. Pang, A. J. Cairns, Y. Liu, Y. Belmabkhout, H. C. Zeng and M. Eddaoudi, *J. Am. Chem. Soc.*, 2013, **135**, 10234–10237.
33 C. Huo, M. Li, X. Huang, H. Yang and S. Mann, *Langmuir*, 2014, **30**, 15047–15052.
34 W. Cao, R. Huang, W. Qi, R. Su and Z. He, *ACS Appl. Mater. Interfaces*, 2015, **7**, 465–473.
35 M. Maas, T. Bollhorst, R. N. Zare and K. Rezwan, *Part. Part. Syst. Charact.*, 2014, **31**, 1067–1071.
36 V. N. Paunov and M. in het Panhuis, *Nanotechnology*, 2005, **16**, 1522.
37 M. Karg, Y. Lu, E. Carbó-Argibay, I. Pastoriza-Santos, J. Pérez-Juste, L. M. Liz-Marzán and T. Hellweg, *Langmuir*, 2009, **25**, 3163–3167.
38 P. F. Noble, O. J. Cayre, R. G. Alargova, O. D. Velev and V. N. Paunov, *J. Am. Chem. Soc.*, 2004, **126**, 8092–8093.
39 K. L. Thompson, P. Chambon, R. Verber and S. P. Armes, *J. Am. Chem. Soc.*, 2012, **134**, 12450–12453.

40 Z. Wang, M. C. M. van Oers, F. P. J. T. Rutjes and J. C. M. van Hest, *Angew. Chem., Int. Ed.*, 2012, **51**, 10746–10750.
41 R. Chandrawati, L. Hosta-Rigau, D. Vanderstraaten, S. A. Lokuliyana, B. Städler, F. Albericio and F. Caruso, *ACS Nano*, 2010, **4**, 1351–1361.
42 J. T. Russell, Y. Lin, A. Böker, L. Su, P. Carl, H. Zettl, J. He, K. Sill, R. Tangirala, T. Emrick, K. Littrell, P. Thiyagarajan, D. Cookson, A. Fery, Q. Wang and T. P. Russell, *Angew. Chem., Int. Ed.*, 2005, **44**, 2420–2426.
43 X. Huang, M. Li, D. C. Green, D. S. Williams, A. J. Patil and S. Mann, *Nat. Commun.*, 2013, **4**, 2239.
44 M. Li, R. L. Harbron, J. V. M. Weaver, B. P. Binks and S. Mann, *Nat. Chem.*, 2013, **5**, 529–536.
45 M. Li, X. Huang, T.-Y. D. Tang and S. Mann, *Curr. Opin. Chem. Biol.*, 2014, **22**, 1–11.
46 S. Sun, M. Li, F. Dong, S. Wang, L. Tian and S. Mann, *Small*, 2016, **12**, 1920–1927.
47 R. Tamate, T. Ueki and R. Yoshida, *Angew. Chem., Int. Ed.*, 2016, **55**, 5179–5183.
48 X. Huang, A. J. Patil, M. Li and S. Mann, *J. Am. Chem. Soc.*, 2014, **136**, 9225–9234.
49 J. Song, L. Cheng, A. Liu, J. Yin, M. Kuang and H. Duan, *J. Am. Chem. Soc.*, 2011, **133**, 10760–10763.
50 P. Huang, J. Lin, W. Li, P. Rong, Z. Wang, S. Wang, X. Wang, X. Sun, M. Aronova, G. Niu, R. D. Leapman, Z. Nie and X. Chen, *Angew. Chem., Int. Ed.*, 2013, **52**, 13958–13964.
51 Y. Jiang, R. Tang, B. Duncan, Z. Jiang, B. Yan, R. Mout and V. M. Rotello, *Angew. Chem., Int. Ed.*, 2015, **54**, 506–510.
52 J. Song, X. Yang, O. Jacobson, P. Huang, X. Sun, L. Lin, X. Yan, G. Niu, Q. Ma and X. Chen, *Adv. Mater.*, 2015, **27**, 4910–4917.
53 Z. Lu and Y. Yin, *Chem. Soc. Rev.*, 2012, **41**, 6874–6887.
54 J. K. Stolarczyk, A. Deak and D. F. Brougham, *Adv. Mater.*, 2016, **28**, 5400–5424.
55 O. D. Velev, K. Furusawa and K. Nagayama, *Langmuir*, 1996, **12**, 2374–2384.
56 O. D. Velev, K. Furusawa and K. Nagayama, *Langmuir*, 1996, **12**, 2385–2391.
57 O. D. Velev and K. Nagayama, *Langmuir*, 1997, **13**, 1856–1859.
58 S. U. Pickering, *J. Chem. Soc., Trans.*, 1907, **91**, 2001–2021.
59 W. Ramsden, *Proc. R. Soc. London*, 1903, **72**, 156–164.
60 F. J. Rossier-Miranda, C. G. P. H. Schroën and R. M. Boom, *Colloids Surf., A*, 2009, **343**, 43–49.
61 J. Wu and G.-H. Ma, *Small*, 2016, **12**, 4633–4648.
62 K. L. Thompson, M. Williams and S. P. Armes, *J. Colloid Interface Sci.*, 2015, **447**, 217–228.
63 H. N. Yow and A. F. Routh, *Langmuir*, 2008, **25**, 159–166.
64 S. Laïb and A. F. Routh, *J. Colloid Interface Sci.*, 2008, **317**, 121–129.
65 O. J. Cayre, P. F. Noble and V. N. Paunov, *J. Mater. Chem.*, 2004, **14**, 3351.
66 C. Wang, H. Liu, Q. Gao, X. Liu and Z. Tong, *ChemPhysChem*, 2007, **8**, 1157–1160.
67 H. Duan, D. Wang, N. S. Sobal, M. Giersig, D. G. Kurth and H. Möhwald, *Nano Lett.*, 2005, **5**, 949–952.
68 K. L. Thompson, S. P. Armes, J. R. Howse, S. Ebbens, I. Ahmad, J. H. Zaidi, D. W. York and J. A. Burdis, *Macromolecules*, 2010, **43**, 10466–10474.
69 P. Arumugam, D. Patra, B. Samanta, S. S. Agasti, C. Subramani and V. M. Rotello, *J. Am. Chem. Soc.*, 2008, **130**, 10046–10047.
70 A. Walsh, K. L. Thompson, S. P. Armes and D. W. York, *Langmuir*, 2010, **26**, 18039–18048.
71 A. Schmid, J. Tonnar and S. P. Armes, *Adv. Mater.*, 2008, **20**, 3331–3336.
72 Y. Chen, C. Wang, J. Chen, X. Liu and Z. Tong, *J. Polym. Sci., Part A: Polym. Chem.*, 2009, **47**, 1354–1367.
73 S. A. F. Bon, S. Cauvin and P. J. Colver, *Soft Matter*, 2007, **3**, 194–199.
74 O. J. Cayre and S. Biggs, *J. Mater. Chem.*, 2009, **19**, 2724.
75 *Colloidal Particles at Liquid Interfaces*, ed. B. P. Binks and T. S. Horozov, Cambridge University Press, Cambridge, New York, 1st edn, 2006.
76 P. Pieranski, *Phys. Rev. Lett.*, 1980, **45**, 569–572.
77 B. P. Binks and J. H. Clint, *Langmuir*, 2002, **18**, 1270–1273.
78 Y. Lin, H. Skaff, T. Emrick, A. D. Dinsmore and T. P. Russell, *Science*, 2003, **299**, 226–229.
79 *Particle-Stabilized Emulsions and Colloids*, ed. T. Ngai and S. Bon, Royal Society of Chemistry, Cambridge, 2014.
80 G. Boniello, C. Blanc, D. Fedorenko, M. Medfai, N. B. Mbarek, M. In, M. Gross, A. Stocco and M. Nobili, *Nat. Mater.*, 2015, **14**, 908–911.
81 G. Meng, J. Paulose, D. R. Nelson and V. N. Manoharan, *Science*, 2014, **343**, 634–637.
82 M. Destribats, S. Gineste, E. Laurichesse, H. Tanner, F. Leal-Calderon, V. Héroguez and V. Schmitt, *Langmuir*, 2014, **30**, 9313–9326.
83 H. Wang, V. Singh and S. H. Behrens, *J. Phys. Chem. Lett.*, 2012, **3**, 2986–2990.
84 D. M. Kaz, R. McGorty, M. Mani, M. P. Brenner and V. N. Manoharan, *Nat. Mater.*, 2012, **11**, 138–142.
85 L. Isa, E. Amstad, K. Schwenke, E. D. Gado, P. Ilg, M. Kröger and E. Reimhult, *Soft Matter*, 2011, **7**, 7663–7675.
86 M. Maas, C. C. Ooi and G. G. Fuller, *Langmuir*, 2010, **26**, 17867–17873.
87 M. E. Leunissen, A. van Blaaderen, A. D. Hollingsworth, M. T. Sullivan and P. M. Chaikin, *Proc. Natl. Acad. Sci. U. S. A.*, 2007, **104**, 2585–2590.
88 J. Zwanikken and R. van Roij, *Phys. Rev. Lett.*, 2007, **99**, 178301.
89 M. Oettel, *Phys. Rev. E: Stat., Nonlinear, Soft Matter Phys.*, 2007, **76**, 041403.
90 P. A. Kralchevsky, I. B. Ivanov, K. P. Ananthapadmanabhan and A. Lips, *Langmuir*, 2005, **21**, 50–63.
91 X. Quan, C. Peng, J. Dong and J. Zhou, *Soft Matter*, 2016, **12**, 3352–3359.
92 L. Isa, F. Lucas, R. Wepf and E. Reimhult, *Nat. Commun.*, 2011, **2**, 438.
93 A. Stocco, G. Su, M. Nobili, M. In and D. Wang, *Soft Matter*, 2014, **10**, 6999–7007.
94 B. M. Weon, J. S. Lee, J. T. Kim, J. Pyo and J. H. Je, *Curr. Opin. Colloid Interface Sci.*, 2012, **17**, 388–395.

95 D. O. Grigoriev, J. Krägel, V. Dutschk, R. Miller and H. Möhwald, *Phys. Chem. Chem. Phys.*, 2007, **9**, 6447–6454.
96 O. S. Deshmukh, D. van den Ende, M. C. Stuart, F. Mugele and M. H. G. Duits, *Adv. Colloid Interface Sci.*, 2015, **222**, 215–227.
97 A. J. Mendoza, E. Guzmán, F. Martínez-Pedrero, H. Ritacco, R. G. Rubio, F. Ortega, V. M. Starov and R. Miller, *Adv. Colloid Interface Sci.*, 2014, **206**, 303–319.
98 Z. Niu, J. He, T. P. Russell and Q. Wang, *Angew. Chem., Int. Ed.*, 2010, **49**, 10052–10066.
99 R. McGorty, J. Fung, D. Kaz and V. N. Manoharan, *Mater. Today*, 2010, **13**, 34–42.
100 F. Leal-Calderon and V. Schmitt, *Curr. Opin. Colloid Interface Sci.*, 2008, **13**, 217–227.
101 C. Zeng, H. Bissig and A. D. Dinsmore, *Solid State Commun.*, 2006, **139**, 547–556.
102 A. Böker, J. He, T. Emrick and T. P. Russell, *Soft Matter*, 2007, **3**, 1231.
103 D. Wang, H. Duan and H. Möhwald, *Soft Matter*, 2005, **1**, 412.
104 E. Vignati, R. Piazza and T. P. Lockhart, *Langmuir*, 2003, **19**, 6650–6656.
105 B. P. Binks, *Curr. Opin. Colloid Interface Sci.*, 2002, **7**, 21–41.
106 A. B. Subramaniam, M. Abkarian and H. A. Stone, *Nat. Mater.*, 2005, **4**, 553–556.
107 A. S. Utada, E. Lorenceau, D. R. Link, P. D. Kaplan, H. A. Stone and D. A. Weitz, *Science*, 2005, **308**, 537–541.
108 D. Lee and D. A. Weitz, *Adv. Mater.*, 2008, **20**, 3498–3503.
109 D. Lee and D. A. Weitz, *Small*, 2009, **5**, 1932–1935.
110 S. Zhou, J. Fan, S. S. Datta, M. Guo, X. Guo and D. A. Weitz, *Adv. Funct. Mater.*, 2013, **23**, 5925–5929.
111 R. K. Shah, J.-W. Kim and D. A. Weitz, *Langmuir*, 2009, **26**, 1561–1565.
112 J. S. Sander and A. R. Studart, *Langmuir*, 2011, **27**, 3301–3307.
113 J. I. Park, Z. Nie, A. Kumachev, A. I. Abdelrahman, B. P. Binks, H. A. Stone and E. Kumacheva, *Angew. Chem.*, 2009, **121**, 5404–5408.
114 E. Tumarkin, J. I. Park, Z. Nie and E. Kumacheva, *Chem. Commun.*, 2011, **47**, 12712.
115 Z. Nie, J. I. Park, W. Li, S. A. F. Bon and E. Kumacheva, *J. Am. Chem. Soc.*, 2008, **130**, 16508–16509.
116 J. Zhang, R. J. Coulston, S. T. Jones, J. Geng, O. A. Scherman and C. Abell, *Science*, 2012, **335**, 690–694.
117 J. He, L. Wang, Z. Wei, Y. Yang, C. Wang, X. Han and Z. Nie, *ACS Appl. Mater. Interfaces*, 2013, **5**, 9746–9751.
118 L. Wang, Y. Liu, J. He, M. J. Hourwitz, Y. Yang, J. T. Fourkas, X. Han and Z. Nie, *Small*, 2015, **11**, 3762–3767.
119 F. Caruso, H. Lichtenfeld, M. Giersig and H. Möhwald, *J. Am. Chem. Soc.*, 1998, **120**, 8523–8524.
120 F. Caruso, *Adv. Mater.*, 2001, **13**, 11–22.
121 Y. Wang, A. S. Angelatos and F. Caruso, *Chem. Mater.*, 2008, **20**, 848–858.
122 X. W. (David) Lou, L. A. Archer and Z. Yang, *Adv. Mater.*, 2008, **20**, 3987–4019.
123 F. Caruso, *Chem. – Eur. J.*, 2000, **6**, 413–419.
124 J. Guo, B. L. Tardy, A. J. Christofferson, Y. Dai, J. J. Richardson, W. Zhu, M. Hu, Y. Ju, J. Cui, R. R. Dagastine, I. Yarovsky and F. Caruso, *Nat. Nanotechnol.*, 2016, **11**, 1105–1111.
125 M. S. Fleming, T. K. Mandal and D. R. Walt, *Chem. Mater.*, 2001, **13**, 2210–2216.
126 S.-W. Kim, M. Kim, W. Y. Lee and T. Hyeon, *J. Am. Chem. Soc.*, 2002, **124**, 7642–7643.
127 D. Mertz, J. Cui, Y. Yan, G. Devlin, C. Chaubaroux, A. Dochter, R. Alles, P. Lavalle, J. C. Voegel, A. Blencowe, P. Auffinger and F. Caruso, *ACS Nano*, 2012, **6**, 7584–7594.
128 D. Mertz, H. Wu, J. S. Wong, J. Cui, P. Tan, R. Alles and F. Caruso, *J. Mater. Chem.*, 2012, **22**, 21434.
129 D. Mertz, C. Affolter-Zbaraszczuk, J. Barthès, J. Cui, F. Caruso, T. F. Baumert, J.-C. Voegel, J. Ogier and F. Meyer, *Nanoscale*, 2014, **6**, 11676–11680.
130 K. Gawlitza, S. T. Turner, F. Polzer, S. Wellert, M. Karg, P. Mulvaney and R. von Klitzing, *Phys. Chem. Chem. Phys.*, 2013, **15**, 15623.
131 B. Du, Z. Cao, Z. Li, A. Mei, X. Zhang, J. Nie, J. Xu and Z. Fan, *Langmuir*, 2009, **25**, 12367–12373.
132 T. Bollhorst, S. Jakob, J. Köser, M. Maas and K. Rezwan, *J. Mater. Chem. B*, 2017, DOI: 10.1039/c6tb03069f.
133 M. Destribats, V. Schmitt and R. Backov, *Langmuir*, 2010, **26**, 1734–1742.
134 R. T. Rosenberg and N. R. Dan, *J. Colloid Interface Sci.*, 2010, **349**, 498–504.
135 R. T. Rosenberg and N. R. Dan, *J. Colloid Interface Sci.*, 2011, **354**, 478–482.
136 R. T. Rosenberg and N. Dan, *J. Biomater. Nanobiotechnol.*, 2011, **02**, 1–7.
137 T. Huang, H. Li, L. Huang, S. Li, K. Li and Y. Zhou, *Langmuir*, 2016, **32**, 991–996.
138 L. Zhang, K. Yu and A. Eisenberg, *Science*, 1996, **272**, 1777–1779.
139 Y. Yu and A. Eisenberg, *J. Am. Chem. Soc.*, 1997, **119**, 8383–8384.
140 C. Tanford, *Science*, 1978, **200**, 1012–1018.
141 D. Chandler, *Nature*, 2005, **437**, 640–647.
142 Y. Mai and A. Eisenberg, *Chem. Soc. Rev.*, 2012, **41**, 5969–5985.
143 P. Tanner, P. Baumann, R. Enea, O. Onaca, C. Palivan and W. Meier, *Acc. Chem. Res.*, 2011, **44**, 1039–1049.
144 J. He, X. Huang, Y.-C. Li, Y. Liu, T. Babu, M. A. Aronova, S. Wang, Z. Lu, X. Chen and Z. Nie, *J. Am. Chem. Soc.*, 2013, **135**, 7974–7984.
145 J. He, P. Zhang, T. Babu, Y. Liu, J. Gong and Z. Nie, *Chem. Commun.*, 2012, **49**, 576–578.
146 A. K. Boal, F. Ilhan, J. E. DeRouchey, T. Thurn-Albrecht, T. P. Russell and V. M. Rotello, *Nature*, 2000, **404**, 746–748.
147 E. R. Zubarev, J. Xu, A. Sayyad and J. D. Gibson, *J. Am. Chem. Soc.*, 2006, **128**, 15098–15099.
148 R. B. Grubbs, *Nat. Mater.*, 2007, **6**, 553–555.
149 J. Hu, T. Wu, G. Zhang and S. Liu, *J. Am. Chem. Soc.*, 2012, **134**, 7624–7627.
150 C. Yi, S. Zhang, K. T. Webb and Z. Nie, *Acc. Chem. Res.*, 2017, **50**, 12–21.
151 J. Song, G. Niu and X. Chen, *Bioconjugate Chem.*, 2017, **28**, 105–114.
152 J. Song, J. Zhou and H. Duan, *J. Am. Chem. Soc.*, 2012, **134**, 13458–13469.
153 J. Song, Z. Fang, C. Wang, J. Zhou, B. Duan, L. Pu and H. Duan, *Nanoscale*, 2013, **5**, 5816–5824.

154 J. Song, L. Pu, J. Zhou, B. Duan and H. Duan, *ACS Nano*, 2013, **7**, 9947–9960.
155 J. Song, X. Yang, O. Jacobson, L. Lin, P. Huang, G. Niu, Q. Ma and X. Chen, *ACS Nano*, 2015, **9**, 9199–9209.
156 J. Song, P. Huang and X. Chen, *Nat. Protoc.*, 2016, **11**, 2287–2299.
157 Z. Nie, D. Fava, M. Rubinstein and E. Kumacheva, *J. Am. Chem. Soc.*, 2008, **130**, 3683–3689.
158 D. Fava, Z. Nie, M. A. Winnik and E. Kumacheva, *Adv. Mater.*, 2008, **20**, 4318–4322.
159 J. Lin, S. Wang, P. Huang, Z. Wang, S. Chen, G. Niu, W. Li, J. He, D. Cui, G. Lu, X. Chen and Z. Nie, *ACS Nano*, 2013, **7**, 5320–5329.
160 J. He, Z. Wei, L. Wang, Z. Tomova, T. Babu, C. Wang, X. Han, J. T. Fourkas and Z. Nie, *Angew. Chem., Int. Ed.*, 2013, **52**, 2463–2468.
161 T. Bian, L. Shang, H. Yu, M. T. Perez, L.-Z. Wu, C.-H. Tung, Z. Nie, Z. Tang and T. Zhang, *Adv. Mater.*, 2014, **26**, 5613–5618.
162 Y. Liu, J. He, K. Yang, C. Yi, Y. Liu, L. Nie, N. M. Khashab, X. Chen and Z. Nie, *Angew. Chem., Int. Ed.*, 2015, **54**, 15809–15812.
163 K. J. M. Bishop, *Angew. Chem., Int. Ed.*, 2016, **55**, 1598–1600.
164 M. S. Nikolic, C. Olsson, A. Salcher, A. Kornowski, A. Rank, R. Schubert, A. Frömsdorf, H. Weller and S. Förster, *Angew. Chem.*, 2009, **121**, 2790–2792.
165 Y. Guo, S. Harirchian-Saei, C. M. S. Izumi and M. G. Moffitt, *ACS Nano*, 2011, **5**, 3309–3318.
166 A. D. Bangham and R. W. Horne, *J. Mol. Biol.*, 1964, **8**, IN2-668-IN10.
167 A. D. Bangham, M. M. Standish and J. C. Watkins, *J. Mol. Biol.*, 1965, **13**, 238–IN27.
168 A. D. Bangham, *Chem. Phys. Lipids*, 1993, **64**, 275–285.
169 T. M. Allen and P. R. Cullis, *Adv. Drug Delivery Rev.*, 2013, **65**, 36–48.
170 W. T. Al-Jamal and K. Kostarelos, *Nanomedicine*, 2007, **2**, 85–98.
171 E. Amstad and E. Reimhult, *Nanomedicine*, 2011, **7**, 145–164.
172 J. N. Cha, H. Birkedal, L. E. Euliss, M. H. Bartl, M. S. Wong, T. J. Deming and G. D. Stucky, *J. Am. Chem. Soc.*, 2003, **125**, 8285–8289.
173 S. Lecommandoux, O. Sandre, F. Chécot, J. Rodriguez-Hernandez and R. Perzynski, *Adv. Mater.*, 2005, **17**, 712–718.
174 G. Gopalakrishnan, C. Danelon, P. Izewska, M. Prummer, P.-Y. Bolinger, I. Geissbühler, D. Demurtas, J. Dubochet and H. Vogel, *Angew. Chem., Int. Ed.*, 2006, **45**, 5478–5483.
175 S.-H. Park, S.-G. Oh, J.-Y. Mun and S.-S. Han, *Colloids Surf., B*, 2006, **48**, 112–118.
176 L. Paasonen, T. Laaksonen, C. Johans, M. Yliperttula, K. Kontturi and A. Urtti, *J. Controlled Release*, 2007, **122**, 86–93.
177 S.-H. Park, S.-G. Oh, K.-D. Suh, S.-H. Han, D. J. Chung, J.-Y. Mun, S.-S. Han and J.-W. Kim, *Colloids Surf., B*, 2009, **70**, 108–113.
178 S.-H. Park, S.-G. Oh, J.-Y. Mun and S.-S. Han, *Colloids Surf., B*, 2005, **44**, 117–122.
179 W. T. Al-Jamal, K. T. Al-Jamal, B. Tian, L. Lacerda, P. H. Bomans, P. M. Frederik and K. Kostarelos, *ACS Nano*, 2008, **2**, 408–418.
180 L. Feng, X. Kong, K. Chao, Y. Sun, Q. Zeng and Y. Zhang, *Mater. Chem. Phys.*, 2005, **93**, 310–313.
181 W. Mueller, K. Koynov, K. Fischer, S. Hartmann, S. Pierrat, T. Basché and M. Maskos, *Macromolecules*, 2009, **42**, 357–361.
182 G. D. Bothun, A. E. Rabideau and M. A. Stoner, *J. Phys. Chem. B*, 2009, **113**, 7725–7728.
183 M. Krack, H. Hohenberg, A. Kornowski, P. Lindner, H. Weller and S. Förster, *J. Am. Chem. Soc.*, 2008, **130**, 7315–7320.
184 X. Zhang, Y. Yang, J. Tian and H. Zhao, *Chem. Commun.*, 2009, 3807–3809.
185 Y. Mai and A. Eisenberg, *J. Am. Chem. Soc.*, 2010, **132**, 10078–10084.
186 M. R. Rasch, E. Rossinyol, J. L. Hueso, B. W. Goodfellow, J. Arbiol and B. A. Korgel, *Nano Lett.*, 2010, **10**, 3733–3739.
187 M. R. Rasch, Y. Yu, C. Bosoy, B. W. Goodfellow and B. A. Korgel, *Langmuir*, 2012, **28**, 12971–12981.
188 M. R. Preiss and G. D. Bothun, *Expert Opin. Drug Delivery*, 2011, **8**, 1025–1040.
189 M. Schulz, A. Olubummo and W. H. Binder, *Soft Matter*, 2012, **8**, 4849.
190 S. J. Soenen, G. V. Velde, A. Ketkar-Atre, U. Himmelreich and M. De Cuyper, *WIREs Nanomed. Nanobiotechnol.*, 2011, **3**, 197–211.
191 E. Amstad, J. Kohlbrecher, E. Müller, T. Schweizer, M. Textor and E. Reimhult, *Nano Lett.*, 2011, **11**, 1664–1670.
192 D. Qiu, X. An, Z. Chen and X. Ma, *Chem. Phys. Lipids*, 2012, **165**, 563–570.
193 D. Qiu and X. An, *Colloids Surf., B*, 2013, **104**, 326–329.
194 K. Katagiri, Y. Imai, K. Koumoto, T. Kaiden, K. Kono and S. Aoshima, *Small*, 2011, **7**, 1683–1689.
195 Q. Wei, T. Li, G. Wang, H. Li, Z. Qian and M. Yang, *Biomaterials*, 2010, **31**, 7332–7339.
196 C. Sanson, O. Diou, J. Thévenot, E. Ibarboure, A. Soum, A. Brûlet, S. Miraux, E. Thiaudière, S. Tan, A. Brisson, V. Dupuis, O. Sandre and S. Lecommandoux, *ACS Nano*, 2011, **5**, 1122–1140.
197 H. Oliveira, E. Pérez-Andrés, J. Thevenot, O. Sandre, E. Berra and S. Lecommandoux, *J. Controlled Release*, 2013, **169**, 165–170.
198 R. J. Hickey, A. S. Haynes, J. M. Kikkawa and S.-J. Park, *J. Am. Chem. Soc.*, 2011, **133**, 1517–1525.
199 R. J. Hickey, J. Koski, X. Meng, R. A. Riggleman, P. Zhang and S.-J. Park, *ACS Nano*, 2014, **8**, 495–502.
200 R. J. Hickey, Q. Luo and S.-J. Park, *ACS Macro Lett.*, 2013, **2**, 805–808.
201 Y. Liu, Y. Li, J. He, K. J. Duelge, Z. Lu and Z. Nie, *J. Am. Chem. Soc.*, 2014, **136**, 2602–2610.
202 Y. Liu, X. Yang, Z. Huang, P. Huang, Y. Zhang, L. Deng, Z. Wang, Z. Zhou, Y. Liu, H. Kalish, N. M. Khachab, X. Chen and Z. Nie, *Angew. Chem., Int. Ed.*, 2016, **55**, 15297–15300.
203 C. C. Berton-Carabin and K. Schroën, *Annu. Rev. Food Sci. Technol.*, 2015, **6**, 263–297.

204 K. L. Thompson, M. Williams and S. P. Armes, *J. Colloid Interface Sci.*, 2015, **447**, 217–228.
205 J. Huo, M. Marcello, A. Garai and D. Bradshaw, *Adv. Mater.*, 2013, **25**, 2717–2722.
206 X.-W. Xu, X.-M. Zhang, C. Liu, Y.-L. Yang, J.-W. Liu, H.-P. Cong, C.-H. Dong, X.-F. Ren and S.-H. Yu, *J. Am. Chem. Soc.*, 2013, **135**, 12928–12931.
207 Y.-S. Cho, G.-R. Yi, J.-M. Lim, S.-H. Kim, V. N. Manoharan, D. J. Pine and S.-M. Yang, *J. Am. Chem. Soc.*, 2005, **127**, 15968–15975.
208 Z. Rozynek and A. Józefczak, *Eur. Phys. J.: Spec. Top.*, 2016, **225**, 741–756.
209 P. Datskos, G. Polizos, M. Bhandari, D. A. Cullen and J. Sharma, *RSC Adv.*, 2016, **6**, 26734–26737.
210 Y. Yin, R. M. Rioux, C. K. Erdonmez, S. Hughes, G. A. Somorjai and A. P. Alivisatos, *Science*, 2004, **304**, 711–714.
211 B. Liu and H. C. Zeng, *J. Am. Chem. Soc.*, 2004, **126**, 16744–16746.
212 B. Liu and H. C. Zeng, *J. Am. Chem. Soc.*, 2004, **126**, 8124–8125.
213 B. Liu and H. C. Zeng, *Chem. Mater.*, 2007, **19**, 5824–5826.
214 M. in het Panhuis and V. N. Paunov, *Chem. Commun.*, 2005, 1726.
215 Y. Nonomura and N. Kobayashi, *J. Colloid Interface Sci.*, 2009, **330**, 463–466.
216 D. Wang, C. Song, Z. Hu and X. Fu, *J. Phys. Chem. B*, 2005, **109**, 1125–1129.
217 A. B. Subramaniam, J. Wan, A. Gopinath and H. A. Stone, *Soft Matter*, 2011, **7**, 2600.
218 L. Zhang, F. Zhang, Y.-S. Wang, Y.-L. Sun, W.-F. Dong, J.-F. Song, Q.-S. Huo and H.-B. Sun, *Soft Matter*, 2011, **7**, 7375–7381.
219 A. Kumar, B. J. Park, F. Tu and D. Lee, *Soft Matter*, 2013, **9**, 6604–6617.
220 N. Zhao and M. Gao, *Adv. Mater.*, 2009, **21**, 184–187.
221 H. Yang, F. Liang, Y. Chen, Q. Wang, X. Qu and Z. Yang, *NPG Asia Mater.*, 2015, **7**, e176.
222 C. H. J. Evers, J. A. Luiken, P. G. Bolhuis and W. K. Kegel, *Nature*, 2016, **534**, 364–368.
223 B. Samanta, D. Patra, C. Subramani, Y. Ofir, G. Yesilbag, A. Sanyal and V. M. Rotello, *Small*, 2009, **5**, 685–688.
224 A. Kaiser, T. Liu, W. Richtering and A. M. Schmidt, *Langmuir*, 2009, **25**, 7335–7341.
225 I. Akartuna, E. Tervoort, A. R. Studart and L. J. Gauckler, *Langmuir*, 2009, **25**, 12419–12424.
226 H. Liu, C. Wang, Q. Gao, J. Chen, B. Ren, X. Liu and Z. Tong, *Int. J. Pharm.*, 2009, **376**, 92–98.
227 P. K. Jain and M. A. El-Sayed, *Chem. Phys. Lett.*, 2010, **487**, 153–164.
228 Y. Lin, H. Skaff, A. Böker, A. D. Dinsmore, T. Emrick and T. P. Russell, *J. Am. Chem. Soc.*, 2003, **125**, 12690–12691.
229 H. Skaff, Y. Lin, R. Tangirala, K. Breitenkamp, A. Böker, T. P. Russell and T. Emrick, *Adv. Mater.*, 2005, **17**, 2082–2086.
230 D. Patra, F. Ozdemir, O. R. Miranda, B. Samanta, A. Sanyal and V. M. Rotello, *Langmuir*, 2009, **25**, 13852–13854.
231 Y. Jeong, B. Duncan, M.-H. Park, C. Kim and V. M. Rotello, *Chem. Commun.*, 2011, **47**, 12077.
232 B. Radt, T. A. Smith and F. Caruso, *Adv. Mater.*, 2004, **16**, 2184–2189.
233 A. S. Angelatos, B. Radt and F. Caruso, *J. Phys. Chem. B*, 2005, **109**, 3071–3076.
234 E. Glogowski, R. Tangirala, J. He, T. P. Russell and T. Emrick, *Nano Lett.*, 2007, **7**, 389–393.
235 D. Liu, F. Zhou, C. Li, T. Zhang, H. Zhang, W. Cai and Y. Li, *Angew. Chem., Int. Ed.*, 2015, **54**, 9596–9600.
236 S. Anandhakumar, M. Sasidharan, C.-W. Tsao and A. M. Raichur, *ACS Appl. Mater. Interfaces*, 2014, **6**, 3275–3281.
237 D. Radziuk, D. G. Shchukin, A. Skirtach, H. Möhwald and G. Sukhorukov, *Langmuir*, 2007, **23**, 4612–4617.
238 G. Kaur, J. He, J. Xu, S. Pingali, G. Jutz, A. Böker, Z. Niu, T. Li, D. Rawlinson, T. Emrick, B. Lee, P. Thiyagarajan, T. P. Russell and Q. Wang, *Langmuir*, 2009, **25**, 5168–5176.
239 P. van Rijn and A. Böker, *J. Mater. Chem.*, 2011, **21**, 16735.
240 B. A. Rhodes, I. Zolle and H. N. Wagner, *J. Clin. Res.*, 1968, **16**, 245–250.
241 J. M. Gallo, C. T. Hung and D. G. Perrier, *Int. J. Pharm.*, 1984, **22**, 63–74.
242 R. Arshady, *J. Controlled Release*, 1990, **14**, 111–131.
243 O. P. Tiourina and G. B. Sukhorukov, *Int. J. Pharm.*, 2002, **242**, 155–161.
244 N. G. Balabushevich, O. P. Tiourina, D. V. Volodkin, N. I. Larionova and G. B. Sukhorukov, *Biomacromolecules*, 2003, **4**, 1191–1197.
245 Z. An, H. Möhwald and J. Li, *Biomacromolecules*, 2006, **7**, 580–585.
246 Z. An, C. Tao, G. Lu, H. Möhwald, S. Zheng, Y. Cui and J. Li, *Chem. Mater.*, 2005, **17**, 2514–2519.
247 W. Tong, C. Gao and H. Möhwald, *Colloid Polym. Sci.*, 2008, **286**, 1103–1109.
248 L. Duan, Q. He, X. Yan, Y. Cui, K. Wang and J. Li, *Biochem. Biophys. Res. Commun.*, 2007, **354**, 357–362.
249 W. Qi, X. Yan, L. Duan, Y. Cui, Y. Yang and J. Li, *Biomacromolecules*, 2009, **10**, 1212–1216.
250 D. Mertz, P. Tan, Y. Wang, T. K. Goh, A. Blencowe and F. Caruso, *Adv. Mater.*, 2011, **23**, 5668–5673.
251 S. Fujii, A. Aichi, M. Muraoka, N. Kishimoto, K. Iwahori, Y. Nakamura and I. Yamashita, *J. Colloid Interface Sci.*, 2009, **338**, 222–228.
252 P. van Rijn, H. Park, K. Özlem Nazli, N. C. Mougin and A. Böker, *Langmuir*, 2013, **29**, 276–284.
253 B. T. Nguyen, T. Nicolai and L. Benyahia, *Langmuir*, 2013, **29**, 10658–10664.
254 Y. Song, U. Shimanovich, T. C. T. Michaels, Q. Ma, J. Li, T. P. J. Knowles and H. C. Shum, *Nat. Commun.*, 2016, **7**, 12934.
255 X. Huang, M. Li and S. Mann, *Chem. Commun.*, 2014, **50**, 6278–6280.
256 X. Liu, P. Zhou, Y. Huang, M. Li, X. Huang and S. Mann, *Angew. Chem.*, 2016, **128**, 7211–7216.
257 S. Mann, *Acc. Chem. Res.*, 2012, **45**, 2131–2141.
258 J. Fothergill, M. Li, S. A. Davis, J. A. Cunningham and S. Mann, *Langmuir*, 2014, **30**, 14591–14596.
259 R. K. Kumar, M. Li, S. N. Olof, A. J. Patil and S. Mann, *Small*, 2013, **9**, 357–362.

260 K. Akkarachaneeyakorn, M. Li, S. A. Davis and S. Mann, *Langmuir*, 2016, **32**, 2912–2919.
261 M. Li, X. Huang and S. Mann, *Small*, 2014, **10**, 3291–3298.
262 A. J. Worthen, L. M. Foster, J. Dong, J. A. Bollinger, A. H. Peterman, L. E. Pastora, S. L. Bryant, T. M. Truskett, C. W. Bielawski and K. P. Johnston, *Langmuir*, 2014, **30**, 984–994.
263 T. Nallamilli, B. P. Binks, E. Mani and M. G. Basavaraj, *Langmuir*, 2015, **31**, 11200–11208.
264 T. G. Mason, J. N. Wilking, K. Meleson, C. B. Chang and S. M. Graves, *J. Phys.: Condens. Matter*, 2006, **18**, R635.
265 C. A. S. Batista, R. G. Larson and N. A. Kotov, *Science*, 2015, **350**, 1242477.
266 Q. Li, U. Jonas, X. S. Zhao and M. Kappl, *Asia-Pac. J. Chem. Eng.*, 2008, **3**, 255–268.
267 C. P. Whitby, D. Fornasiero, J. Ralston, L. Liggieri and F. Ravera, *J. Phys. Chem. C*, 2012, **116**, 3050–3058.
268 T. Bollhorst, T. Grieb, A. Rosenauer, G. Fuller, M. Maas and K. Rezwan, *Chem. Mater.*, 2013, **25**, 3464–3471.
269 S. Sihler, A. Schrade, Z. Cao and U. Ziener, *Langmuir*, 2015, **31**, 10392–10401.
270 A. Schrade, Z. Cao, K. Landfester and U. Ziener, *Langmuir*, 2011, **27**, 6689–6700.
271 S. Li, B. A. Moosa, J. G. Croissant and N. M. Khashab, *Angew. Chem.*, 2015, **54**, 6804–6808.
272 K. Chen, S. Zhou, S. Yang and L. Wu, *Adv. Funct. Mater.*, 2015, **25**, 1035–1041.
273 F. Caruso, R. A. Caruso and H. Möhwald, *Chem. Mater.*, 1999, **11**, 3309–3314.
274 F. Caruso and H. Möhwald, *Langmuir*, 1999, **15**, 8276–8281.
275 R. A. Caruso, A. Susha and F. Caruso, *Chem. Mater.*, 2001, **13**, 400–409.
276 M. Chen, L. Wu, S. Zhou and B. You, *Macromolecules*, 2004, **37**, 9613–9619.
277 M. Chen, S. Zhou, B. You and L. Wu, *Macromolecules*, 2005, **38**, 6411–6417.
278 M. J. Percy, C. Barthet, J. C. Lobb, M. A. Khan, S. F. Lascelles, M. Vamvakaki and S. P. Armes, *Langmuir*, 2000, **16**, 6913–6920.
279 M. J. Percy and S. P. Armes, *Langmuir*, 2002, **18**, 4562–4565.
280 M. J. Percy, V. Michailidou, S. P. Armes, C. Perruchot, J. F. Watts and S. J. Greaves, *Langmuir*, 2003, **19**, 2072–2079.
281 S. Fortuna, C. A. L. Colard, A. Troisi and S. A. F. Bon, *Langmuir*, 2009, **25**, 12399–12403.
282 R. Chen, D. J. G. Pearce, S. Fortuna, D. L. Cheung and S. A. F. Bon, *J. Am. Chem. Soc.*, 2011, **133**, 2151–2153.
283 K. Isenbügel, H. Ritter, R. Branscheid and U. Kolb, *Macromol. Rapid Commun.*, 2010, **31**, 2121–2126.
284 S. Zhou, A. Sugawara-Narutaki, S. Tsuboike, J. Wang, A. Shimojima and T. Okubo, *Langmuir*, 2015, **31**, 13214–13220.
285 B. Y. Guan, L. Yu and X. W. (David) Lou, *Adv. Mater.*, 2016, **28**, 9596–9601.
286 F. Caruso, A. S. Susha, M. Giersig and H. Möhwald, *Adv. Mater.*, 1999, **11**, 950–953.
287 F. Caruso, M. Spasova, A. Susha, M. Giersig and R. A. Caruso, *Chem. Mater.*, 2000, **13**, 109–116.
288 V. Salgueiriño-Maceira, M. Spasova and M. Farle, *Adv. Funct. Mater.*, 2005, **15**, 1036–1040.
289 S.-L. Shen, W. Wu, K. Guo, H. Meng and J.-F. Chen, *Colloids Surf., A*, 2007, **311**, 99–105.
290 P. Arosio, J. Thévenot, T. Orlando, F. Orsini, M. Corti, M. Mariani, L. Bordonali, C. Innocenti, C. Sangregorio, H. Oliveira, S. Lecommandoux, A. Lascialfari and O. Sandre, *J. Mater. Chem. B*, 2013, **1**, 5317–5328.
291 N. J. Halas, S. Lal, W.-S. Chang, S. Link and P. Nordlander, *Chem. Rev.*, 2011, **111**, 3913–3961.
292 M. Rycenga, C. M. Cobley, J. Zeng, W. Li, C. H. Moran, Q. Zhang, D. Qin and Y. Xia, *Chem. Rev.*, 2011, **111**, 3669–3712.
293 P. K. Jain, X. Huang, I. H. El-Sayed and M. A. El-Sayed, *Acc. Chem. Res.*, 2008, **41**, 1578–1586.
294 Z. Liang, A. Susha and F. Caruso, *Chem. Mater.*, 2003, **15**, 3176–3183.
295 M. Karg and T. Hellweg, *J. Mater. Chem.*, 2009, **19**, 8714.
296 P. B. Landon, A. H. Mo, C. Zhang, C. D. Emerson, A. D. Printz, A. F. Gomez, C. J. DeLaTorre, D. A. M. Colburn, P. Anzenberg, M. Eliceiri, C. O'Connell and R. Lal, *ACS Appl. Mater. Interfaces*, 2014, **6**, 9937–9941.
297 J. Tian, L. Yuan, M. Zhang, F. Zheng, Q. Xiong and H. Zhao, *Langmuir*, 2012, **28**, 9365–9371.
298 L. Cheng, A. Liu, S. Peng and H. Duan, *ACS Nano*, 2010, **4**, 6098–6104.
299 L. Wu, U. Glebe and A. Böker, *Polym. Chem.*, 2015, **6**, 5143–5184.
300 H. Deng, Y. Zhong, M. Du, Q. Liu, Z. Fan, F. Dai and X. Zhang, *Theranostics*, 2014, **4**, 904–918.
301 Y. Zhang and H. Zhao, *Langmuir*, 2016, **32**, 3567–3579.
302 K. Niikura, N. Iyo, T. Higuchi, T. Nishio, H. Jinnai, N. Fujitani and K. Ijiro, *J. Am. Chem. Soc.*, 2012, **134**, 7632–7635.
303 K. Niikura, N. Iyo, Y. Matsuo, H. Mitomo and K. Ijiro, *ACS Appl. Mater. Interfaces*, 2013, **5**, 3900–3907.
304 J. Wei, K. Niikura, T. Higuchi, T. Kimura, H. Mitomo, H. Jinnai, Y. Joti, Y. Bessho, Y. Nishino, Y. Matsuo and K. Ijiro, *J. Am. Chem. Soc.*, 2016, **138**, 3274–3277.
305 X. An, F. Zhang, Y. Zhu and W. Shen, *Chem. Commun.*, 2010, **46**, 7202–7204.
306 R. M. Gorgoll, T. Tsubota, K. Harano and E. Nakamura, *J. Am. Chem. Soc.*, 2015, **137**, 7568–7571.
307 Y.-C. Yeh, R. Tang, R. Mout, Y. Jeong and V. M. Rotello, *Angew. Chem., Int. Ed.*, 2014, **53**, 5137–5141.
308 F. Caruso and H. Möhwald, *J. Am. Chem. Soc.*, 1999, **121**, 6039–6046.
309 C. Schüler and F. Caruso, *Macromol. Rapid Commun.*, 2000, **21**, 750–753.
310 F. Caruso, H. Fiedler and K. Haage, *Colloids Surf., A*, 2000, **169**, 287–293.
311 F. Caruso and C. Schüler, *Langmuir*, 2000, **16**, 9595–9603.
312 Y. Lvov and F. Caruso, *Anal. Chem.*, 2001, **73**, 4212–4217.
313 T. Li, Z. Niu, T. Emrick, T. P. Russell and Q. Wang, *Small*, 2008, **4**, 1624–1629.
314 E. Phillips, O. Penate-Medina, P. B. Zanzonico, R. D. Carvajal, P. Mohan, Y. Ye, J. Humm, M. Gönen, H. Kalaigian, H. Schöder, H. W. Strauss, S. M. Larson, U. Wiesner and M. S. Bradbury, *Sci. Transl. Med.*, 2014, **6**, 260ra149.
315 M. S. Bradbury, M. Pauliah, P. Zanzonico, U. Wiesner and S. Patel, *WIREs Nanomed. Nanobiotechnol.*, 2016, **8**, 535–553.

316 C. Caltagirone, A. Bettoschi, A. Garau and R. Montis, *Chem. Soc. Rev.*, 2015, **44**, 4645–4671.
317 S. E. Kim, L. Zhang, K. Ma, M. Riegman, F. Chen, I. Ingold, M. Conrad, M. Z. Turker, M. Gao, X. Jiang, S. Monette, M. Pauliah, M. Gonen, P. Zanzonico, T. Quinn, U. Wiesner, M. S. Bradbury and M. Overholtzer, *Nat. Nanotechnol.*, 2016, **11**, 977–985.
318 Y. Pan, J.-P. Volkmer, K. E. Mach, R. V. Rouse, J.-J. Liu, D. Sahoo, T. C. Chang, T. J. Metzner, L. Kang, M. van de Rijn, E. C. Skinner, S. S. Gambhir, I. L. Weissman and J. C. Liao, *Sci. Transl. Med.*, 2014, **6**, 260ra148.
319 H. Soo Choi, W. Liu, P. Misra, E. Tanaka, J. P. Zimmer, B. Itty Ipe, M. G. Bawendi and J. V. Frangioni, *Nat. Biotechnol.*, 2007, **25**, 1165–1170.
320 D. Pissuwan, T. Niidome and M. B. Cortie, *J. Controlled Release*, 2011, **149**, 65–71.
321 J. Dobson, *Gene Ther.*, 2006, **13**, 283–287.
322 Y.-X. J. Wang, *Quant. Imaging Med. Surg.*, 2011, **1**, 35–40.
323 R. Weissleder, M. Nahrendorf and M. J. Pittet, *Nat. Mater.*, 2014, **13**, 125–138.
324 S. Zanganeh, G. Hutter, R. Spitler, O. Lenkov, M. Mahmoudi, A. Shaw, J. S. Pajarinen, H. Nejadnik, S. Goodman, M. Moseley, L. M. Coussens and H. E. Daldrup-Link, *Nat. Nanotechnol.*, 2016, **11**, 986–994.
325 K. Zarschler, L. Rocks, N. Licciardello, L. Boselli, E. Polo, K. P. Garcia, L. De Cola, H. Stephan and K. A. Dawson, *Nanomedicine*, 2016, **12**, 1663–1701.
326 Y. Liu, J.-J. Yin and Z. Nie, *Nano Res.*, 2014, **7**, 1719–1730.
327 H. F. Krug and P. Wick, *Angew. Chem., Int. Ed.*, 2011, **50**, 1260–1278.
328 H. F. Krug, *Angew. Chem., Int. Ed.*, 2014, **53**, 12304–12319.
329 A. Nel, T. Xia, L. Mädler and N. Li, *Science*, 2006, **311**, 622–627.
330 M. Yu and J. Zheng, *ACS Nano*, 2015, **9**, 6655–6674.
331 M. Longmire, P. L. Choyke and H. Kobayashi, *Nanomedicine*, 2008, **3**, 703–717.
332 N. Khlebtsov and L. Dykman, *Chem. Soc. Rev.*, 2011, **40**, 1647–1671.
333 N. Bertrand, J. Wu, X. Xu, N. Kamaly and O. C. Farokhzad, *Adv. Drug Delivery Rev.*, 2014, **66**, 2–25.
334 A. M. Smith, M. C. Mancini and S. Nie, *Nat. Nanotechnol.*, 2009, **4**, 710–711.
335 X. Huang, I. H. El-Sayed, W. Qian and M. A. El-Sayed, *J. Am. Chem. Soc.*, 2006, **128**, 2115–2120.
336 A. Agarwal, S. W. Huang, M. O'Donnell, K. C. Day, M. Day, N. Kotov and S. Ashkenazi, *J. Appl. Phys.*, 2007, **102**, 064701.
337 S. Laurent, S. Dutz, U. O. Häfeli and M. Mahmoudi, *Adv. Colloid Interface Sci.*, 2011, **166**, 8–23.
338 B. Gleich and J. Weizenecker, *Nature*, 2005, **435**, 1214–1217.
339 M. H. Pablico-Lansigan, S. F. Situ and A. C. S. Samia, *Nanoscale*, 2013, **5**, 4040.
340 H. E. Daldrup-Link, D. Golovko, B. Ruffell, D. G. DeNardo, R. Castaneda, C. Ansari, J. Rao, G. A. Tikhomirov, M. F. Wendland, C. Corot and L. M. Coussens, *Clin. Cancer Res.*, 2011, **17**, 5695–5704.
341 P. H. R. Keen, N. K. H. Slater and A. F. Routh, *Langmuir*, 2014, **30**, 1939–1948.
342 C. Zhang, C. Hu, Y. Zhao, M. Möller, K. Yan and X. Zhu, *Langmuir*, 2013, **29**, 15457–15462.
343 Y. Zhao, Y. Li, D. E. Demco, X. Zhu and M. Möller, *Langmuir*, 2014, **30**, 4253–4261.
344 F. Porta and A. Kros, *Part. Part. Syst. Charact.*, 2013, **30**, 606–613.
345 M. Ray, R. Tang, Z. Jiang and V. M. Rotello, *Bioconjugate Chem.*, 2015, **26**, 1004–1007.
346 C. S. Kim, R. Mout, Y. Zhao, Y.-C. Yeh, R. Tang, Y. Jeong, B. Duncan, J. A. Hardy and V. M. Rotello, *Bioconjugate Chem.*, 2015, **26**, 950–954.
347 J. Hardie, Y. Jiang, E. R. Tetrault, P. C. Ghazi, G. Y. Tonga, M. E. Farkas and V. M. Rotello, *Nanotechnology*, 2016, **27**, 374001.
348 R. Tang, Z. Jiang, M. Ray, S. Hou and V. M. Rotello, *Nanoscale*, 2016, **8**, 18038–18041.
349 T.-Y. Liu and T. C. Huang, *Acta Biomater.*, 2011, **7**, 3927–3934.
350 H. De Oliveira, J. Thevenot and S. Lecommandoux, *WIREs Nanomed. Nanobiotechnol.*, 2012, **4**, 525–546.
351 L. Tang, X. Yang, Q. Yin, K. Cai, H. Wang, I. Chaudhury, C. Yao, Q. Zhou, M. Kwon, J. A. Hartman, I. T. Dobrucki, L. W. Dobrucki, L. B. Borst, S. Lezmi, W. G. Helferich, A. L. Ferguson, T. M. Fan and J. Cheng, *Proc. Natl. Acad. Sci. U. S. A.*, 2014, **111**, 15344–15349.
352 N. Chen, H. Wang, Q. Huang, J. Li, J. Yan, D. He, C. Fan and H. Song, *Small*, 2014, **10**, 3603–3611.
353 J. J. Li, D. Hartono, C.-N. Ong, B.-H. Bay and L.-Y. L. Yung, *Biomaterials*, 2010, **31**, 5996–6003.
354 P. Agostinis, K. Berg, K. A. Cengel, T. H. Foster, A. W. Girotti, S. O. Gollnick, S. M. Hahn, M. R. Hamblin, A. Juzeniene, D. Kessel, M. Korbelik, J. Moan, P. Mroz, D. Nowis, J. Piette, B. C. Wilson and J. Golab, *Ca-Cancer J. Clin.*, 2011, **61**, 250–281.
355 P. L. Choyke, *Sci. Transl. Med.*, 2014, **6**, 260fs44.
356 Y. Jeong, S. T. Kim, Y. Jiang, B. Duncan, C. S. Kim, K. Saha, Y.-C. Yeh, B. Yan, R. Tang, S. Hou, C. Kim, M.-H. Park and V. M. Rotello, *Nanomedicine*, 2016, **11**, 1571–1578.
357 H.-Y. Huang, H.-L. Liu, P.-H. Hsu, C.-S. Chiang, C.-H. Tsai, H.-S. Chi, S.-Y. Chen and Y.-Y. Chen, *Adv. Mater.*, 2015, **27**, 655–661.
358 X. Cai, F. Yang and N. Gu, *Theranostics*, 2012, **2**, 103–112.
359 S. Unnikrishnan and A. L. Klibanov, *Am. J. Roentgenol.*, 2012, **199**, 292–299.
360 T. B. Brismar, D. Grishenkov, B. Gustafsson, J. Härmark, Å. Barrefelt, S. V. V. N. Kothapalli, S. Margheritelli, L. Oddo, K. Caidahl, H. Hebert and G. Paradossi, *Biomacromolecules*, 2012, **13**, 1390–1399.
361 A. A. Barrefelt, T. B. Brismar, G. Egri, P. Aspelin, A. Olsson, L. Oddo, S. Margheritelli, K. Caidahl, G. Paradossi, L. Dähne, R. Axelsson and M. Hassan, *EJNMMI Res.*, 2013, **3**, 12.
362 L. Duan, F. Yang, L. Song, K. Fang, J. Tian, Y. Liang, M. Li, N. Xu, Z. Chen, Y. Zhang and N. Gu, *Soft Matter*, 2015, **11**, 5492–5500.
363 B. Y. S. Kim, J. T. Rutka and W. C. W. Chan, *N. Engl. J. Med.*, 2010, **363**, 2434–2443.
364 V. J. Venditto and F. C. Szoka Jr., *Adv. Drug Delivery Rev.*, 2013, **65**, 80–88.

365 M. L. Etheridge, S. A. Campbell, A. G. Erdman, C. L. Haynes, S. M. Wolf and J. McCullough, *Nanomedicine*, 2013, **9**, 1–14.
366 E. Blanco, H. Shen and M. Ferrari, *Nat. Biotechnol.*, 2015, **33**, 941–951.
367 S. Wilhelm, A. J. Tavares, Q. Dai, S. Ohta, J. Audet, H. F. Dvorak and W. C. W. Chan, *Nat. Rev. Mat.*, 2016, **1**, 16014.
368 J. P. A. Ioannidis, *PLoS Med.*, 2016, **13**, e1002049.
369 M. Björnmalm, M. Faria and F. Caruso, *J. Am. Chem. Soc.*, 2016, **138**, 13449–13456.
370 R. Bawa, G. F. Audette and I. Rubinstein, *Handbook of Clinical Nanomedicine: Nanoparticles, Imaging, Therapy and Clinical Applications*, Pan Stanford, 2015.
371 R. A. Petros and J. M. DeSimone, *Nat. Rev. Drug Discovery*, 2010, **9**, 615–627.
372 S. M. Moghimi, A. C. Hunter and J. C. Murray, *Pharmacol. Rev.*, 2001, **53**, 283–318.
373 Y. Geng, P. Dalhaimer, S. Cai, R. Tsai, M. Tewari, T. Minko and D. E. Discher, *Nat. Nanotechnol.*, 2007, **2**, 249–255.
374 H. Cabral, Y. Matsumoto, K. Mizuno, Q. Chen, M. Murakami, M. Kimura, Y. Terada, M. R. Kano, K. Miyazono, M. Uesaka, N. Nishiyama and K. Kataoka, *Nat. Nanotechnol.*, 2011, **6**, 815–823.
375 A. E. Nel, L. Mädler, D. Velegol, T. Xia, E. M. V. Hoek, P. Somasundaran, F. Klaessig, V. Castranova and M. Thompson, *Nat. Mater.*, 2009, **8**, 543–557.
376 J. A. Kim, C. Åberg, A. Salvati and K. A. Dawson, *Nat. Nanotechnol.*, 2012, **7**, 62–68.
377 J. V. Jokerst, T. Lobovkina, R. N. Zare and S. S. Gambhir, *Nanomedicine*, 2011, **6**, 715–728.
378 S. Schöttler, G. Becker, S. Winzen, T. Steinbach, K. Mohr, K. Landfester, V. Mailänder and F. R. Wurm, *Nat. Nanotechnol.*, 2016, **11**, 372–377.
379 S. Tenzer, D. Docter, J. Kuharev, A. Musyanovych, V. Fetz, R. Hecht, F. Schlenk, D. Fischer, K. Kiouptsi, C. Reinhardt, K. Landfester, H. Schild, M. Maskos, S. K. Knauer and R. H. Stauber, *Nat. Nanotechnol.*, 2013, **8**, 772–781.
380 A. Salvati, A. S. Pitek, M. P. Monopoli, K. Prapainop, F. B. Bombelli, D. R. Hristov, P. M. Kelly, C. Åberg, E. Mahon and K. A. Dawson, *Nat. Nanotechnol.*, 2013, **8**, 137–143.
381 S. Schöttler, K. Landfester and V. Mailänder, *Angew. Chem., Int. Ed.*, 2016, **55**, 2016.
382 K. P. García, K. Zarschler, L. Barbaro, J. A. Barreto, W. O'Malley, L. Spiccia, H. Stephan and B. Graham, *Small*, 2014, **10**, 2516–2529.
383 D. F. Moyano, K. Saha, G. Prakash, B. Yan, H. Kong, M. Yazdani and V. M. Rotello, *ACS Nano*, 2014, **8**, 6748–6755.
384 M. Benezra, E. Phillips, M. Overholtzer, P. B. Zanzonico, E. Tuominen, U. Wiesner and M. S. Bradbury, *Small*, 2015, **11**, 1721–1732.
385 S. G. Elci, Y. Jiang, B. Yan, S. T. Kim, K. Saha, D. F. Moyano, G. Yesilbag Tonga, L. C. Jackson, V. M. Rotello and R. W. Vachet, *ACS Nano*, 2016, **10**, 5536–5542.
386 A. Elsaesser and C. V. Howard, *Adv. Drug Delivery Rev.*, 2012, **64**, 129–137.
387 H. F. Krug, *Angew. Chem., Int. Ed.*, 2014, **53**, 12304–12319.
388 E. Lepeltier, L. Nuhn, C.-M. Lehr and R. Zentel, *Nanomedicine*, 2015, **10**, 3147–3166.
389 R. Toy and K. Roy, *Bioengineering Translational Medicine*, 2016, **1**, 47–62.
390 B. Lee Chung, M. J. Toth, N. Kamaly, Y. J. Sei, J. Becraft, W. J. M. Mulder, Z. A. Fayad, O. C. Farokhzad, Y. Kim and R. Langer, *Nano Today*, 2015, **10**, 759–776.
391 C. de Souza Carvalho, N. Daum and C.-M. Lehr, *Adv. Drug Delivery Rev.*, 2014, **75**, 129–140.
392 N. Vogel, M. Retsch, C.-A. Fustin, A. del Campo and U. Jonas, *Chem. Rev.*, 2015, **115**, 6265–6311.
393 H. Zheng, R. K. Smith, Y. Jun, C. Kisielowski, U. Dahmen and A. P. Alivisatos, *Science*, 2009, **324**, 1309–1312.
394 N. de Jonge and F. M. Ross, *Nat. Nanotechnol.*, 2011, **6**, 695–704.

